New mixed-mode methacrylate-based polymeric monoliths prepared via complexation with cyclodextrins employed as stationary phases for capillary electrochromatography

Dissertation

zur

Erlangung des Doktorgrades

der Naturwissenschaften

(Dr. rer. nat)

dem

Fachbereich Chemie

der Philipps-Universität Marburg

Vorgelegt von

Fuad Al-Rimawi

aus

Ramallah/Palästina

Marburg/Lahn 2007

Die vorliegende Arbeit entstand in der Zeit von April 2004 bis Juli 2007 unter der Leitung von Prof. Dr. Ute Pyell am Fachbereich Chemie der Philipps-Universität Marburg.

Vom Fachbereich Chemie der Philipps-Universität Marburg als Dissertation am 28. 06. 2007 angenommen

Erstgutachter: Prof. Dr. Ute Pyell
Zweitgutachter: Prof. Dr. Andreas Seubert

Tag der mündlichen Prüfung am 23.07.2007

Gedruckt mit Unterstützung des Deutschen Akademischen Austauschdienstes

To my family, my Wife,

My son (Yousef),

To my Homeland

Palestine

Acknowledgments

I would like to thank Prof. Dr. Ute Pyell for her kind supervision, valuable guidance and her keen interest in my research project throughout my stay at her laboratory. Also I thank Prof. Dr. Andreas Seubert for fruitful discussions regarding my laboratory work.

Thanks are also due to Dr. Uwe Linne for providing the μ-LC instrument, Dr. Andreas Schaper for carrying out the SEM measurements, Frau Czerny for performing porosity analysis. I also acknowledge Prof. Dr. Thomas Schrader and his research group for providing the software for nonlinear regression calculations.

My thanks are extended also to my colleagues in AK Pyell (Carolin Huhn, Annika Wahl, Barbara Hermann, Jan Rittgan, Susanne Dieckmann) and my colleagues at Philipps-Universität Marburg (Sajid Malik from Biology department, Wael Derwish and Yasser Elgamel from Chemistry department) for their cooperation and nice company. I thank also my short-practical students Sebastian Kamps and Markus Rauber.

I am grateful to Deutscher Akademischer Austauschdienst (DAAD) for the financial support throughout my stay in Germany.

I can not end without thanking my family for their encouragement and love throughout my stay at Philipps-Unvirsität Marburg, Germany. This thesis is dedicated to them.

Table of Contents

List of abbreviations and symbols

A	Coefficient of eddy diffusion
AMPS	2-acrylamido-2-methyl-1-propanesulfonic acid
APS	Ammonium persulfate
AS	Ammonium sulfate
B	Coefficient of longitudinal diffusion or complex formation constant
B_D	Complex dissociation constant
C_{12}	Dodecyl methacrylate
C_{18}	Octadecyl methacrylate
C_6	Cyclohexyl methacrylate
c_{aq}	Molar concentration of free solute in the mobile phase
c_{com}	Molar concentration of complexed solute in the mobile phase
CD	Cyclodextrin
CE	Capillary electrophoresis
CEC	Capillary electrochromatography
c_m	Molar concentration of an analyte in the mobile phase
C_m	Coefficient of the resistance to mass transfer in the mobile phase
CMC	Critical micellar concentration
c_s	Molar concentration of free solute in the stationary phase
C_s	Coefficient of the resistance to mass transfer in the stationary phase
%C	Crosslinker concentration
d	Capillary diameter
DMAA	*N*,*N*-dimethylacrylamide
DMF	Dimethylformamide
E	Applied electric field

EOF	Electroosmotic Flow
F	Volume flow rate
F_k	Faraday constant
FT-IR	Fourierr Transform Infrared Spectroscopy
H	Plate height
HEMA	2-hydroxyethyl methacrylate
HPLC	High performance liquid chromatography
^{1}H NMR	Nuclear magnetic resonance
^{1}H NOESY	Nuclear Overhauser Enhancement Spectroscopy
I	Ionic strength
I.D.	Inner diameter
ISEC	Inverse size-exclusion chromatography
K	Partitioning coefficient
K_p	Permeability
k	Retention factor
k_{app}	Apparent retention factor
k_c	Corrected retention factor
k_{obs}	Observed retention factor
K_{distr}	Distribution coefficient
K^o	Specific permeability
L	Length of a separation bed
LC	Liquid chromatography
L_{eff}	Effective length of a capillary
L_{tot}	Total length of a capillary
MA	Methylacrylamide
MEKC	Micellar electrokinetic chromatography

N	Plate number
n_{CH2}	Methylene selectivity
O.D.	Outer diameter
OT-CEC	Open-tubular electrochromatography
PDA	Piperazinediacrylamide
pH*	Apparent pH
p*I*	Isoelectric point
q	Charge
r	Radius
R	Gas constant or resolution
ROESY	Rotating frame Overhauser Effect Spectroscopy
S^2	Variance
SDS	Sodium Dodecyl Sulfate
SEM	Scanning electron microscopy
T	Temperature
t_0	Hold-up time
TEM	Transmission electron microscopy
TEMED	Tetramethylethylenediamine
THF	Tetrahydrofuran
t_R	Retention time
%T	Total monomer concentration
U	Applied voltage
u	Linear velocity
UV	Ultraviolet
v	Migration velocity
v_{eo}	Linear velocity of electroosmotic flow

v_{ep}	Electrophoretic velocity
V_m	Volume of the mobile phase
V_s	Volume of the stationary phase
VSA	Vinylsulfonic acid
W	Width at the baseline of a peak
$w^{0.5}$	Width at half the maximum height of a peak
x	Distance
X	Mole fraction
$\overline{X}_j$	Arithmetic average within a group
$\overline{X}_g$	Total average
α	Selectivity factor
α_{meth}	Methylene selectivity
γ	Surface tension
δ	Thickness of the electrical double layer or chemical shift
δ_{HG}	Chemical shift of the complexed guest
δ_G	Chemical shift of the free guest
δ_{obs}	Observed chemical shift
Δa	Standard error of the y-intercept
Δb	Standard error of the slope
ΔB	Standard error of the complex formation constant
ΔG	Change in the free energy
Δp	Pressure difference
$\Delta\delta$	Change in the chemical shift
$\Delta\delta_{max}$	Maximum chemical shift
ε	Electric permittivity or total porosity
ε_r	Relative permittivity of the medium (dielectric constant)

ε_o	Permittivity of vacuum
ζ	Zeta-Potential
η	Viscosity
θ	Angle
κ	Debye-Hueckel parameter (reciprocal of the double layer thickness)
μ_{eo}	Electroosmotic mobility
μ_{ep}	Electrophoretic mobility
σ	Surface charge density or standard deviation
σ^2	Variance
φ	Phase ratio
χ	Electric conductivity
ψ	Electric potential
$\varphi_{Methanol}$	Volume fraction of methanol in the mobile phase

1 Introduction and Objectives

Capillary electrochromatography (CEC) is a capillary-format separation technique that combines aspects of both chromatography and capillary electrophoresis (CE). As in CE, the mobile phase is driven in CEC by electroosmosis while applying high voltage across the column. As in HPLC, CEC requires a stationary phase. The flat flow profile of the electroosmotic flow (EOF) results in the reduction of band broadening due to the decrease in resistance to mass transfer in the mobile phase (C_m) and the eddy diffusion (A) parameters in the Van-Deemter equation. Therefore, higher separation efficiency can be obtained in CEC in comparison to μ-LC keeping all other parameters constant. CEC has been employed for the separation of a wide spectrum of analytes.

The stationary phase in CEC plays a dual role. It provides sites for the required interaction of the analytes with the stationary phase and the charge density at the interface stationary phase/mobile phase is responsible for the generation of the electroosmotic flow. Packed-columns, open-tubular columns, as well as monolithic columns have been employed as stationary phases for CEC.

Monolithic materials, which emerged during the last decade, are materials, which consist of a continuous rod of a rigid macroporous polymer. The simplicity of their *in-situ* preparation in capillaries, the absence of frits and the large variety of polymerizable monomers make monolithic separation materials an attractive alternative to capillaries packed with a particulate material. These materials have quickly become a well-established stationary phase format for CEC. There are two main types of monolithic materials, silica-based and organic polymer-based monoliths. The polymeric continuous beds exhibit following features: simple preparation, facile adaptability to fine-tune the selectivity of the separation system as well as the direction and velocity of the EOF. Organic monoliths for CEC are prepared by *in-situ* free radical polymerization of a mixture of monomers dissolved in a porogenic liquid in the presence of an initiator (system) inside a capillary.

Several types of organic monoliths were investigated as continuous beds in CEC. For water-soluble monomers an aqueous buffer can be used for dissolving the polymerization mixture. However, in case of more hydrophobic water-insoluble monomers, organic solvents or a mixture of an organic solvent with aqueous buffer is needed. An alternative to the use of organic solvents is the solubilization of water-insoluble monomers in aqueous medium by host-guest complexation using cyclodextrins.

The objective of this work is the preparation of polymeric monoliths as stationary phases for CEC employing solubilization by complexation with cyclodextrins. Free radical copolymerization has been performed in aqueous solution with a cyclodextrin-solubilized hydrophobic monomer, a water-soluble crosslinker (piperazinediacrylamide), and a charged monomer (vinylsulfonic acid).

This thesis focuses also on the investigation of the host/guest complexes of the hydrophobic monomers with different types of cyclodextrin; application of capillary electromigration techniques (capillary electrochromatography (CEC) and micellar electrokinetic chromatography (MEKC)) and spectroscopic methods (^{1}H NMR and ^{1}H NOESY spectroscopy) to investigate interactions between cyclodextrins (α-CD, statistically methylated ß-CD, hydroxypropyl-ß-CD, and 2-hydroxypropyl-γ-CD) and different methacrylates (adamantyl, isobornyl, cyclohexyl and phenyl methacrylate).

Another aim of this work has been the investigation of the chromatographic properties of these monolithic stationary phases using CEC and to compare them with the chromatographic properties of a packed HPLC-column filled with octadecyl silica gel. Chromatographic properties of these monoliths were investigated with aqueous and non-aqueous mobile phases with hydrophobic and polar analytes and with neutral and with charged analytes. Beside a characterization of the contributions of hydrophobic, Van-der-Waals and Coulomb interactions to the observed retention, in this work, the potential of the stationary phases synthesized for the separation of positively charged analytes (alkylanilines, amino acids, and peptides) was intended to be elucidated.

2 Theoretical Background

2.1 Capillary electrochromatography

Capillary electrochromatography (CEC) can be considered as a hybrid of CE and HPLC. From another point of view, it is a liquid chromatographic method in which the mobile phase is electroosmotically driven through the chromatographic bed. CEC combines the selectivity of HPLC and the efficiency of CE [1]. Analytes are separated according to differences in the partitioning constant between the stationary phase and the mobile phase, and/or to differences in the electrophoretic mobility. In CEC the mobile phase is driven through the chromatographic column (while applying high voltage across the column) by electroosmotic flow (EOF), the pumping mechanism known from CE, whereas in HPLC a mechanical pump drags the liquid through the column. As in CE, small diameter (typically 50-100 μm) columns with favourable surface area-to-volume ratio are employed to minimize thermal gradients from ohmic heating, which can have an adverse effect on band width. CEC differs crucially from CE, however, in that the separation principle is the difference in the partitioning of the analyte between the mobile phase and stationary phase [1].

CEC has many advantages compared to HPLC. High separation efficiencies can be obtained in CEC in comparison to HPLC. This is mainly due to the characteristics of the electroosmotic flow. The flat or plug-like flow velocity profile in EOF results in the reduction of band broadening for a solute zone as it passes through the column due to the decrease in resistance to mass transfer in the mobile phase (C_m) and the eddy diffusion (A) parameters in the Van-Deemter equation, which increases the column efficiency. Furthermore, the electrically driven flow rate is independent of the particle diameter and column length as in pressure-driven flow. Therefore, smaller particles and larger columns can be used which further increases column efficiency. In pressure-driven flow, however, the pressure depends directly on the column length and is inversely on the square of the particle diameter, therefore, for practical pressures, generally used particle diameters are seldom less than 3 μm with column length restricted to approximately 25 cm. The combined effect of reduced particle diameter, increased column length and plug flow leads to CEC efficiencies of typically 200000 plates per meter, and substantially improved resolution [2]. With such high efficiencies, CEC can show higher column peak capacity, which is the number of peaks, which can be separated in a chromatogram. It should also be emphasized that in first approximation the mobile phase velocity in CEC is independent of the mean channel diameter, which makes possible to use separation beds in CEC, which might be not

appropriate for μ-LC because of their low permeability. Another advantage of CEC is that the mobile phase consumption is much lower than in HPLC [2].

CEC has proved to be a versatile separation method for different classes of compounds. Examples, among others, are the applications in the biochemical (amines and amino acids, peptides, proteins, nucleosides and nucleotides, and carbohydrates), pharmaceutical (steroids, acidic and basic drugs), environmental and industrial fields (inorganic anions and cations, synthetic polymers, polyaromatics, pesticides, insecticides, and herbicides). Also the separation of chiral compounds is possible [1-3].

2.2 Electrophoresis and electroosmosis

Electrophoresis is the migration of charged species in an electrical field. Cations migrate toward the cathode and anions are attracted toward the anode, while neutral solutes are not attracted to either electrode. Conventionally electrophoresis has been performed in layers of gel or paper. The traditional electrophoresis equipment offered a low level of automation and long analysis times. Detection of the separated bands was performed by post-separation visualisation. The analysis times were long as only relatively low voltages could be applied before excessive heat formation caused loss of separation.

Performing electrophoretic separations in capillaries, which has been appeared in early-1980s, is now known as capillary electrophoresis [4]. It offers the possibility of automated analytical equipment, fast analysis time and on-line detection of the separated peaks. Heat generated inside the capillary is effectively dissipated through the walls of the capillary, which allows high voltages to be used to achieve rapid separations. A section of the capillary is used for on-capillary detection i.e. no external detection cell is required. The output from an electrophoresis run is called an electropherogram.

Separation by electrophoresis is based on differences in solute migration velocity in an electric field. The migration velocity of a charged species v can be given by

$$v = \mu_e E \quad (1)$$

Where μ_e is the electrophoretic mobility, E is the applied electric field which is the applied voltage U divided by total length of the capillary L_{tot}, i.e. $E = U/L_{tot}$.

The mobility is a characteristic constant for a species. It is strongly dependent on the properties of the solution. The mobility is determined by the electric force that the charged

species experiences, balanced by its frictional force through the medium, which gives the relation

$$\mu_e = \frac{q}{6\pi\eta r} \tag{2}$$

where q is the charge of the charged species, r is the hydrodynamic radius of the charged species, η is the solution viscosity. From this equation, it is evident that small, highly charged species (i.e. high charge to size ratio) have higher mobilities compared to large, minimally charged species.

Electroosmotic flow is a bulk flow of liquid through a capillary caused by an electrical voltage applied across the capillary, which has surface charge on the interior wall. When a glass capillary is filled with a buffer, silanol groups (-Si-OH) on the surface of the capillary dissociate to form negatively charged groups ($Si\text{-}O^-$). A layer of positively charged counterions, which are present in the bulk solution, will be attracted to the negative surface (Fig. 1). These cations are tightly held in the Stern layer. Even with an applied voltage, they move very slowly i.e. this Stern layer is nearly immobile. Just above Stern layer is another diffuse layer of cations and anions that move with the electric field. This layer is called Gouy layer. The boundary between the Stern layer and Gouy layer is the Stern plane, Fig. 1, while the plane of shear is within the Gouy layer. As it is seen from Fig. 1, the electric potential decreases with distance in a linear fashion across the Stern layer. Across the diffuse region and into the bulk solution, the decay in electric potential is exponential ($\psi \rightarrow 0$ as $x \rightarrow \infty$). The distance over which electric potential falls by e^{-1} is called double layer thickness δ. The thickness of this layer, which is typically only a few nanometers, depends inversely on the square root of the ionic strength of the mobile phase I, temperature T and the electric permittivity of the mobile phase ε. The reciprocal of the double layer thickness, κ, also known as the Debye-Hueckel parameter, is given by the relation,

$$\kappa = \frac{1}{\delta} = \sqrt{\frac{2\,I\,F_k^{\,2}}{RT\varepsilon_0\varepsilon_r}} \tag{3}$$

where δ is the Debye length (double layer thickness), F_k is the Faraday constant, R is the gas constant, ε_o is the permittivity of vacuum, ε_r is the relative permittivity of the medium (dielectric constant). The electric permittivity is related to ε_0 and ε_r as follows,

$$\varepsilon = 4\pi\,\varepsilon_0\,\varepsilon_r \tag{4}$$

The electrical potential at the shear plane is known as the zeta potential ζ. The zeta potential depends on the surface charge density σ and on the double layer thickness [1].

When an electric field is applied across the capillary, the cations and anions in the diffuse Gouy layer start to migrate towards the cathode dragging the rest of the fluid in the capillary, creating a bulk flow of liquid in the capillary [1-2, 5-6].

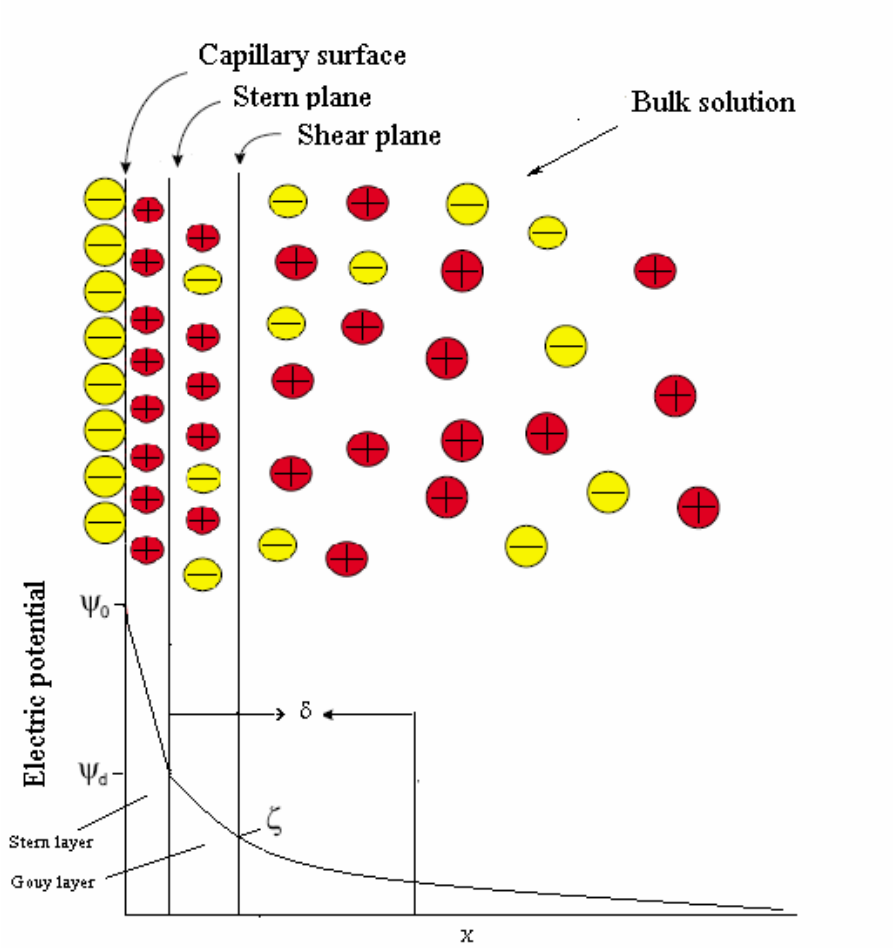

Fig. 1. Schematic representation of the structure of the electric double layer; plot of electric potential ψ vs. distance x [1].

When the radius of the capillary is large compared to the thickness of the electrical double layer, the electroosmotic mobility μ_{eo} is given by the Smoluchowski equation [1,2]:

$$\mu_{eo} = \frac{\varepsilon_0 \varepsilon_r \zeta}{\eta} \tag{5}$$

From this equation, it is evident that the electroosmotic mobility is dependent on the zeta potential which is strongly affected by the solution properties. For example, pH of the

solution influences strongly the net surface charge density. The dielectric constant to viscosity ratio (ε_r/η) of the solution affects also the electroosmotic mobility.

The linear velocity of EOF v_{eo} in an electrolyte solution depends on the electroosmotic mobility μ_{eo} and the electric field strength [1,2],

$$v_{eo} = \mu_{eo} E = \frac{\varepsilon_0 \varepsilon_r \zeta}{\eta} E \tag{6}$$

The linear velocity of the EOF can be determined from the effective length of the capillary L_{eff}, which is the length from the inlet to the detection window, and the hold-up time t_0 as follows,

$$v_{eo} = \frac{L_{eff}}{t_0} \tag{7}$$

By substitution the value of v_{eo} (from Eq. 7) in Eq. 6 and replacing E with U/L_{tot}, the following formula for the electroosmotic mobility is obtained,

$$\mu_{eo} = \frac{L_{eff} L_{tot}}{t_0 U} \tag{8}$$

where L_{tot} is the total length of the capillary (length from the inlet to the outlet).

The flow velocity profile in electrochromatography differs from the velocity profile of the parabolic flow of pressure-driven flow in HPLC [1]. The flow profile is nearly plug-like since it originates essentially from the capillary wall, but it depends on the diameter of the capillary d and the double layer thickness δ. The flow profile is only independent of the capillary diameter when $d >> \delta$. As d approaches δ, double layer overlap occurs with a simultaneous reduction in flow velocity, until a parabolic flow profile is obtained when d and δ are similar [1-2].

2.3 Fundamentals of chromatography

In chromatographic separations, analytes distribute themselves between the mobile phase and the stationary phase. The equilibrium constant of the distribution of an analyte between the mobile phase and stationary phase K is called a partitioning coefficient, and is defined as,

$$K = \frac{c_s}{c_m} \tag{9}$$

where c_s is the molar concentration of the analyte in the stationary phase, and c_m is the molar concentration of the analyte in the mobile phase.

The retention factor k is an important parameter used to describe the migration velocity of an analyte in the separation bed. It is defined as,

$$k = K\frac{V_s}{V_m} \tag{10}$$

where the ratioV_s/V_m is called the phase ratio, where V_s is the volume of the stationary phase, and V_m is the volume of the mobile phase.

The retention factor k is independent of the length of the column or the velocity of the mobile phase. It can be determined from the retention time t_R of an anlyte which is the time it takes after sample injection for the anayte to reach the detector, and from the dead time t_0 which is the time needed for the unretained solute to reach the detector,

$$k = \frac{t_R - t_0}{t_0} \tag{11}$$

The measure of the selectivity of a separation system is the selectivity factor α, which is defined as,

$$\alpha = \frac{k_2}{k_1} \qquad (k_2 > k_1) \tag{12}$$

where k_2, k_1 is the retention factor of Analyte 2 and 1, respectively.

The resolution R provides a quantitative measure of the ability of a chromatographic system to separate two analytes. Resolution is defined as,

$$R = 2\frac{t_{R2} - t_{R1}}{w_1 + w_2} = 1.18\frac{t_{R2} - t_{R1}}{w_1^{0.5} + w_2^{0.5}} \tag{13}$$

Where t_{R1}, t_{R2} is the retention time of Analyte 1 and 2, respectively. w_1, w_2 is the width at the baseline of Peak 1 and 2, respectively. $w_1^{0.5}$, $w_2^{0.5}$ is the width at half its maximum height of Peak 1 and 2, respectively.

In chromatography, two related terms for measuring the efficiency of a separation are widely used; the plate height H and the plate number N. The two terms are related by the equation

$$N = \frac{L}{H} \tag{14}$$

Where L is the length of the separation bed.

Formally, the efficiency of a chromatographic column increases with increasing number of plates and decreasing plate height. The plate number can be calculated for an analyte from the parameters of a chromatogram as follows,

$$N = 5.54\left(\frac{t_R}{w_{0.5}}\right)^2 \tag{15}$$

The plate number is usually normalized on the length of the chromatographic bed in order to compare the efficiency independent of the column length.

Chromatographic bands are generally assumed to be Gaussian in shape. Gaussian curves are obtained when replicate values of a measurement are plotted as a function of the frequency of their occurrence. The Gaussian function is the same as the (normal) probability density function or normal error function. The Gaussian function is directly related to the variance σ^2 and to the standard deviation σ of a measurement [7]. Therefore, it is convenient to define the efficiency of a column in terms of variance per unit length of the column, that is, the plate height is given by,

$$H = \frac{\sigma^2}{L} \tag{16}$$

The terms plate height and number of theoretical plates are based on a theoretical study of Martin and Synge [8] in which they treated a chromatographic column as if it were made up of numerous discrete narrow layers called theoretical plates. At each plate, equilibration of the distribution of the analyte between the mobile phase and the stationary phase was assumed to take place. Movement of the analyte in the column was then treated as a stepwise transfer of equilibrated mobile phase from one plate to the next. In fact, the equilibrium state can never be realized with the mobile phase in constant motion [7]. Band broadening occurs due to eddy diffusion, longitudinal diffusion of an analyte from the concentrated center of a band to the more dilute regions ahead and behind the band center, that is, toward and opposed to the direction of the mobile phase. Resistance to mass transfer of the analyte in the mobile phase C_m and stationary phase C_s contribute also to the band broadening. C_s and C_m coefficients arise because the equilibrium between the mobile phase and the stationary phase is established so slowly that a chromatographic column always operates under nonequilibrium conditions [7]. These factors are summarized in the Van-Deemter equation,

$$H = A + \frac{B}{u} + C_m u + C_s u \tag{17}$$

where A, B are coefficients of eddy diffusion, longitudinal diffusion, respectively, u is the linear velocity of the mobile phase.

The eddy diffusion term A, which leads to a broadened band, arises from the different pathways travelled by the analyte through a packed column. The A term contribution to H is reduced by packing columns with smaller particles, and with using homogenous packing material. Electroosmotic propulsion of the mobile phase allows the use of much smaller particles since there is no maximum pressure limit, and the flat profile generated reduces the variation of the different paths (streams) travelled by the analyte. Furthermore, in packed column chromatography, EOF velocity is independent of channel diameter (in the limit of no double layer overlap), thus variations in flow velocity between regions of the column differing in packing structure will be small in an electrically driven system, as depicted schematically in Fig. 2a [1]. Another important feature of the flat streaming profile of electroosmotic flow (compared to the parabolic streaming profile generated by pressure difference-induced laminar flow) is reduction of the band broadening due to mass transfer resistance in the mobile phase C_m (Fig. 2b), since this term depends on the different streaming profiles of the mobile phase through the column. The lower contributions of A and C_m terms to the band broadening in Van-Deemter equation results in increase in the efficiency in CEC compared to HPLC (Fig 2c). Jiang et al. [9] observed a nearly flat H-u curve for CEC compared to HPLC for thiourea (Fig. 3). A decrease in A and C terms by a factor of two to four has also been observed in CEC compared to μ –HPLC using the same column [10-11].

(a)

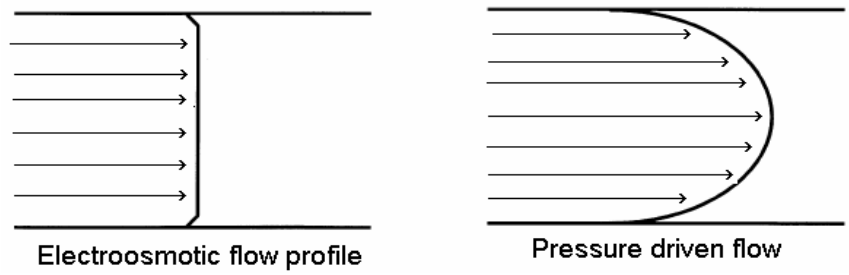

(b)

(c)

Fig. 2. (a) Representation of flow velocity profiles through channels of varying diameter (Arrows represent mean velocity vectors), (b) Comparison of the velocity profiles, (c) Effect on peak shapes [1].

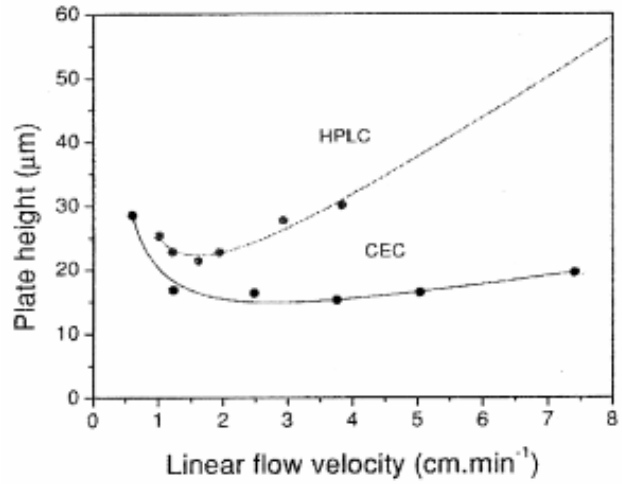

Fig. 3. Comparison of Van Deemter curves under electro- and pressure-driven conditions. Column: poly(alkylmethacrylate) monolith containing sulfonic acid functionalities, 41.5 cm (8.5 cm from detection window to outlet). Mobile phase 20% (v/v) sodium phosphate buffer (5 mmol L^{-1}, pH 7) and 80% acetonitrile, sample thiourea [9].

2.4 Instrumentation

CEC can be performed using the same instrumentation as for CE, although minor modifications, such as pressurization at both ends of the capillary, are often required to prevent bubble formation in the packed capillary. In contrast to HPLC, no pump is needed for CEC instrumentation. The instrumentation required to perform CEC is illustrated in Fig. 4. The inlet of the column is dipped into the inlet reservoir, while the outlet is dipped into the outlet reservoir. The inlet reservoir is replaced with the sample reservoir when performing an injection. Injection of a sample is performed directly into the high-voltage end of the separation capillary, mostly by electrokinetic injection. In this case, the vessel with mobile phase is replaced by a vessel containing the sample and a programmed voltage is applied for a few seconds. With electrokinetic injection the sample is dragged into the capillary by the effect of electroosmosis. In the case of neutral analytes, no discrimination of sample constituents takes place. The simplicity of electrokinetic injection compared to the difficulty of injecting a few nonoliters via a mechanical injection device into a stream of pressureized mobile phase constitutes an important advantage of CEC over micro-HPLC [6].

The high voltage power supply is used to apply an electric potential between the inlet and outlet reservoirs. For normal operation, a potential in the region of 30 kV is applied to the inlet reservoir while the outlet reservoir is held at electrical ground. The detector is placed close to the outlet and connected to a data collection device.

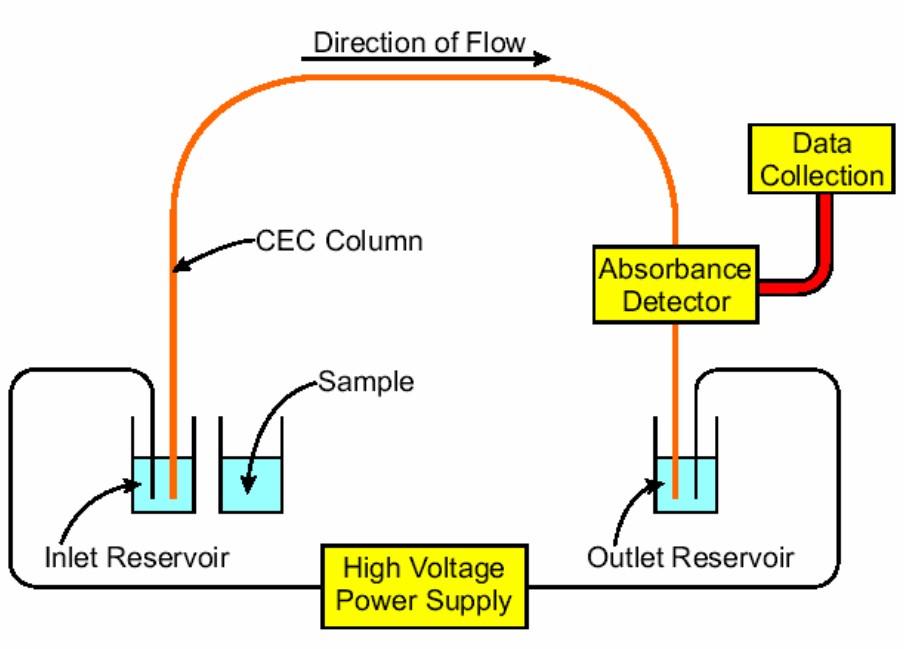

Fig. 4. Schematic representation of the components of a CEC instrument [2].

Basically, in CEC the same detection techniques are applicable as in CE: photometric detection, fluorimetric detection, or amperometric detection. Furthermore, the coupling of CEC with mass spectrometry has been realized mainly by employing electrospray ionization [12-13]. Also, the coupling of CEC with NMR spectroscopy has been reported [14]. In order to minimize band broadening, detection in CEC is usually performed on-column in an empty segment of the capillary after the outlet frit. The internal diameter (I.D.) of the capillary column, therefore, determines the path length over which the absorbance is measured. The shorter pathlength limits inherently the sensitivity of CEC compared to HPLC and micro-HPLC, where flow cells with higher path lengths are employed. Stead et al. compared the separation of steroids in plasma and found that CEC is 100-fold less sensitive than HPLC [15].

2.5 Mobile phases for CEC

Mobile phase plays a dual role in CEC. It is the eluent, and in combination with the stationary phase, it is also the charge carrier producing electroosmotic flow. Thus, parameters such as ionic strength, conductivity, Joule heating, viscosity, and double layer thickness which are functions of composition and temperature of the mobile phase are much more important in CEC than in HPLC [16]. Also, in CEC, optimization of the composition of the mobile phase must consider not only retention of solutes and selectivity of the chromatographic system (as in HPLC) but also observed electroosmotic mobility and achieved chromatographic efficiency. In CEC as in CE, the mobile phase has to be buffered to produce the electroosmotic flow needed for the propulsion of mobile phase across the capillary [17].

2.6 Column technology

As the mobile phase for CEC, the stationary phase for CEC has a dual function. It provides interaction sites for the solutes, and plays the dominant role in the generation of the electroosmotic flow, hence the propagation of the mobile phase through the chromatographic bed. Therefore, the stationary phase for CEC should have ionisable groups. The dissociated silanol groups on the surface of silica gel can provide the negative charges required for EOF [18]. Based on differences in column format, three modes of CEC can be distinguished: packed columns, open tubular and continuous beds/monoliths.

2.6.1 Packed-bed columns

Packed-columns have been used for CEC [19-26]. In the first years of the development of CEC, columns were used packed with the silica particles that had been developed for HPLC. They offer the advantage of the ability to use the large variety of stationary phases already available for HPLC. Typically, 50-100 μm inner diameter columns are employed packed with HPLC-type stationary phase particles (modified porous silica particles). The silica matrix of such particles usually provides enough surface charge to enable the generation of a substantial EOF. These packing beds have also a high loading capacity. Also, longer capillary lengths as well as very small particle sizes can be utilized in CEC-packed-bed columns without problems since the bulk fluid is generated electroosmotically in CEC, i.e., there is no backpressure as in HPLC. However, this type of stationary phases suffers from some problems. The major drawback is the frits, which are needed at both inlet and outlet to support the beds. It has been suspected that the differences in surface chemistries between the stationary phase and the frit, and the change in EOF in moving from the packed region to the empty capillary may contribute to bubble formation [27]. In addition to the required frits, the packed column-format has other technical problems: none of the standard methods to pack columns with small beads will give sufficiently uniform beds in narrow bore tubes, and therefore pressurized electrode chambers are required to avoid bubble formation.

A typical CEC column is shown in Fig. 5, with the configuration being a packed section of capillary, where the separation occurs, followed by an open section of capillary beginning at the absorbance detection window. The packed section of the capillary is stabilized by retaining frits, and since it is not transparent, detection is performed after the separation medium.

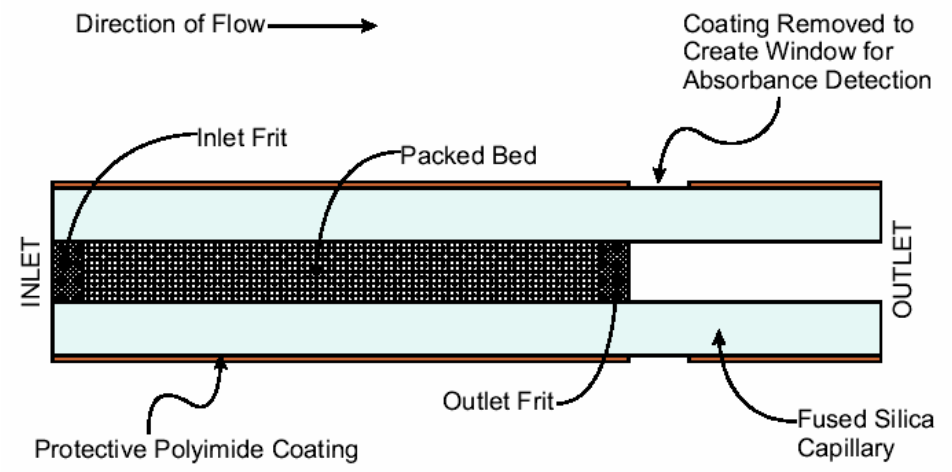

Fig. 5. Schematic representation of a packed capillary for CEC [10].

2.6.2 Open tubular columns

Another mode of CEC is open-tubular electrochromatography (OT-CEC) [28-36]. In OT-CEC, the stationary phase is attached in a thin layer to the inner wall of a capillary with small inner diameter (smaller than 25 μm). This may increase the separation efficiency compared with a packed column because the eddy diffusion contribution is eliminated. The method gives also high resolution when the inner diameter is small, which, however, gives low sensitivity in on-tube UV-detection due to the very short light path. Furthermore, the loadability of OT-CEC is low compared to packed-column CEC, and lower retention factors are usually obtained.

2.6.3 Monolithic stationary phases for CEC

Limitations of packed-column as well as open-tubular CEC stationary phases have triggered the development of various alternative approaches. One of these approaches is monolithic column technology. Monolithic columns containing in situ prepared monolithic separation media based on organic polymer or silica can be prepared. The preparation of organic polymer monoliths is simple and straightforward. They are prepared by in situ free radical polymerization of a mixture of monomers dissolved in a porogenic liquid in the presence of an initiator (system) inside a capillary or a microfluidic chip. The salt concentration in the polymerization mixture plays an important role in the creation of the desired flow-through channels within the polymeric matrix. The macroporosity of the resulting polymeric continuous phase results from phase separation of the solid polymer from the porogenic liquid during the polymerization process.

The polymerization solution can be introduced into the capillary by several methods: using an injection syringe connected to the capillary, the siphoning introduction, using a simple vacuum injection system, or by using a standard filling device as used for coating capillary GC columns which uses a pressure of up to 0.5 MPa or a plastic syringe [37].

The simple preparation of monoliths avoids the problems related to both frit formation and packing. Additionally, columns of virtually any length and shape are easily accessible. Another advantage is that the polymerization mixture can be prepared from a wide variety of monomers, allowing a nearly unlimited choice of both matrix and surface chemistries. This flexibility enables the easy tailoring of both the interactions that are required for specific separation modes and the level of generated EOF. Additionally, the control that can be exerted over the polymerization process enables the optimization of the porous properties of

the monolith, as well as the flow rate and chromatographic efficiency of the system. This novel type of stationary phases which emerged during the last decade [38-51] has also attracted increasing attention in liquid chromatography because of its in-situ, ease preparation, unique properties, and low flow resistance as compared to conventional columns packed with particles. These stationary phases have been the subject of several reviewers in recent years [52-56].

The first monolith has been prepared by Hjerten et al. in 1989 [38] based on a copolymer of acrylic acid and N,N'-methylenebisacrylamide. This monolith has been employed as cation-exchange-stationary phase for HPLC for the separation of model proteins [38]. Baba et al. [57] has prepared polyacrylamide gel-filled fused silica capillaries in 1992, which are similar to those used for capillary gel electrophoresis. The capillary was filled with an aqueous polymerization mixture containing monovinyl and divinyl (crosslinking) acrylamide-based monomers as well as a redox free radical initiating system, such as ammonium peroxodisulfate and tetramethylethylenediamine (TEMED). Initiation of the polymerization process begins immediately upon mixing of all the components at room temperature. Therefore, the reaction mixture was used immediately. The polymerization process is normally allowed to proceed overnight to afford a capillary filled with a continuous bed of gel. The resulting gel is a very soft, highly swollen material, which contains no more than 5% solid polymer. These capillaries have been used for the separation of complex mixtures of nucleic acids. The retention mechanism is sieving rather than interaction of the solutes with the matrix. Fujimoto et al. [42] has also prepared in 1995 an acrylamide-based monolith for CEC by copolymerization of an aqueous solution of acrylamide/ N,N'methylenebisacrylamide, and acrylamide/2-acrylamido-2-methyl-1-propanesulfonic acid (AMPS) inside a fused-silica capillary. Despite the lack of chemical attachment to the inner wall of the capillary, these crosslinked gels showed fair physical stability. Again in this system, Fujimoto et al. concluded that the mechanism of separation was sieving rather than an interaction of the solutes with the matrix [58].

In 1997, Hjerten et al. has prepared in-situ continuous beds for both electrochromatography and reversed-phase liquid chromatography of some aromatic hydrocarbons [39]. The original approach was complex, requiring several steps including the modification of the capillary surface with 3-(trimethoxysilyl)propyl methacrylate, two individual polymerizations, and a chemical functionalization. The initial polymer matrix was formed by copolymerizing a dilute aqueous solution of 2-hydroxyethyl methacrylate (HEMA) and piperazine diacrylate using a

standard redox initiation system in the presence of a high concentration of ammonium sulfate. The pores of this matrix were then filled with another polymerization mixture containing allyl glycidyl ether and dextran sulfate, and the second polymerization proceeded within the pores of the initial matrix leading to the “immobilization”of the charged dextran within the newly formed composite to produce the required EOF for CEC capillaries. Eventually, reaction of both epoxide and hydroxyl functionalities with 1,2-epoxyoctadecane led to the covalent functionalization of the matrix with a number of C18 chains.

The same group subsequently proposed a much simpler one-step procedure with the polymerization mixture consisting of an aqueous solution of acrylamide, piperazine diacrylamide, and vinylsulfonic acid with added stearyl methacrylate or butyl methacrylate to control the hydrophobicity of the gel [41]. Since neither of these non-polar monomers is soluble in water, a surfactant was added to the mixture, followed by sonication to form an emulsion of the hydrophobic monomer in the aqueous solution. Once initiated, the mixture was immediately drawn into an acryloylated capillary, where the polymerization was completed. The presence of the strongly acidic sulfonic acid functionalities afforded EOF that remained constant over a broad pH range. Separation of five polycyclic aromatic hydrocarbons has been achieved in 5 minutes in a 25 μm capillary [41].

Maruska [37] has given an overview about the synthesis of water-soluble acrylamide-based monoliths. These monoliths are hydrophilic and therefore retention of analytes in the reversed-phase is very low. In order to increase the retention of solutes in the reversed-phase with the monolithic stationary phase, hydrophobic monomers have to be used in order to increase the hydrophobicity of the stationary phase. Replacement of the hydrophilic acrylamide with the more hydrophobic N-isopropylacrylamide, in combination with functionalization of the capillary wall with 3-(trimethoxysilyl)propyl methacrylate [59], afforded a monolith covalently attached to the capillary wall. The CEC-separation of hydrophobic neutral compounds obtained using this polymeric stationary phase exhibits many of the characteristics typical of reversed-phase chromatography, including a linear dependence of the retention factor k on the volume fraction of an organic modifier present in an organic/aqueous mobile phase. This led to the conclusion that, in contrast to the original polyacrylamide-based gels, size-exclusion was no longer the primary mode of separation.

Ericson et al. [40] has prepared in 1999 a monolithic capillary column for a CEC separation of proteins. The preparation process involves a polymerization initiated by ammonium peroxodisulfate–TEMED in a system consisting of two phases: an aqueous phase typically a

solution of acrylamide and piperazine diacrylamide in a mixture of a buffer solution and dimethylformamide, and an immiscible, highly hydrophobic phase consisting of octadecyl methacrylate (for reversed-phase retention) [40]. Continuous sonication for 45 minutes was required in order to emulsify the octadecyl methacrylate and form a dispersion of fine polymer particles. Following this, another portion of initiator was added to the system to restart the polymerization of two newly added monomers, dimethyldiallylammonium chloride (for the generation of EOF) and piperazine diacrylamide. The resulting partly polymerized dispersion was then forced into a methacryloylated capillary using pressure and, finally, the polymerization process was carried out to completion. This allowed the excellent separation of proteins in either the co-EOF or counter-EOF mode.

Palm and Novotny simplified the incorporation of highly hydrophobic monomers into acrylamide-based matrices [60]. Rather than forming dispersion by sonication, mixtures of aqueous buffer and *N*-methylformamide were used to prepare homogeneous polymerization solutions containing acrylamide, methylene bisacrylamide, acrylic acid, and C4, C6, C12, or C18 alkyl acrylate [60-61]. Zhang and El Rassi prepared also monolithic stationary phases incorporating dodecyl ligands where the polymerization mixture is dissolved in an N-methylformamide/aqueous buffer solution [62].

Hoegger and Freitag used a similar procedure to that described by Hjerten for the preparation of acrylamide monoliths and performed a systematic evaluation of the preparation and chromatographic behaviour of these monoliths [63–65]. Initially, a polymerization mixture consisting of *N*,*N*-dimethylacrylamide (DMAA), methacrylamide (MA), and vinylsulfonic acid (VSA) was used and butyl acrylate or hexyl acrylate were added to control the hydrophobicity of the monolith. The retention mechanism for a series of neutral aromatic compounds was found to be neither pure reverse-phase nor pure normal-phase, even when monoliths containing large percentage of C_6 ligand were used, suggesting that in this case the separation mechanism is not solely controlled by differences in hydrophobicity. In 2003, these authors prepared similar monoliths from mixtures of piperazine diacrylamide, VSA and DMAA for the separation of charged biomolecules by CEC using a mixed-mode separation mechanism [64]. The effect of increasing the concentration of ammonium sulfate in the polymerization mixture was investigated, with the result that there is an increase in the mean pore diameter with increasing salt concentration as determined from both mercury intrusion porosimetry data and decrease in column back pressure. Furthermore, no difference in EOF was observed for the three different columns prepared. The effects of variations in mobile and

stationary phase composition on the separations were also considered. Changes in the stationary phase composition were also investigated with DMAA replaced by MA, 2-hydroxyethyl methacrylate or 2-hydroxyethyl acrylate in the polymerization mixture. Retention in each case followed the expected trends based on the relative monomer hydrophilicity. In 2004, Freitag [66] used monolithic columns prepared from methacrylamide, piperazinediacrylamide, and vinylsulfonic acid for the separation of phenols and amino acids in both CEC and nano-HPLC mode.

Polystyrene-based monoliths were also prepared for CEC. Gusev et al. [67] has first reported the preparation of polystyrene-based porous rigid monolithic capillary columns for CEC by polymerizing mixtures of chloromethylstyrene and divinylbenzene in the presence of various porogenic solvents such as methanol, ethanol, propanol, toluene, and formamide. The reactive chloromethyl moieties incorporated into the monolith served as sites for the introduction of quaternary ammonium functionalities with the pores of the monolith filled with *N*,*N*-dimethyloctylamine. Zhang et al. [68] further reported the preparation of a porous polymer monolith for CEC separation of proteins and peptides by copolymerizing chloromethylstyrene and ethylene dimethacrylate in the presence of propanol and formamide. The chloromethyl functionalities were subsequently modified with *N*,*N*-dimethylbutylamine to form a positively charged chromatographic surface with fixed butyl chains. In 2003, Jin et al. [69] reported the preparation of polystyrene-based monoliths by polymerizing styrene, divinylbenzene and methacrylic acid in the presence of toluene and isooctane as the porogenic solvents. These stationary phases were used for the separation of a wide range of analytes.

In addition to acrylamide- and styrene-based monoliths, preparations of methacrylate-based monoliths have also been reported. The preparation of methacrylate-based monolithic stationary phases was extensively investigated by Svec and co-workers [70-73]. In 1996, they have prepared a methacrylate-based monolith [70] by a simple copolymerization of ethylene dimethacrylate, butyl methacrylate, and 2-acrylamido-2-methyl-1-propanesulfonic acid in the presence of ternary porogenic system consisting of various proportions of water, 1-propanol, and 1,4-butanediol. In the following years, many other groups have also prepared methacrylate-based monoliths using the same approach [74-75]. Recently, Augustin et al. [76] has prepared methacrylate-based polymeric stationary phases for CEC by free radical copolymerization of butyl or hexyl acrylate, 1,3-butanediol diacrylate in a porogenic mixture containing acetonitrile, ethanol, and 5 mmol L^{-1} phosphate buffer. This polymeric stationary phase has been used for the separation of alkylbenzene derivatives.

2.6.4 Microchips

In addition to capillary columns, microchip-based CEC devices have also been fabricated. Kutter et al. [77] demonstrated open-tubular electrochromatography (OT-EC) using isocratic and gradient elution on microchips modified with a C_{18} stationary phase for separation of fluorescent dyes. Regnier's group has developed C_{18} and polymer coated monolithic support structure on poly(dimethylsiloxane) chips for OT-EC and LC [78]. Peptides from tryptic digests of proteins were separated isocratically in less than 10 minutes in CEC mode on these novel microchips. Mixed mode, continuous beds possessing both C_3 and sulfonic acid ligands obtained by in situ polymerization in the channels of microchips have also been used for CEC of antidepressant drugs [79].

2.7 Host-guest complexation using cyclodextrins

Mostly polymerization of monoliths was performed in organic solvents. For water-soluble monomers, an aqueous buffer can be used for dissolving the polymerization mixture. However, in case of more hydrophobic water-insoluble monomers, organic solvents or a mixture of an organic solvent with aqueous buffer is needed. An alternative to the use of organic solvents is the solubilization of water-insoluble monomers in aqueous medium by host-guest complexation using cyclodextrins [80].

Cyclodextrins are obtained by degradation of starch. They are cyclic oligosaccharides consisting of 6 (α), 7(β), or 8 (γ) glucopyranose units joined by α-1,4 linkage forming a torus-shaped ring structure. The primary hydroxy groups in position 6 are located at the narrow side of the torus, whereas the secondary glucopyranose OH-groups are located at the wider side of the torus (Fig. 6). Due to their polar hydrophilic outer shell and relatively hydrophobic cavity, they are able to form host-guest complexes by inclusion of suitable hydrophobic molecules (Fig. 7). The formation of these complexes leads to significant changes of the solubility and reactivity of the guest molecules, but without any chemical modification. Thus, water insoluble molecules may become completely water-soluble simply by mixing them with an aqueous solution of a native cyclodextrin or a cyclodextrin-derivative, e.g. methylated or hydroxypropylated cyclodextrin. Hydrogen bonds and hydrophobic interactions are responsible for the stability of the complexes [80].

For the host-guest complexation, a thermodynamic equilibrium is reached between the free cyclodextrin and the free guest with the host-guest complex, which can be described by the mass action law [81]:

$$[CD] + [G] \; f \quad [CD\text{-}G] \tag{18}$$

For this equilibrium, according to the law of mass action, the complex formation constant or stability constant B is defined as [81]:

$$B = \frac{[CD\text{-}G]}{[CD][G]} \tag{19}$$

Based on this knowledge, the behaviour of CD-complexes of various monomers e.g methacrylates or acrylamides has been investigated. Complexed monomers can be successfully polymerised via free radicals in aqueous solution [80]. The procedure of solubilization of hydrophobic monomers by complex formation with water-soluble cyclodextrins and subsequent reaction of the formed host-guest complexes by free radical polymerization or copolymerization in aqueous solution has been introduced into polymer chemistry in 1997 by Ritter and co-workers [82-90]. The free radical homopolymerization of *tert*-butyl methacrylate–cyclodextrin host–guest complexes [89], the free radical homopolymerization of cyclohexyl and phenyl methacrylate–cyclodextrin host–guest complexes [83], the free radical homopolymerization of *N*-methacryloyl-1-aminononane–cyclodextrin host–guest complexes [84] and the free radical copolymerization of hydrophobic acrylate–cyclodextrin host–guest complexes [85, 87, 88] and methacrylate–cyclodextrin host–guest complexes [86] were reported. The formation of the complexes can be verified by FT-IR, ^{1}H NMR, 2D-NOESY or ROESY NMR spectroscopy. Ritter and co-workers have found that in nearly all cases the resulting polymer precipitates rapidly in high yields and the cyclodextrin slips off step by step from the growing chain and thus remains soluble in the water phase, which can be recycled [80].

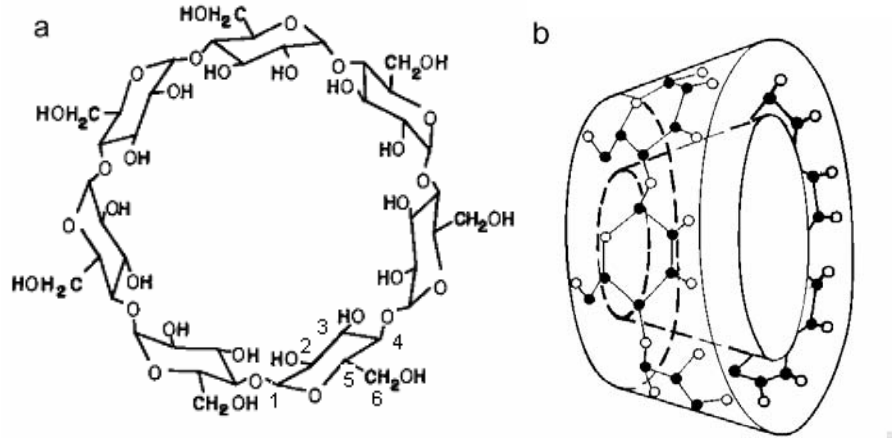

Fig. 6. (a) Chemical structure and (b) the toroidal shape of the ß-cyclodextrin molecule [80].

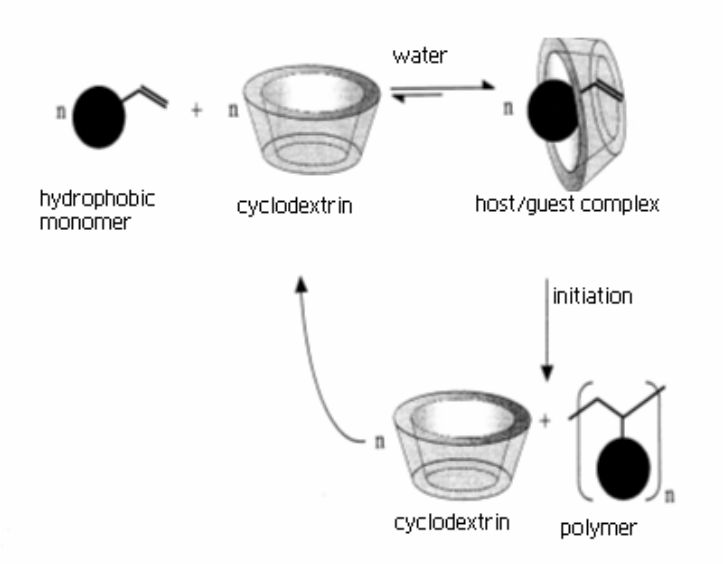

Fig. 7. Solubilization of hydrophobic monomers by cyclodextrin in aqueous solution followed by free radical polymerization [80].

The development in the solubilization of hydrophobic monomers in aqueous solution by water-soluble cyclodextrins led to apply this method in the preparation of monolithic stationary phases incorporating hydrophobic monomers solubilized in aqueous solution. Likewise, Wahl et al. [91] prepared such monolithic stationary phase for CEC by copolymerizing different water-insoluble crosslinking bisacrylamides solubilized with statistically methylated-β-cyclodextrin in aqueous solution.

3 Experimental

3.1 Pre-treatment of the capillary

For CEC experiments, fused-silica capillaries with inner diameter of 100 µm and outer diameter of 360 µm are used. Capillaries are coated with polyimide layer to give them flexibility without breaking. As the first step, the fused silica capillaries were pretreated with 3-(trimethoxysilyl) propyl methacrylate (bind silane), using the method described by Hjerten [92]. The capillary was first flushed with acetone, hydrochloric acid solution (0.1 M), sodium hydroxide solution (0.1 M), water, and finally with acetone. Then, a 30% v/v solution of bind silane in acetone was pumped through the capillary for 15 minutes and left overnight filled with this solution. After silanization, the capillaries were washed out with acetone and water.

3.2 Synthesis of the monolithic stationary phases

For the polymerization reaction, the hydrophobic methacrylate monomers were solubilized in aqueous phosphate buffer (100 mmol L^{-1}, pH 7.0, for preparation see the appendix) with methylated-ß-cyclodextrin, then piperazinediacrylamide (PDA), vinylsulfonic acid (VSA), and ammonium sulfate were added (Monoliths 1-4, Tab. 1). Filling the capillary with the polymerization mixture was done with an in-house manufactured capillary-filling apparatus (Fig. 8). This simple glass apparatus with a 3-way cock is connected to a pump and an argon cylinder. The polymerization mixture in a vial is brought into this apparatus, which is covered with a thread cover. First, the mixture was degassed for 10 minutes with help of a membrane vacuum pump and refilling with argon. Then, 10 µL of 2.5% (w/v) ammonium persulfate (APS) and 10 µL of 2.5% tetramethylethylenediamine (TEMED) solution were added and briefly mixed. Subsequently, the capillary is dipped into the reaction mixture, and with help of an argon pressure (ca. 1 bar) the reaction mixture is passed into the capillary. The ends of the capillary were sealed with silicon grease and the polymerization was allowed to proceed overnight at room temperature. Afterwards, the filled capillary was rinsed with distilled water for two hours with the help of an HPLC pump (50-100 bar) and a flow splitter. During the rinsing process, the detection window was created in the capillary by burning off a short section of the outer polyimide coating and pyrrolyzing and removing the monolith inside by a stream of water. Finally, the capillary is installed in the CEC apparatus (with effective length of 15.0 cm which corresponds to a total length of 21.0 cm) and rinsed with the mobile phase.

For the preparation of the polar monolithic stationary phase used in CD-modified CEC study (Monolith 5) the same procedure was employed but using N-isoporopylacrylamide instead of

the hydrophobic monomer (Tab. 1). The monoliths with varied molar fractions of vinylsulfonic acid were also prepared employing the same procedure but using different volumes of vinylsulfonic acid in the polymerization mixtures (Monoliths 6-14, Tab. 1). The monoliths with different total monomer concentrations (%T) (7.0, 10.0, 14.0, and 21.0, Monoliths 15-18) were prepared by using different volumes of buffer for the polymerization mixtures (Tab. 1). The monoliths with varied molar fractions of the hydrophobic monomer were prepared by replacing the hydrophobic monomer gradually by a hydrophilic monomer (methacrylamide) so that different monoliths with different masses of hydrophobic monomer in the polymerization mixture are prepared with the same total monomer concentration (%T) and percentage of crosslinker (%C) (see Tab. 2).

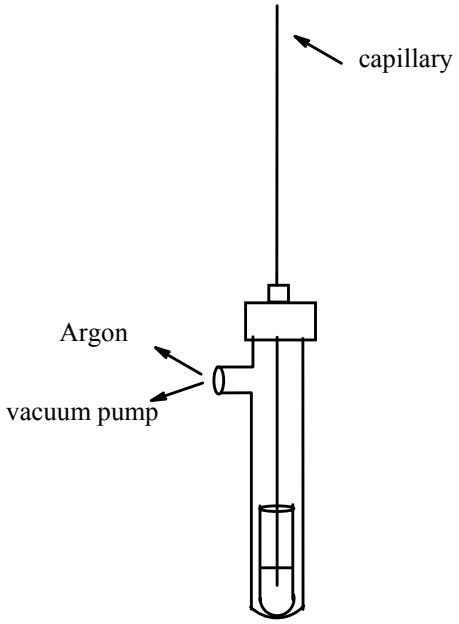

Fig. 8. The in-house manufactured capillary-filling apparatus.

Tab. 1. Composition of the polymerization mixtures of the monoliths employed during this work.

Monolith number	Hydrophobic monomer (50 mg)	Statistically methylated-β-CD (mg)	PDA (mg)	VSA (25% w/w), µL	Buffer volume (mL)	%T (w/v)
1	Isobornyl methacrylate	300	35	10	0.6	14.2
2	Adamantyl methacrylate	300	35	10	0.6	14.2
3	Cyclohexyl methacrylate	450	35	10	0.6	14.2
4	Phenyl methacrylate	450	35	10	0.6	14.2
5	N-isopropylacrylamide	/	35	10	0.6	14.2
6-9	Isobornyl methacrylate	300	35	[a]	0.6	14.2
10-14	Adamantyl methacrylate	300	35	[b]	0.6	14.2
15-18	Isobornyl methacrylate	300	35	10	[c]	[c]

Crosslinker concentration (%C): 41.2 (w/w)

Ammonium sulfate: 50 mg/mL,

APS (2.5% w/v): 10 µL

TEMED (2.5% w/v): 10 µL

[a] Different volumes of VSA (5, 10, 15, and 20 µL, 2.5% w/v) were added to the polymerization mixtures.

[b] Different volumes of VSA (1, 5, 10, 20, and 40 µL, 2.5% w/v) were added to the polymerization mixtures.

[c] Different volumes of buffer (1.20, 0.850, 0.600, and 0.472 mL) were used in the polymerization mixtures to obtain monoliths with various %T (7.0, 10.0, 14.0, and 21.0).

Tab. 2. Composition of the polymerization mixtures of the monoliths with different molar fraction of the hydrophobic monomer (in 0.6 mL buffer).

Monolith number	Hydrophobic monomer (mg)	Statistically methylated-β-CD (mg)*)	Statistically methylated-β-CD (mg)**)	MA (mg)	PDA (mg)
1, 2, 3, 4	50	300	450	0	35
19 a,b,c,d	40	240	360	10	35
20 a,b,c,d	30	180	270	20	35
21 a,b,c,d	20	120	180	30	35
22 a,b,c,d	10	60	90	40	35
23	0	0	0	50	35

*) For isobornyl and adamantyl methacrylate, **) For cyclohexyl and phenyl methacrylate
Total monomer concentration (%T):14.2 (w/v), Crosslinker concentration (%C): 41.2 (w/w)
Ammonium sulfate: 50 mg/mL, VSA (25% w/w): 10 µL
APS (2.5% w/v): 10 µL, TEMED (2.5% w/v): 10 µL
a,b,c,d refers to monoliths with isobornyl, adamantyl, cyclohexyl, and phenyl methacrylate, respectively.

3.3 CEC instrument

In essence, CE instruments can be employed for CEC measurements. The capillary holder is designed curved which may have an adverse effect on the monolithic material. Therefore, an inhouse-built CEC instrument was designed by Wahl et al. [91], in which the capillary remains straight (Fig. 9). This CEC apparatus was already described in [91] and consists of a Spellman CZE 1000R high-voltage generator (Plainview, NY, USA) with an in-house manufactured electronic steering unit for controlled electrokinetic injection, a Spectra 100 UV-VIS detector (Thermo Separation Products, San Jose, CA, USA) with detection cell for in-capillary detection, and a Shimadzu (Kyoto, Japan) LC-10 AD HPLC pump for conditioning of the separation capillary with new mobile phase under pressure. Data treatment and recording was with EZ-Chrom 6.6 (Scientific Software, San Ramon, CA, USA).

In this scheme, the outlet side of the capillary is attached with a T-fitting made of stainless steel acting as the cathode. The inlet side of the capillary is immersed into a vial with mobile phase, which can be also used for sample injection using another vial containing sample solution. Injection is performed electrokinetically where a voltage is applied between both

ends of the capillary solution for a specific time. To start the measurement, the sample vial is replaced with the mobile phase vial.

A high voltage source for separation is applied between the anodic platinum wire electrode immersed in the vial of mobile phase or sample solution, and the cathodic stainless steel T-fitting. For every new mobile phase, it is necessary that the voltage is increased slowly until the required voltage for chromatographic measurements is reached, otherwise bubbles might appear inside the capillary.

For a new measurement with a mobile phase, the capillary is conditioned with mobile phase for 20-30 minutes using an HPLC pump with 50-100 bar. The capillary can be easily washed with the mobile phase using the HPLC pump without the need to detach it from the CEC apparatus. For the measurements, the HPLC pump is switched off so that the external pressure has no effect on the separations.

The capillary is installed in the CEC instrument in such a way that the transparent section of the capillary matches the radiation course of the UV-visible detector. This in-capillary detection technique reduces the extra-column band broadening.

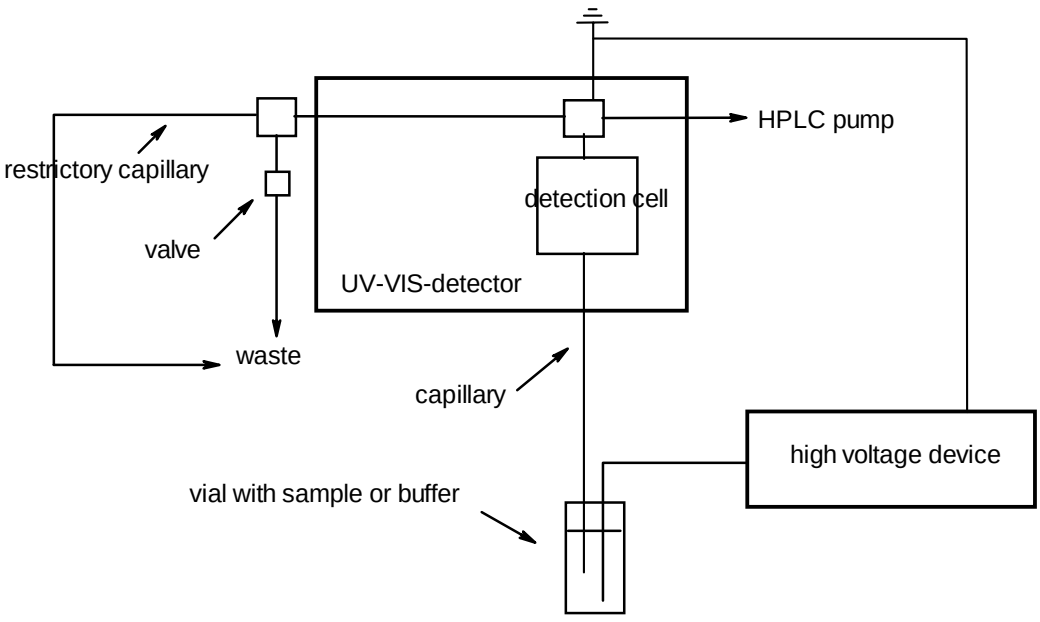

Fig. 9. Home-built CEC instrument used during this work.

3.4 Other instruments

CE and MEKC experiments were carried out on a P/ACE 2200 CE system (Beckman, Munich, Germany) with UV detector and Gold V810 software.

For the HPLC experiments, instrumentation with UV-VIS detector (L-4250, Merck-Hitachi, Darmstadt, Germany) and pump (L-6200 A, Merck-Hitachi) was used. A column (125 × 4 mm) packed with Kromasil 5 C18 (d_p = 5 µm) from Chromatographie Service GmbH (Germany) was used.

The µ-LC used was an Ultimate (Dionex, Idstein) equipped with a Famos autosampler (Dionex, Idstein) with UV detector (Dionex, Idstein).

HI 8817 pH meter (HANNA instruments, Kehl, Germany), and LF 191 conductometer (WTW, Weinheim, Germany) were used to measure the pH and the electric conductivity of the mobile phase.

^{1}H-NMR and ^{13}C NMR measurements (standard pulse sequence, mixing time 500 ms) were carried out on an ARX200 (Bruker, Karlsruhe, Germany). ^{1}H-NOESY spectra were recorded with a DRX600 spectrometer (Bruker, Karlsruhe, Germany).

3.5 Preparation of the mobile phases

Different water/methanol mobile phases buffered with 0.05% (3.5 mmol L^{-1}) triethylamine and 0.02% (3.6 mmol L^{-1}) acetic acid, apparent pH (pH*) = 6.5-7.0, electric conductivity = 120 µS/cm have been used for the reversed phase studies. pH* is the pH for a solution containing an organic solvent measured with a pH meter calibrated with aqueous standards. For the normal phase separations, different methanol/acetonitrile mobile phases, buffered with 0.01% triethylamine (0.7 mmol L^{-1}) and 0.06% acetic acid (10.8 mmol L^{-1}), pH* = 7.0-7.50, electric conductivity = 120-150 µS/cm have been used. In this work, triethylamine/acetic acid was used as buffer system since it has lower conductivity compared to other buffers like phosphate, acetate, or borate buffers. Higher electric conductivity leads to a high current strength and consequently high Joule heating which in turn affects adversely the chromatographic separation (radial temperature gradient induces band broadening).

Other mobile phases have been used during this work, which will be indicated in the individual experiments.

3.6 Analytes tested

Different categories of analytes were used in this work. Alkylphenones (acetophenone, propiophenone, butyrophenone, and valerophenone) were used as hydrophobic analytes. As hydrophilic analytes, different phenolic compounds (3-ethoxy-4-hydroxybenzaldehyde (ethylvanillin), 3-methoxy-4-hydroxybenzaldehyde (vanillin), 4-hydroxybenzaldehyde, and resorcinol) were used. Nitrotoluenes (4-nitrotoluene, 2,4-dinitrotoluene, and 2,4,6-trinitrotoluene), which have intermediate polarity between the phenones and the phenolic compounds were also used. Different alkylanilines (4-ethyl-, 4-propyl-, 4-butyl-, 4-pentyl-, and 4-hexylaniline), which have both hydrophobic (alkyl group) and hydrophilic (amino group) structure units were also used in this study. Fig. 10 shows the chemical structures of these analytes. These different groups of analytes differ in their charge. Alkylanilines can be positively charged, phenolic analytes can be negatively charged depending on the pH, while nitrotoluenes and phenones are neutral at any pH.

Different amino acids (L-phenylalanine, L-tryptophan, and L-histidine), several di- and tripeptides (Phe-Phe-Phe, Phe-Phe, H-Phe-Tyr-OH, H-Phe-Glu-OH, and H-Phe-Arg-OH) were also used for this study. Their characteristics and chemical structures are summarized in Tab. 3.

For CEC experiments, sample solutions (150-250 ppm) were prepared in the mobile phase. Sample injection was performed electrokinetically (6 kV for 3 seconds). UV detection was at a wavelength of 230 nm (213 nm for peptides). Dimethylformamide (DMF) was used as unretained EOF marker. The effective length of the capillary is 15 cm (inlet-to-detector, corresponding to a total length of 21 cm). For peptides, a solution of the analyte (5000 mg L^{-1}) were prepared in water, then diluted to 1000 mg L^{-1} in the mobile phase.

For HPLC and μ-LC experiments, sample solutions (150-250 ppm) were prepared in the mobile phase. UV detection was set at a wavelength of 230 nm. Dimethylformamide was used as marker of the hold-up time.

For MEKC experiments, sodium dodecylsulfate (SDS) was used as micelle-forming surfactant, thiourea was used as marker of the hold-up time, and quinine hydrochloride served as marker of the migration time of the micelles. Sodium borate buffer (10 mmol L^{-1}, pH 9.0) with 100 mmol L^{-1} SDS containing different concentrations of cyclodextrin was used as separation buffer. For MEKC as well as for CE, sample solutions (150-200 ppm) were prepared in the mobile phase. Sample injection was performed hydrodynamically (5 psi for 5

s). UV detection was at a wavelength of 214 nm. The effective length of the capillary is 20.4 cm (inlet-to-detector) corresponding to a total length of 28 cm.

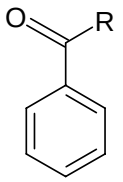

alkylphenones
R = CH_3: acetophenone
R = C_2H_5: propiophenone
R = C_3H_7: butyrophenoe
R = C_4H_9: valerophenone

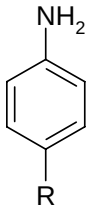

alkylanilines
R = C_2H_5: 4-ethylaniline
R = C_3H_7: 4-propylaniline
R = C_4H_9: 4-butylaniline
R = C_5H_{11}: 4-pentylaniline
R = C_6H_{13}: 4-hexylaniline

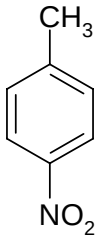

4-nitrotoluene

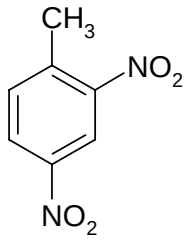

2,4-dinitrotoluene

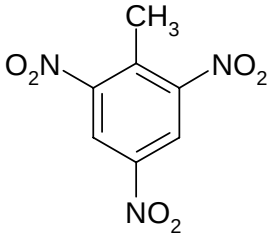

2,4,6-trinitrotoluene

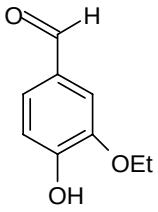

3-ethoxy-4-hydroxy benzaldehyde

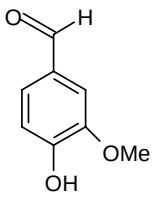

3-methoxy-4-hydroxy benzaldehyde

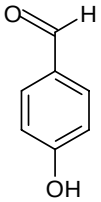

4-hydroxybenzaldehyde

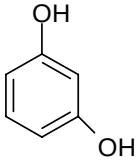

resorcinol

Fig. 10. Chemical structures of the analytes used.

Tab. 3. Chemical structures and isoelectric point values of the amino acids and peptides used in this study.

Name	Type	pI	Structure
L-phenylalanine (phe)	hydrophobic	5.49	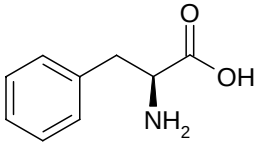
L-tryptophan (trp)	hydrophobic	5.89	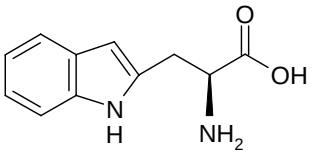
L-histidine (his)	basic	7.60	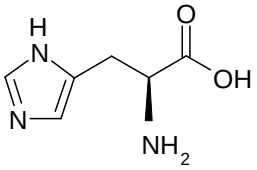
Phe-Phe	hydrophobic	5.49	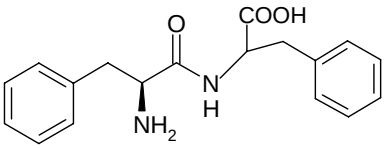
Phe-Phe-Phe	hydrophobic	5.49	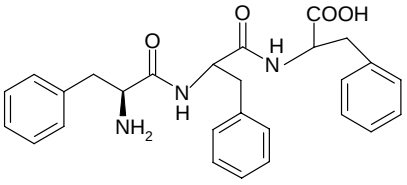
H-Phe-Tyr-OH	hydrophobic	5.57	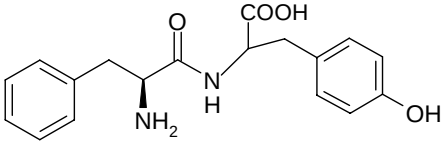
H-Phe-Arg-OH	basic	10.76	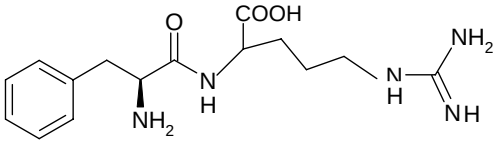
H-Phe-Glu-OH	acidic	3.15	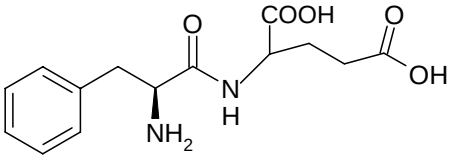

4 Results and Discussion

4.1 Selection of the hydrophobic monomers

Acrylamide-based monolithic stationary phases prepared from water-soluble monomers are hydrophilic, therefore, retention factors in reversed-phase chromatography are low. In order to increase the hydrophobicity of the organic monolith, more hydrophobic structure units are required, which have to be introduced by including more hydrophobic monomers into the polymerization mixture. Hence different monomers with hydrophobic groups: cyclohexyl methacrylate (C_6), dodecyl methacrylate (C_{12}), and octadecyl methacrylate (C_{18}) were selected. It is expected that monoliths prepared from these hydrophobic monomers in aqueous solution after solubilization via complexation with water-soluble cyclodextrins show higher hydrophobicity, and consequently higher retention factors in reversed-phase chromatography. However, a large molar ratio of cyclodextrin/monomer was needed to solubilize C_{12} and C_{18} in aqueous solution (molar ratio of 4 or 6 methylated-ß-cyclodextrin/monomer, respectively), while a molar ratio of only 1.15 methylated-ß-cyclodextrin/monomer is needed to dissolve cyclohexyl methacrylate. This poor solubility of C_{12} and C_{18} in aqueous solution using cyclodextrins limits the amount of these monomers that can be included in the polymerization mixture. The behavior of these two monomers can be explained by their low complex formation constant with cyclodextrins. For these reasons, these two monomers were excluded from those monomers suited for the synthesis of monolithic stationary phases.

These findings depict that monomers with cyclic groups like cyclohexyl methacrylate have a better solubility in aqueous solution with cyclodextrins, and presumably a higher complex formation constant compared to monomers with a linear alkyl chain, like C_{12} and C_{18}. Therefore for further studies, monomers with cyclic hydrophobic groups that can fit well in the cavity of ß-cyclodextrin were selected (like adamantyl, isobornyl, cyclohexyl, and phenyl groups). It is known in the literature that adamantane has a very large complex formation constant with ß-cyclodextrin [93] due to the near perfect size match between this group and the cavity of ß-cyclodextrin. Therefore, for further studies, following methacrylates were selected: adamantyl-, isobornyl-, cyclohexyl-, and phenyl methacrylate (Fig. 11). The numbers in these structures will be referred to in the discussion of ^{1}H NMR and ^{1}H NOESY spectra.

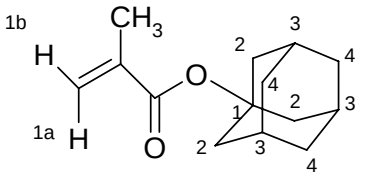

Adamantyl methacrylate

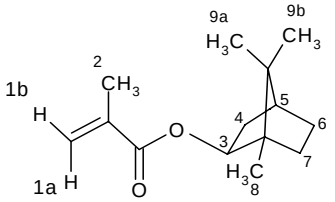

Isobornyl methacrylate

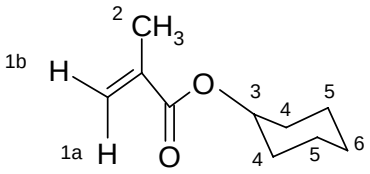

Cyclohexyl methacrylate

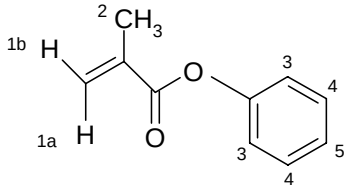

Phenyl methacrylate

Fig. 11. Chemical structure of methacrylate monomers used in this work.

4.2 Solubilization of the hydrophobic monomers by host-guest complexation

Polymerization of water-soluble acrylamides can be performed in aqueous solution. However, if hydrophobic monomers are to be included into the organic monolith, then mixtures of an aqueous buffer with an organic solvent have to be employed as porogenic liquid. Different monolithic stationary phases with different hydrophobic monomers were synthesized in organic solvents like isopropanol, formamide, N-methylformamide, or N,N-dimethylformamide or in a mixture of organic solvents with aqueous buffer [54].

In this study, polymerization of hydrophobic methacrylate monomers in aqueous media solubilized via host-guest complexation with water-soluble cyclodextrins was investigated. Polymerization with cyclodextrins as a readily solubilizing agent is an attractive alternative to polymerization in an organic solvent. If the acrylate group is not included into the cavity, the reactivity of the complexed acrylate is not reduced compared to the uncomplexed molecule [83].

The selected hydrophobic methacrylates were solubilized in water using different types of cyclodextrin (methylated-ß-CD, hydroxypropyl ß-CD, α-CD, and 2-hydroxypropyl γ-CD). These cyclodextrins were selected according to their solubility in water and their availability at low cost. In a first approach, the molar ratio CD/monomer which was needed for complete solubilization of the methacrylate was determined (Tab. 4). Different molar ratios were needed. For example, 154 mg of α-cyclodextrin, 202 mg of hydroxypropyl-γ-cyclodextrin, 155 mg of hydroxypropyl-ß-CD, and 120 mg of methylated ß-CD were needed to solubilize 20 mg of isobornyl methacrylate in 500 µL water. This corresponds to 1.73, 1.40, 1.10, and

1.0 CD/monomer molar ratio, respectively. Differences in this molar ratio can be attributed mainly to differences in the complex forming constant of the monomer/CD-complex. In order to verify this hypothesis, complex formation constants of the inclusion complexes were determined employing both capillary electromigration and spectroscopic methods, see sections 4.4 and 4.5.

Tab. 4. Molar ratios CD/monomer needed to solubilize a test portion (20 mg) of the hydrophobic methacrylate in 500 µL water.

Monomer	α-CD	Hydroxypropyl-ß-CD	Methylated ß-CD	2-hydroxypropyl-γ-CD
Adamantyl methacrylate	1.60	1.10	1.0	1.20
Isobornyl methacrylate	1.73	1.10	1.0	1.40
Cyclohexyl methacrylate	1.32	1.18	1.15	1.20
Phenyl methacrylate	1.33	1.25	1.15	1.18

4.3 Stoichiometry of the host-guest complexes

Complex stoichiometry of host-guest complexes can be determined from NMR data by means of the method of continuous variations (Job method) [94]. This method involves preparing a series of solutions containing both the host and guest in varying molar fractions so that a complete range of molar ratios is sampled, and where the total concentration of host and guest is constant for each solution. The experimentally observed parameter is a host or guest chemical shift that is sensitive to complex formation. In this method the concentration of the host-guest complex [HG] is equal to $(\Delta\delta/\Delta\delta_{max})[G]_0$ where $\Delta\delta/\Delta\delta_{max}$ is the degree of complexation; $\Delta\delta$ is the change in the chemical shift of a proton due to complex-formation, $\Delta\delta_{max}$ is the maximum chemical shift, and $[G]_0$ is the initial concentration of the guest i.e. $[HG] = (\Delta\delta/\Delta\delta_{max})[G]_0$. Therefore a plot of $\Delta\delta$ $[G]_0$ vs. mole fraction of the guest or host gives information about the stoichiometry of the formed host-guest complex [HG]. However, a plot of $\Delta\delta$ X_G vs. mole fraction is usually drawn since the total concentration of host and guest $([H]_0 + [G]_0)$ is constant for the solutions i.e. $X_G = [G]_0/\text{constant}$ or $[G]_0 = \text{constant} \cdot X_G$. The stoichiometry of the complex can be determined from the maximum of this plot where it is

1:1 when the maximum is at 0.5 while it is 1:2 (one guest to two hosts) or 2:1 (two guests to one host) when the maximum of the plot $\Delta\delta \cdot X_{guest}$ vs. X_{guest} is at 0.33 or 0.67, respectively.

Different solutions of host and guest monomers were prepared in deuterated methanol with different molar fraction of the guest (0.20, 0.30, 0.40, 0.50, 0.60, 0.80, and 1.0) where the total concentration of host and guest remains constant (0.02 mol L^{-1}). NMR spectra of these solutions showed range of chemical shift from 0.0032 to 0.0120 for adamantyl methacrylate, 0.0040 to 0.0070 for isobornyl methacrylate, 0.0013 to 0.0059 for cyclohexyl methacrylate, and 0.0012 to 0.0043 for phenyl methacrylate. Job plots for methacrylate/methylated-ß-cyclodextrin complexes show that their stoichiometry is 1:1 where the maximum of these plots is observed at around 0.5 (Fig. 12).

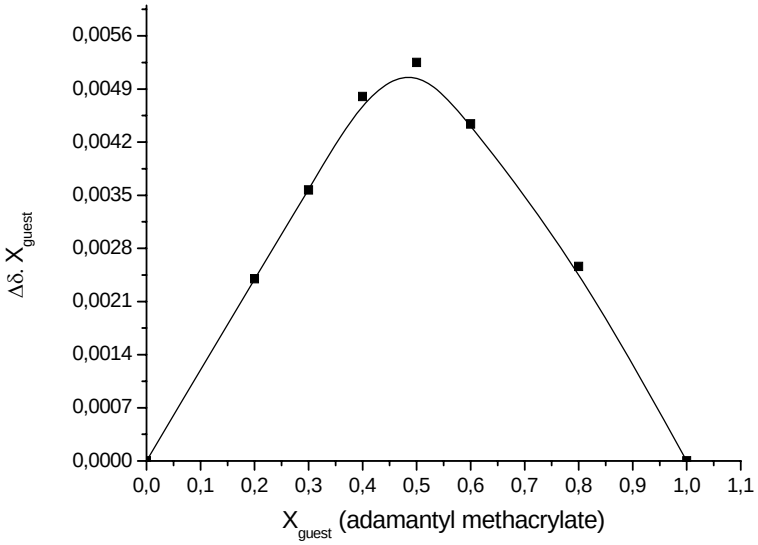

.

(a)

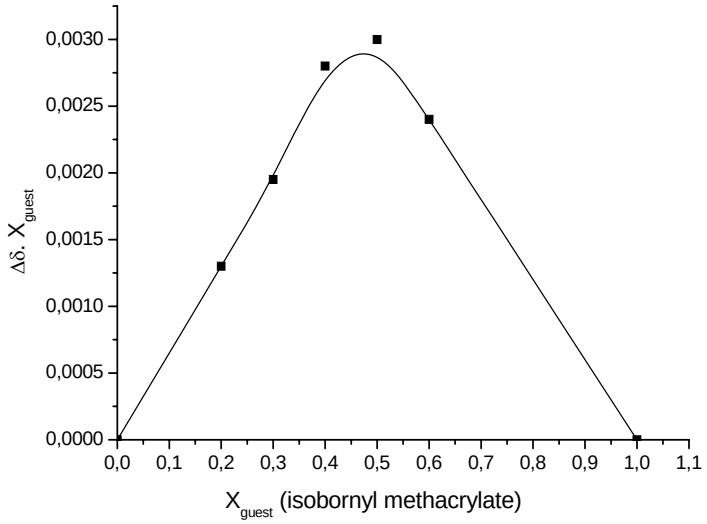

Fig 12. Continued on next page.

(b)

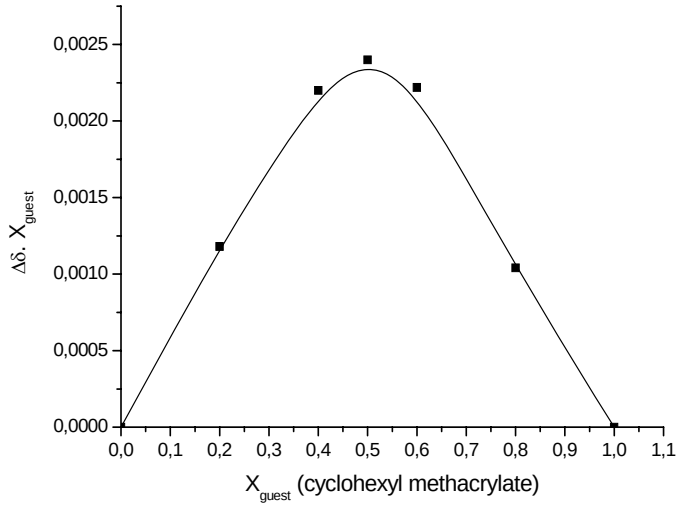

(c)

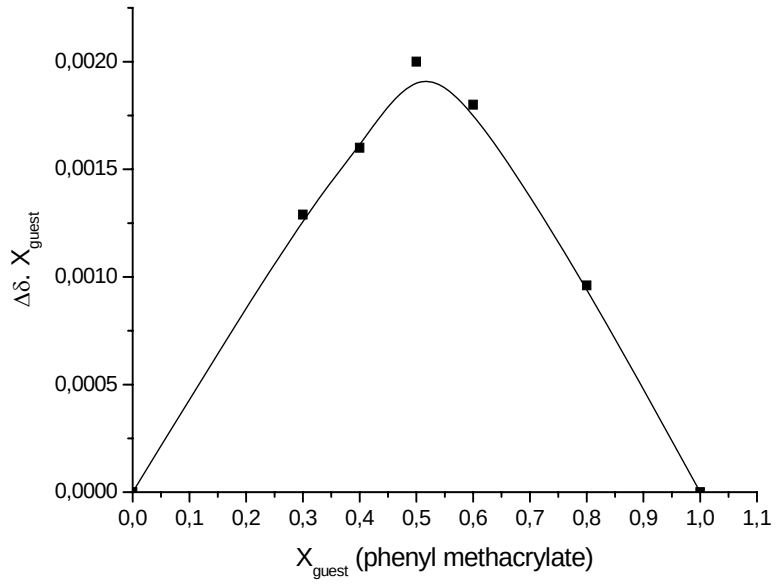

(d)

Fig. 12. Job plots for the methacrylate/methylated-ß-cyclodextrin complexes (a) adamantyl methacrylate (Proton 3) (b) isobornyl methacrylate (Proton 8) (c) cyclohexyl methacrylate (Proton 4) (d) phenyl methacrylate (Proton 3).

4.4 Selection of the best cyclodextrin as solubilizing agent

Cyclodextrin-modified MEKC was developed not only for chiral separations but also for the separation of highly hydrophobic solutes taking advantage of two coupled equilibria, (i) the distribution equilibrium between the micellar and the surrounding phase, and (ii) the complexation equilibrium between the solute and the added cyclodextrin [95]. Highly hydrophobic solutes are difficult to separate by MEKC owing to their extremely high micellar medium/aqueous medium distribution coefficients K_{distr}. In order to improve their separation, reduction of the retention factors is crucial. Addition of cyclodextrin to the separation buffer

results in a reduction of the observed retention factors k_{obs}. The observed retention factor is the ratio of the time spent by the analyte in the pseudostationary phase to the time spent in the surrounding aqueous phase. The observed retention factor therefore is reduced with increasing complex formation constant and with increased concentration of cyclodextrin.

The reduction in k_{obs} with increasing concentration of cyclodextrin was used to demonstrate complex formation of the selected monomers with the cyclodextrins studied and to select the best cyclodextrin as solubilizing agent for these hydrophobic methacrylates in further polymerization reactions. The larger the reduction of the observed retention factor (keeping constant the molar concentration of cyclodextrin) the stronger is the complex between the cyclodextrin and the methacrylate. The observed retention factor k_{obs} was calculated according to the following equation which was derived by Terabe and co-workers [95, 96].

$$k_{obs} = \frac{t_m - t_0}{t_0 \left(1 - \frac{t_m}{t_{mc}}\right)} \qquad (20)$$

where t_m is the migration time of the solute, t_0 is the migration time of a polar marker not interacting with the micelle, ($K_{distr} \rightarrow 0$), and t_{mc} is the migration time of a hydrophobic marker, with $K_{distr} \rightarrow \infty$. As a micelle-forming surfactant sodium dodecylsulfate (SDS) has been used with 100 mmol L^{-1} concentration. Thiourea has been used as polar marker, and quinine hydrochloride served as marker of the migration time of the micelle. It was assumed here that the neutral cyclodextrin does not interact with the bulky marker quinine hydrochloride.

As expected, the observed retention factors of the studied hydrophobic methacrylates were decreased by the addition of any of the cyclodextrins studied to the separation buffer (Tab. 5). The decrease in the observed retention factor is almost identical using a ß-CD or a γ-CD. However, the effect of α-CD is significantly lower. Adamantyl and isobornyl methacrylate had very high retention factors without the addition of a cyclodextrin to the separation buffer; they coelute with the micelle marker ($t_m = t_{mc}$). Addition of a ß-CD or a γ-CD to the separation buffer decreased their retention factors significantly, while their observed retention factors were not affected apparently by the addition of α-cyclodextrin to the separation buffer (Tab. 5). On the other hand the observed retention factors of phenyl or cyclohexyl methacrylate were decreased by the addition of α-cyclodextrin, however to a lower extent when compared to effect of the other cyclodextrins used in this study. These findings indicate that ß- and γ-CDs form stronger complexes with these monomers compared to α-CD. Therefore they are better solubilizing agents for these monomers (see Tab. 4). This

observation can be explained by the improved size match between the cavity of cyclodextrin and the guest. In further studies, only statistically methylated ß-CD was selected as host due to its low price availability and good water solubility.

Tab. 5. Cyclodextrin-modified MEKC, observed retention factors for the methacrylates investigated dependent on the concentration of selected cyclodextrins in the separation buffer (100 mmol L^{-1} SDS, 10 mmol L^{-1} $Na_2B_4O_7$, pH = 9.0), capillary 28.0 (20.4) cm × 50 µm; marker of the hold-up time: thiourea, marker of the migration time of the micelle: quinine hydrochloride.

Ligand	Ligand concentration/ mmol L^{-1}	adamantyl methacrylate	isobornyl methacrylate	cyclohexyl methacrylate	phenyl methacrylate
α-CD	0.0	$t_m = t_{mc}$	$t_m = t_{mc}$	43.3	10.9
	10.0	$t_m = t_{mc}$	$t_m = t_{mc}$	39.5	9.7
	30.0	$t_m = t_{mc}$	$t_m = t_{mc}$	34.2	7.8
	50.0	$t_m = t_{mc}$	$t_m = t_{mc}$	28.4	6.8
hydroxypropyl-β-CD	0.0	$t_m = t_{mc}$	$t_m = t_{mc}$	43.3	10.9
	10.0	37.5	$t_m = t_{mc}$	25.2	9.3
	30.0	3.3	30.6	7.4	3.6
	50.0	1.20	5.82	1.98	1.68
Methylated β-CD	0.0	$t_m = t_{mc}$	$t_m = t_{mc}$	43.3	10.9
	10.0	35.2	$t_m = t_{mc}$	24.2	8.2
	30.0	3.0	20.0	7.0	3.4
	50.0	1.07	3.60	1.92	1.64
hydroxypropyl-γ-CD	0.0	$t_m = t_{mc}$	$t_m = t_{mc}$	43.3	10.9
	10.0	38.0	$t_m = t_{mc}$	25.9	9.5
	30.0	4.0	31.2	8.1	4.0
	50.0	1.3	6.1	2.4	1.8

4.5 Determination of complex formation constants

4.5.1 Capillary electromigration methods

4.5.1.1 Cyclodextrin-modified MEKC

Cyclodextrin-modified MEKC was also used to determine the complex formation constant of the inclusion complexes. Estimation of complex formation constants by MEKC involves adding cyclodextrin to the aqueous buffer and measuring the change in the observed retention factor of an injected solute. In case of complexation with cyclodextrin, the observed retention factor (k*) of a solute is defined as,

$$k^* = \varphi\ K^* \tag{21}$$

where φ is the phase ratio, and K* is the apparent partitioning coefficient which is defined as,

$$K^* = \frac{c_s}{c_{aq} + c_{com}} \tag{22}$$

where c_s is the molar concentration of free solute in the stationary phase, c_{aq} is the molar concentration of free solute in the mobile phase, and c_{com} is the molar concentration of complexed solute in the mobile phase.

If the molar concentration of free cyclodextrin [CD] is assumed to be identical to the total concentration of cyclodextrin, complex formation constant B is defined by the following equation:

$$B = \frac{c_{com}}{c_{aq}[CD]} \tag{23}$$

Substitution of c_{com} in Eq. 22, followed by substitution of K* in Eq. 21 gives,

$$k^* = \frac{\varphi\ c_s}{(c_{aq} + B\ c_{aq}[CD])} \tag{24}$$

$$= k\ \frac{1}{1 + B[CD]} \tag{25}$$

where k is the retention factor in the absence of cyclodextrin ($k = \varphi\ c_s/c_{aq}$)

Rearrangement of this equation yields [97],

$$\frac{1}{k^*} = \frac{1}{k} + \frac{B}{k}[CD] \tag{26}$$

Then by plotting 1/k* against the concentration of cyclodextrin (y-reciprocal plot), the complex formation constant B of a solute with cyclodextrin can be determined (B = slope/y-

intercept) [97-98]. Advantage of this method is the possibility to determine complex formation constants of water-insoluble monomers in pure aqueous media. Also, high and low complex formation constants can be investigated by this method. However, in these studies in all cases a significant deviation of the y-reciprocal plot from linearity and a negative y-intercept were obtained, see Fig. 13 using adamantyl methacrylate as an example, resulting in physically non-interpretable values of the complex formation constant. In order to determine the possible sources of errors which lead to negative intercepts, the validity of the assumptions which were made in deriving the model have to be examined. Three assumptions were made: (i) EOF-marker and t_{mc} marker give true values, however, t_{mc} can be affected by the presence of cyclodextrin in the buffer due to complex formation between the cyclodextrin and the micelle marker. (ii) Phase ratio (ratio of volume of the micellar phase to the volume of the aqueous mobile phase) is not altered by the addition of a CD to the separation electrolyte, however, complex formation between the cyclodextrin and the surfactant monomer can reduce the volume of pseudo-stationary phase which in turn affects the phase ratio. (iii) Concentration of free cyclodextrin is equal to the total concentration of cyclodextrin.

The effect of dissolved cyclodextrin on the critical micellar concentration (CMC) can be used to ascertain whether complex formation between the cyclodextrin and the surfactant monomer plays a significant role. Nair et al. [99] observed that the CMC of SDS was increased almost linearly with the concentration of hydroxylpropyl-ß-cyclodextrin dissolved in 0.05 mol L^{-1} phosphate buffer, pH 7.0. For example, they observed that the CMC for SDS was 3.8 mmol L^{-1} at 3 mmol L^{-1} of hydroxypropyl-ß-cyclodextrin, while it was 45.9 mmol L^{-1} at 50 mmol L^{-1} of this cyclodextrin. These measurements confirm that interactions of the surfactant monomer with the dissolved CD cannot be neglected and can be assumed to be the major reason for the observed nonlinearity and consequently the negative y-intercept.

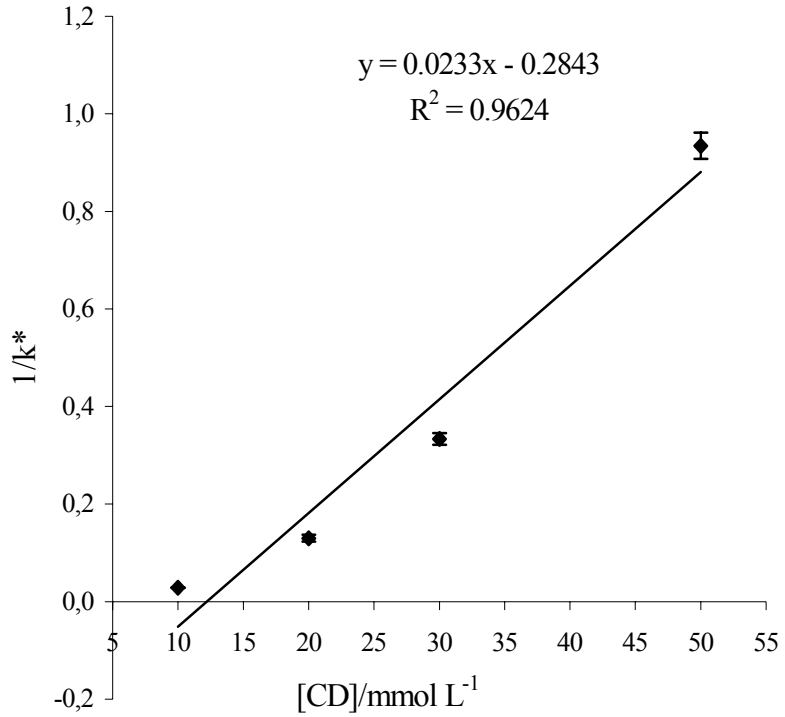

Fig. 13. Cyclodextrin-modified MEKC, 1/k* for adamantyl methacrylate vs. concentration of methylated ß-cyclodextrin present in the separation buffer (100 mmol L^{-1} SDS, 10 mmol L^{-1} $Na_2B_4O_7$, pH=9.0). Each data point is the mean of triplicate measurements, error bar = standard deviation.

4.5.1.2 Cyclodextrin-modified CEC

Interfering complex formation between the cyclodextrin and the surfactant monomer which caused the negative y-intercept in the plot of 1/k* vs. concentration of cyclodextrin in cyclodextrin-modified MEKC led us to use another method of capillary electromigration techniques which does not employ a micellar pseudo-stationary phase. Capillary electrochromatography (CEC) employs a true stationary phase. Therefore the unwanted interactions described in the previous section can be eliminated. Cyclodextrin-modified CEC was employed as a method to study the inclusion complexes of methylated ß-CD with methacrylate guests and to determine their complex formation constants. A very polar polymeric stationary phase was used for the CEC experiments by using N-isopropylacrylamide as monomer in the polymerization mixture (for polymerization conditions, see Tab. 1) in order to avoid possible interactions of cyclodextrin present in the mobile phase with the hydrophobic groups of the stationary phase.

In a first step, alkylphenones (acetophenone, propiophenone, butyrophenone, and valerophenone) were used to test the applicability of this method for the determination of

complex formation constants using Eq. 26. As expected, the observed retention factors for these alkylphenones are decreased with increasing concentration of methylated ß-cyclodextrin indicating host-guest complex formation (Tab. 6). The plot of 1/k* vs. concentration of cyclodextrin is linear with positive y-intercept (Fig. 14) which indicates that with this method the determination of complex formation constants is possible. The observed retention factors for the methacrylates studied are also decreased with increasing concentration of methylated ß-cyclodextrin in the mobile phase (Tab. 7). The decrease in the retention factor is higher for cyclohexyl than for phenyl methacrylate (which is consistent with the results obtained from CD-modified MEKC). With increasing the concentration of CD to 20 mmol L^{-1}, cyclohexyl methacrylate is eluted in front of the unretained EOF marker DMF which can be ascribed to size-exclusion effects. The observed retention factors for adamantyl and isobornyl methacrylate are also decreased with increasing concentration of cyclodextrin but to a higher extent compared to phenyl or cyclohexyl methacrylate. At a very low concentration of the cyclodextrin (1 mmol L^{-1}) there is already elution of the acrylate zone in front of the unretained EOF marker DMF. Therefore, this method was not suited to determine complex formation constants for adamantyl and isobornyl methacrylate. Plotting of 1/k* vs. concentration of cyclodextrin gave a linear relationship with positive y-intercept for phenyl methacrylate (Fig. 15). Each data point represents the average of triplicate measurements, the standard deviation is shown as error bar. In all cases $r^2 \geq 0.98$. For the calculation of the complex formation constant for cyclohexyl methacrylate only two data points were available.

Complex formation constants were calculated for phenyl and cyclohexyl methacrylate (B = slope/y-intercept), (Tab. 8). The standard error of the complex formation constant ΔB was calculated from the standard error of the slope Δb and of the y-intercept Δa according to the error propagation law ($\mathrm{V}B = B\sqrt{(\frac{\mathrm{V}b}{b})^2 + (\frac{\mathrm{V}a}{a})^2}$, where b and a are the slope and the y-intercept). ΔB increases with increasing complex formation constant since the deviation from the linearity for the function (1/k* = f [CD]) increases due to more pronounced size exclusion effects. For the alkylphenones the complex formation constant increases with increasing alkyl chain length. Furthermore, the complex formation constant is higher for cyclohexyl methacrylate than for phenyl methacrylate which can be ascribed to differences in the hydrophobicity of the guest molecule.

As shown in Figs. 14-15, for all compounds investigated a linear dependence of 1/k* on the concentration of cyclodextrin in the mobile phase is observed, clearly indicating the formation

of host-guest complexes with a 1:1 stoichiometry [100-101]. This observation corroborates results obtained in Section 4.3.

Tab. 6. Cyclodextrin-modified CEC, observed retention factors for selected alkylphenones dependent on the concentration of methylated ß-cyclodextrin. Mobile phase: methanol/water (30:70, v/v) buffered with triethylamine/acetic acid, pH* = 7.0, electric conductivity = 120 µS cm^{-1}.

[cyclodextrin], mmol L^{-1}	Acetophenone	Propiophenone	Butyrophenone	Valerophenone
0.0	0.31	0.42	0.56	0.88
10.0	0.19	0.22	0.18	0.18
20.0	0.13	0.14	0.10	0.09
30.0	0.11	0.093	0.073	0.068
50.0	0.07	0.00	0.0	0.0

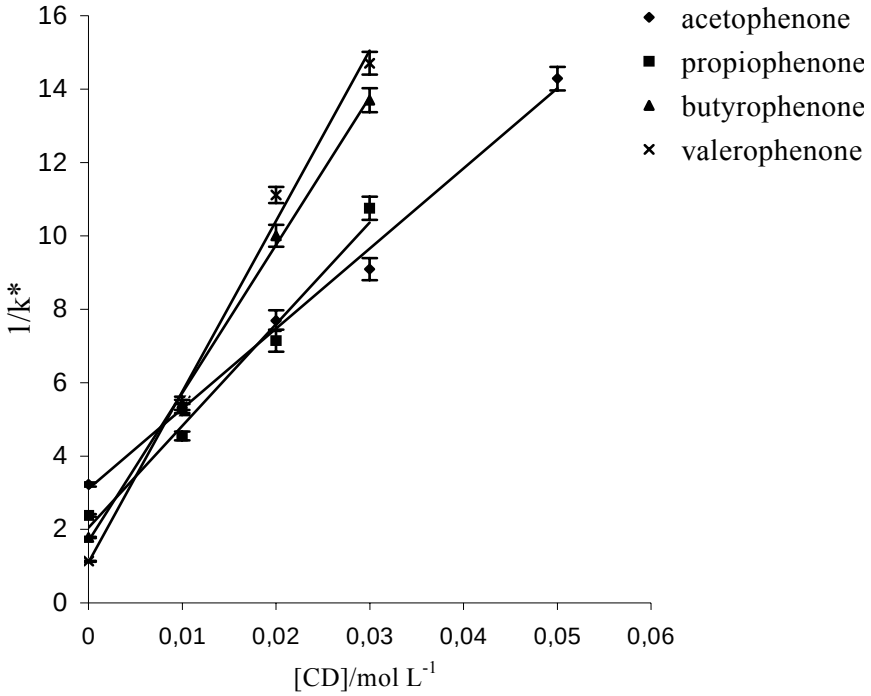

Fig. 14. Cyclodextrin-modified CEC, 1/k* for alkylphenones vs. concentration of methylated ß-cyclodextrin present in the mobile phase (methanol/water, 30:70, v/v) buffered with triethylamine/acetic acid, pH* = 7.0, electric conductivity = 120 µS cm^{-1}. Each data point is the mean of triplicate measurements, error bar = standard deviation.

Tab. 7. Cyclodextrin-modified CEC, observed retention factors for phenyl- and cyclohexyl methacrylate dependent on the concentration of methylated ß-cyclodextrin. Mobile phase: methanol/water (30:70, v/v) buffered with triethylamine/acetic acid, pH* = 7.0, electric conductivity = 120 µS cm^{-1}.

[cyclodextrin], mmol L^{-1}	Phenyl methacrylate	Cyclohexyl methacrylate
0.0	0.62	0.81
1.0	0.51	0.23
5.0	0.28	0.0
10.0	0.17	0.0
20.0	0.083	[a]
30.0	0.047	[a]
50.0	0.0	[a]

[a] Retention factor not accessible due to size-exclusion effects.

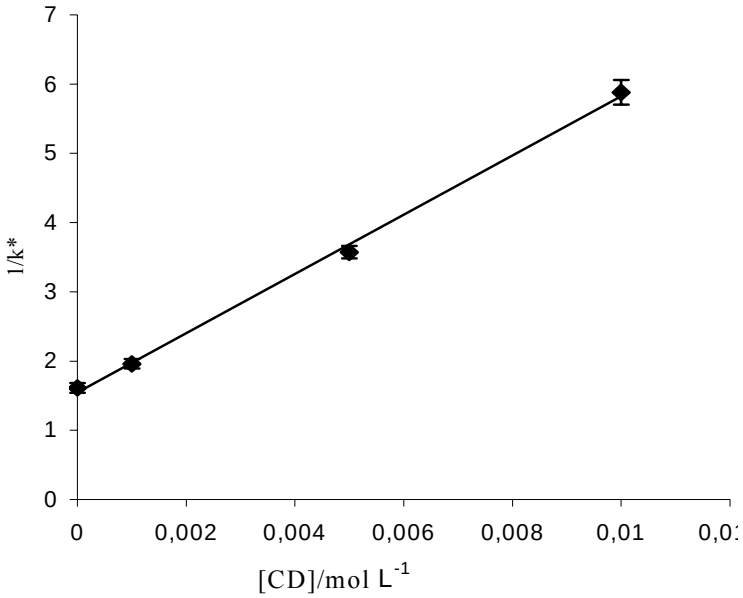

Fig. 15. Cyclodextrin-modified CEC, 1/k* for phenyl methacrylate vs. concentration of methylated ß-cyclodextrin present in the mobile phase (methanol/water, 30:70, v/v) buffered with triethylamine/acetic acid, pH* = 7.0, electric conductivity = 120 µS cm^{-1}. Each data point is the mean of triplicate measurements, error bar = standard deviation.

Tab. 8. Complex formation constants of methylated ß-cyclodextrin/solute complexes determined by cyclodextrin-modified CEC. Mobile phase: methanol/water (30:70, v/v) buffered with triethylamine/acetic acid, pH* = 7.0, electric conductivity = 120 µS cm^{-1}.

Solute	Complex formation constant (± ΔB)
Acetophenone	70 ± 7
Propiophenone	140 ± 33
Butyrophenone	240 ± 37
Valerophenone	420 ± 70
Phenyl methacrylate	930 ± 250
Cyclohexyl methacrylate	2500[a)]

[a)] standard error can not be calculated (only two data points).

4.5.2 Spectroscopic methods

NMR spectroscopy has become one of the most important methods for structural elucidation of biomolecules and organic compounds in solution. The NMR parameters such as chemical shift, nuclear overhauser effect (NOE) are sensitive to short range intermolecular interactions like the inclusion complex formation between cyclodextrin and guest molecules. This method is capable of yielding atomic-level information, which can be used to improve the understanding of cyclodextrin-guest interactions [102]. NMR spectroscopic methods were used to determine the complex formation constant for the host-guest complexes (^{1}H NMR) and to study spatial relationships of cyclodextrin-guest interactions (^{1}H NOESY).

4.5.2.1 ^{1}H NMR chemical shift analysis

^{1}H NMR chemical shift analysis was used to determine the large complex formation constants for adamantyl and isobornyl methacrylate which could not be determined by CEC. This method depends on the change in the chemical shift of the guest (or the host) protons due to complex formation. Only complexes which induce large chemical shift changes can be investigated using this method.

This method was used to determine complex formation constants by measuring the chemical shift changes of the monomer protons (complexation-induced chemical shift CIS) as a function of the cyclodextrin concentration. For a host-guest complex HG,

$$H + G \underset{B_D}{\overset{B}{\rightleftharpoons}} HG \qquad (27)$$

According to the mass action law, the following equations are valid for complex formation constant (B) and complex dissociation constant (B_D)

$$B = \frac{[HG]}{[H][G]} \qquad (28) \qquad B_D = \frac{[H][G]}{[HG]} \qquad (29)$$

where [H] = [CD], [G] = c_{aq} and [HG] = c_{com}, (H, G, and HG were used in this section since these symbols are usually employed in the literature).

For the formation of a 1:1 complex, the initial concentration of host and guest ($[H]_0$ and $[G]_0$) which are known from the preparation of the measured solutions can be expressed as,

$$[H]_0 = [H] + [HG] \qquad (30)$$

$$[G]_0 = [G] + [HG] \qquad (31)$$

Substitution of the value of [H] and [G] in Eq. 29 yields,

$$B_D = \frac{([H]_0 - [HG])([G]_0 - [HG])}{[HG]}$$

$$= \frac{[H]_0[G]_0 - [H]_0[HG] - [G]_0[HG] + [HG]^2}{[HG]} \qquad (32)$$

Transformation of Eq. 32 gives,

$$0 = [HG]^2 + [H]_0[G]_0 - [H]_0[HG] - [G]_0[HG] - B_D[HG]$$

$$= [HG]^2 - ([H]_0 + [G]_0 + B_D)[HG] + [H]_0[G]_0 \qquad (33)$$

The solution of this quadratic equation (Eq. 34) shows that the exact concentration of the complex can be determined when the dissociation constant B_D and the initial concentration of the host and guest are known,

$$[HG] = \frac{1}{2}\left[[H]_0 + [G]_0 + B_D - \sqrt{(B_D + [H]_0 + [G]_0)^2 - 4[H]_0[G]_0}\right] \qquad (34)$$

The molar ratio of host to guest (n(host)/n(guest)) was varied. The NMR spectrum of the mixture depends on complex formation constant B and on the rate of the reaction. The rate of reaction is fast on the NMR time scale and only a time averaged spectrum of the guest (or host) and the host-guest complex is observed [94]. Therefore an observed chemical shift δ_{obs} is obtained which is the weighted average of the chemical shift for the free guest δ_G and the chemical shift of the complexed guest δ_{HG} :

$$\delta_{obs} = X_G\,\delta_G + X_{HG}\,\delta_{HG} \qquad (35)$$

Where X_G, and X_{HG} are the molar fractions of the guest and the complex in equilibrium, which can be expressed as,

$$X_G = \frac{[G]}{[G]+[HG]}, \quad X_{HG} = \frac{[HG]}{[G]+[HG]} \tag{36}$$

Substitution of X_G, and X_{HG} in Eq. 35 yields,

$$\delta_{obs} = \frac{[G]}{[G]_0}\delta_G + \frac{[HG]}{[G]_0}\delta_{HG} \tag{37}$$

Substitution value of [G] in Eq. 37, followed by some transformations gives,

$$\delta_{obs} = \frac{[G]_0 - [HG]}{[G]_0}\delta_G + \frac{[HG]}{[G]_0}\delta_{HG}$$

$$= (1 - \frac{[HG]}{[G]_0})\delta_G + \frac{[HG]}{[G]_0}\delta_{HG}$$

$$= \delta_G - \frac{[HG]}{[G]_0}\delta_G + \frac{[HG]}{[G]_0}\delta_{HG}$$

$$= \delta_G + \frac{[HG]}{[G]_0}(\delta_{HG} - \delta_G) \tag{38}$$

The maximum chemical shift $\Delta\delta_{max}$ of a proton is the chemical shift of the guest proton in the host-guest complex minus the chemical shift of the guest proton,

$$\Delta\delta_{max} = \delta_{HG} - \delta_G \tag{39}$$

Substitution of $\Delta\delta_{max}$ in Eq. 38 gives,

$$\delta_{obs} = \delta_G + \frac{[HG]}{[G]_0}\Delta\delta_{max} \tag{40}$$

By substitution of Eq. 34 in Eq. 40 and substitution of B_D into 1/B gives,

$$\delta_{obs} = \delta_G + \frac{\Delta\delta_{max}}{[G]_0}\frac{1}{2}\left[[H]_0 + [G]_0 + \frac{1}{B} - \sqrt{(\frac{1}{B} + [H]_0 + [G]_0)^2 - 4[H]_0[G]_0}\right] \tag{41}$$

The values of $[G]_0$ and $[H]_0$ as well as the chemical shift change of guest (δ_G) are known. The observed chemical shift (δ_{obs}) is also known from ^{1}H NMR experiments. The change in the chemical shift ($\Delta\delta$) can be determined from the difference between δ_{obs} and δ_G,

$$\Delta\delta = \left|\delta_{obs} - \delta_G\right| \tag{42}$$

Using this relationship, Eq. 41 is transformed into,

$$\Delta\delta = \frac{\Delta\delta_{max}}{[G]_0}\frac{1}{2}\left[[H]_0 + [G]_0 + \frac{1}{B} - \sqrt{(\frac{1}{B} + [H]_0 + [G]_0)^2 - 4[H]_0[G]_0}\right] \tag{43}$$

The values of $[H]_0$ and $[G]_0$ are known, also $\Delta\delta$ is known from the ^{1}H NMR spectra. Complex formation constant B and $\Delta\delta_{max}$ can be obtained from a nonlinear regression of a plot of $\Delta\delta$ vs. the total concentration of the host $[H]_o$ using Sigmaplot software (Jandel Corporation, San

Rafael, CA, USA). The iteration parameters B and $\Delta\delta_{max}$ are varied until the sum of the squares of the deviations between $\Delta\delta^r$ (value obtained from the regression line) and the measured value of $\Delta\delta$ from the ^{1}H NMR experiments is minimum. The goodness of the calculated value of complex formation constant can be checked from the comparison of the approximated value of $\Delta\delta_{max}$ from the Sigmaplot with the measured $\Delta\delta$ in the plateau region (from ^{1}H NMR experiments).

In this study, different solutions of methacrylate with different molar ratios of methylated β-cyclodextrin were prepared in deuterated methanol (100%) and aqueous deuterated methanol (70% CD_3OD, 30% D_2O). The monomers studied are not soluble in pure water, but they are soluble in a mixture of water and methanol (30:70, v/v). Both solutions in pure methanol and in water/methanol were used to study the impact of the solvent composition on the complex formation constant. ^{1}H NMR spectra were recorded and the chemical shift change (Tabs. 9-12) of a selected monomer proton was plotted against the concentration of cyclodextrin (Fig. 16). Complex formation constants were calculated by nonlinear regression of the shifts (Tab. 13). Standard error was calculated from the regression curve. The chemical shift for the protons of phenyl methacrylate was not significantly changed with the addition of cyclodextrin indicating low complex formation constant with cyclodextrin, therefore its complex formation constant could not be determined by this method. However, the chemical shift for several protons of the other methacrylates was changed with increasing the concentration of cyclodextrin indicating host-guest complexation. Adamantyl methacrylate shows the highest chemical shift change compared to other monomers. The change in the chemical shift was larger for the hydrophobic group protons of the monomers than for the protons of the methacrylate group which shows that the hydrophobic group interacts with the cyclodextrin cavity.

The calculated complex formation constants are given in Tab. 13. The highest value was obtained for adamantyl methacrylate (average of three values obtained for three different protons). Isobornyl and cyclohexyl methacrylate show significantly lower complex formation constants. This observation is consistent with a near-perfect size match between the cavity of ß-CD and the adamantyl group [103]. The comparison with results from CD-modified CEC shows that the complex formation constants for different methacrylates with statistically methylated ß-CD can be brought in the order adamantyl methacrylate > isobornyl methacrylate > cyclohexyl methacrylate > phenyl methacrylate.

The methacrylates studied have a higher complex formation constant in aqueous methanol compared to pure methanol (Tab. 13) showing that solvophobic interactions play a dominant role in host-guest complex formation [104]. Additionally, the complex formation constant of cyclohexyl methacrylate determined by the CEC method in water/methanol (70:30, v/v) is much higher than the complex formation constant determined by NMR method in water/methanol (30:70, v/v) (see Tabs. 8, 13). As known, host-guest complex formation constants in methanol/water mixtures are largely dependent on the volume fraction of water. The higher is the volume fraction of water, the higher will be the complex formation constant. The difference in the solvent composition explains the large difference between the value obtained by using the CEC method to the value obtained by using the ^{1}H NMR chemical shift analysis method. Results are in accordance with the assumption that solvophobic interactions are a major driving force for host-guest complex formation.

Tab. 9. ^{1}H NMR changes in the chemical shift ($\Delta\delta$, in ppm) of H_2, H_4, and H_3 for adamantyl methacrylate due to complexation with methylated –ß-CD in 70% CD_3OD.

[methylated-ß-CD], mol L^{-1}	$\Delta\delta$ for H_2	$\Delta\delta$ for H_4	$\Delta\delta$ for H_3
0.0	0.0	0.0	0.0
0.0016	0.018	0.010	0.016
0.0032	0.036	0.018	0.080
0.0063	0.065	0.034	0.148
0.0084	0.077	0.041	0.173
0.0110	0.094	0.048	0.195
0.0210	0.114	0.050	0.219
0.0320	0.117	0.051	0.220

Tab. 10. ^{1}H NMR changes in the chemical shift ($\Delta\delta$, in ppm) of H_{9b} for isobornyl methacrylate due to complexation with methylated –ß-CD in 70% CD_3OD.

[methylated-ß-CD], mol L^{-1}	$\Delta\delta$ for H_{9b}
0.0	0.0
0.00289	0.0237
0.00578	0.0550
0.00964	0.0925
0.0193	0.1400
0.0482	0.1987
0.0675	0.2000

Tab. 11. ^{1}H NMR changes in the chemical shift ($\Delta\delta$, in ppm) of H_4 for cyclohexyl methacrylate due to complexation with methylated –ß-CD in 70% CD_3OD.

[methylated-ß-CD], mol L^{-1}	$\Delta\delta$ for H_4
0.0	0.0
0.00387	0.013
0.00774	0.0163
0.0129	0.020
0.0645	0.042
0.0903	0.050
0.129	0.051

Tab. 12. ^{1}H NMR changes in the chemical shift ($\Delta\delta$, in ppm) of H_4 for phenyl methacrylate due to complexation with methylated –ß-CD in 70% CD_3OD.

[methylated-ß-CD], mol L^{-1}	$\Delta\delta$ for H_4
0.0	0.0
0.00396	0.0038
0.00792	0.0075
0.0132	0.0113
0.0264	0.0175
0.0396	0.0188
0.0660	0.0200
0.0924	0.0210

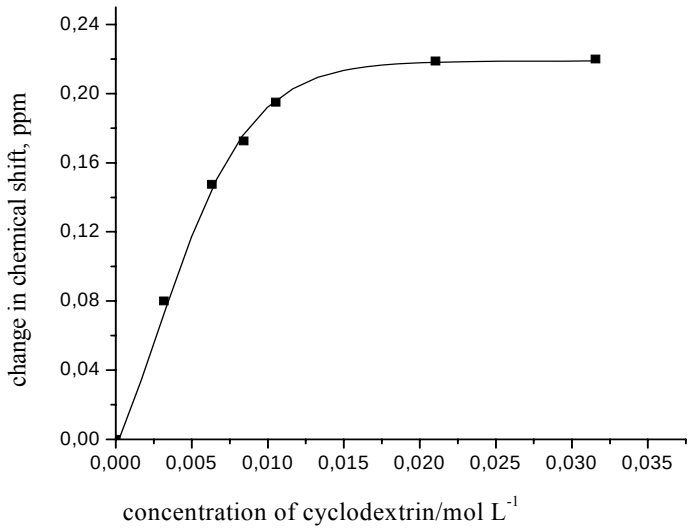

Fig. 16: Change of the chemical shift for H_3 of adamantyl methacrylate monomer (0.014 mol L^{-1}) vs. concentration of methylated ß-cyclodextrin.

Tab. 13. ^{1}H NMR chemical shift analysis, complex formation constants of methylated ß-cyclodextrin/methacrylate complexes determined in CD_3OD and in CD_3OD/D_2O (70:30, v/v).

Monomer	proton	100% CD_3OD	70% CD_3OD
adamantyl methacrylate	H_3	320 ± 90	7360 ± 900
	H_4	300 ± 70	7370 ± 700
	H_2	330 ± 80	7320 ± 800
isobornyl methacrylate	H_{9b}	19 ± 1	97± 15
cyclohexyl methacrylate	H_4	17 ± 1	80 ± 10
phenyl methacrylate	/	(-)[a]	(-)[a]

a) determination not possible

4.5.2.2 ^{1}H NOESY spectra

Two-dimensional NMR experiments like ^{1}H NOESY are performed to investigate the spatial relationships between atoms in host-guest complexes. The intra- and intermolecular nuclear overhauser effect (NOE) takes place through space. This is a result of dipolar interactions of a nucleus with further nucleus spins which depends on the internuclear distance. NOEs can be normally observed only if the nuclei are within 5 Å of each other. The method was improved

by the introduction of 2D-NOE correlated spectroscopy (NOESY) and the first ^{1}H NOESY spectrum of the inclusion complex between α-cyclodextrin and p-nitrophenol was recorded by Yamamato et al. in 1987 [105]. ^{1}H NOESY cross peaks between two nuclei provide evidence that the nuclei are (time averaged) within 5 Å of each other. Consequently, ^{1}H NOESY provides structural information about the formed complex.

^{1}H NOESY spectra for the host-guest complexes were recorded (with 1:1 CD/monomer molar ratio for adamantyl methacrylate or isobornyl methacrylate, and 1.15:1 molar ratio for cyclohexyl or phenyl methacrylate monomers) in 1 mL of deuterated water. The ^{1}H NOESY spectrum of methylated ß-cyclodextrin/adamantyl methacrylate displays clear and strong NOE cross-peaks between the protons of the adamantyl group (H_2-H_4) and the protons of the cyclodextrin cavity (H_3, H_5). This spectrum also showed weaker cross-peaks for H_a, H_b protons of this monomer and the cyclodextrin cavity (Fig. 17a), which indicates that the mobility of the guest monomer is high. Furthermore, ^{1}H NOESY spectra of the isobornyl methacrylate and the cyclohexyl methacrylate cyclodextrin complexes (Fig. 17b, 17c) show cross peaks between the protons of the cyclodextrin cavity (H_3, H_5) and the protons of the hydrophobic group of the monomer (isobornyl or cyclohexyl group). The ^{1}H NOESY spectrum of the phenyl methacrylate cyclodextrin complex (Fig. 17d) displayed much weaker cross peaks compared to the other complexes. These findings are in accordance with the results obtained from the chemical shift analysis which show that the hydrophobic part of the guest monomer is embedded into the cavity of the cyclodextrin.

(a)

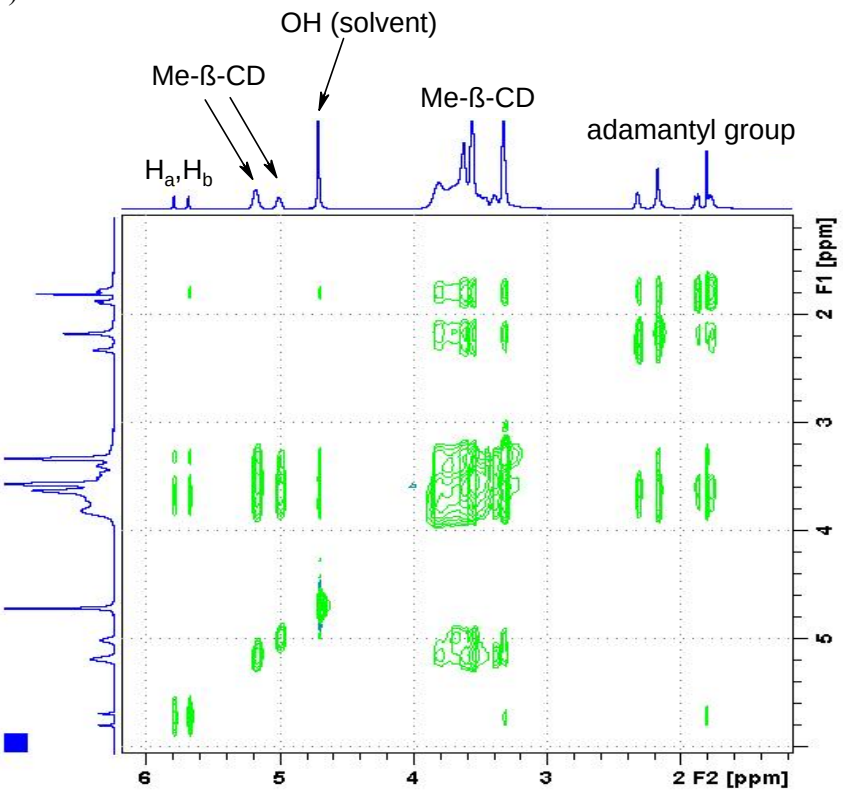

(b)

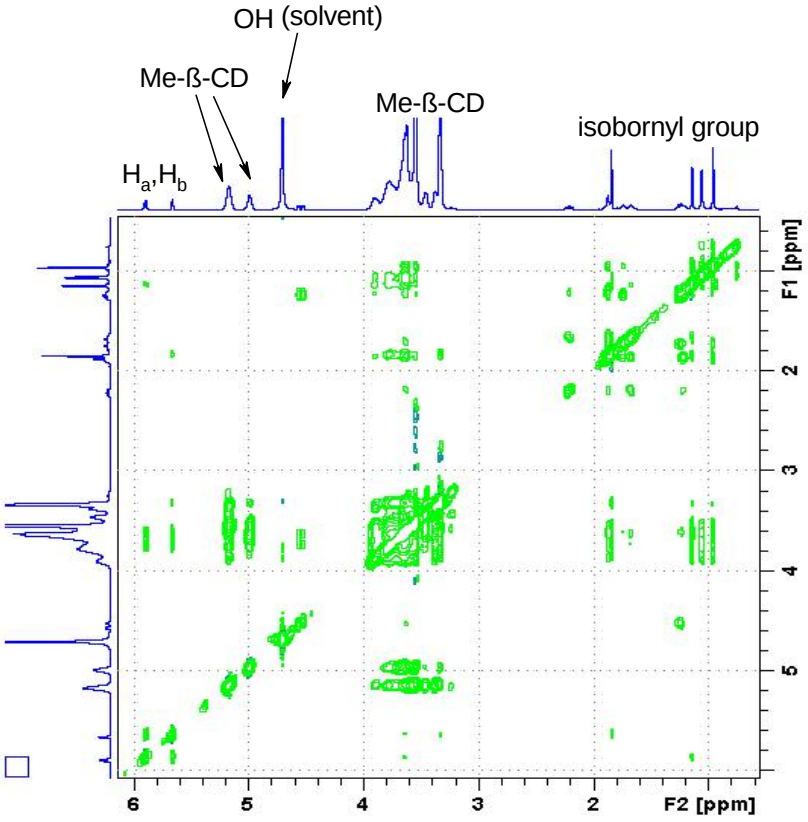

Fig 17a-d. Continued on next page.

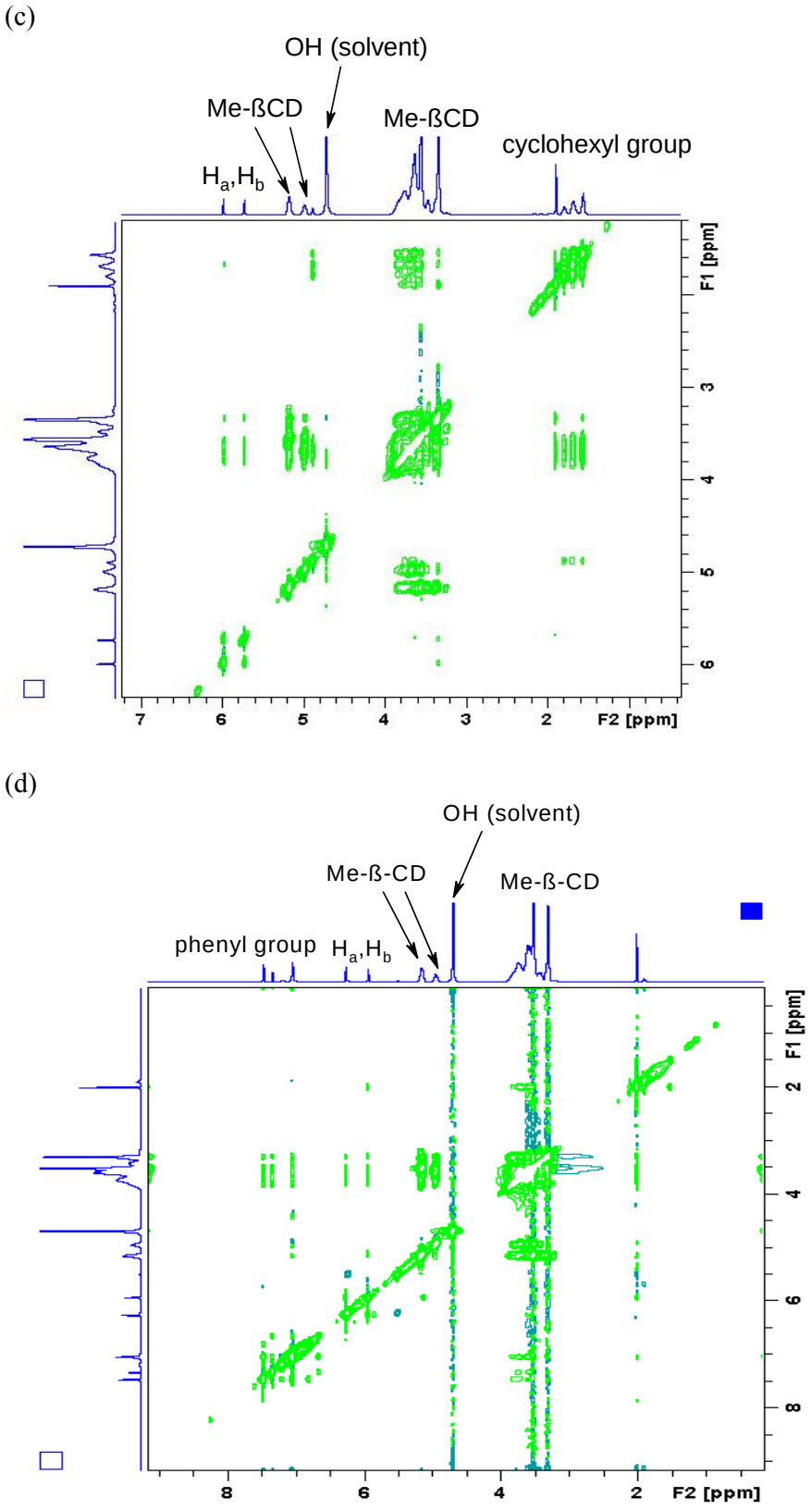

Fig. 17a-d. ^{1}H NOESY spectra of methacrylate/methylated ß-cyclodextrin complexes in D_2O (mixing time 500 ms, 600 MHz), (a) adamantyl methacrylate (b) isobornyl methacrylate (c) cyclohexyl methacrylate (d) phenyl methacrylate.

4.6 Monolith synthesis

Highly crosslinked, macroporous polymeric monoliths for CEC separation were synthesized with different hydrophobic and hydrophilic structure units (mixed-mode monoliths) by polymerization of one hydrophobic monomer e.g. adamantyl methacrylate, a crosslinker e.g. piperazinediacrylamide (PDA), and a negatively charged monomer e.g. vinylsulfonic acid (VSA). Methylacrylamide (MA) is used as polar monomer to obtain monoliths with lower hydrophobicity. Structures of PDA, MA, and VSA are shown in Fig. 18. Monoliths are attached covalently with the capillary inner wall through the pretreatment process with 3-(trimethoxysilyl) propyl methacrylate (bind silane) which reacts with silanol groups on the surface of the fused silica capillary via formation of siloxane groups thereby attaching methacrylate ligands covalently to the wall that are able to form copolymers with the monomers in the polymerization mixture during preparation of the monoliths, see Fig. 19. This pretreatment stabilizes also the monolith against shrinkage and prevents creation of undesired voids [37]. Backpressures up to 200 bar were measured without extrusion or apparent damage of the monolithic column. It can hence be assumed that these monoliths are rigid, and mechanically stable for application in CEC. These monolithic capillaries were also used for a μ-LC system. Again, these monoliths are stable for application in this system.

Monolithic stationary phases for electrochromatographic separations should bear interactive sites for chromatographic retention, and charged moieties in order to assure the generation of a stable EOF. Methacrylate monomers were used to enable chromatographic separation, and vinylsulfonic acid to produce the required EOF for the propulsion of the mobile phase through the chromatographic bed. VSA has been selected since it has a low pKa (ca. 3), therefore, generation of EOF can be achieved even at low pH of the buffered mobile phase. Monolithic stationary phases should also be macroporous with good mechanical permeability. The amount of the lyotrophic salt present in the polymerization mixture (e.g., ammonium sulfate) can affect the porous properties and permeability of the monolithic material. It is usually added to promote pore formation induced by hydrophobic interaction of polymer segments (salting out of the polymer chains). The moment of collapse and hence the formation and final structure of the monolith depends on the nature of the solvent and on the type and concentration of the salting out agent. A study by Hoegger and Freitag [65] showed that the addition of a lyotrophic salt (ammonium sulfate) favors the formation of small nodules especially at higher monomer concentration, and the pore size of the monolith can be modulated through the salt concentration. However, the mass fraction of a crosslinker also affects the pore size distribution and the mechanical properties of the monolith. PDA was

used as crosslinker (with relatively high mass fraction) for the monoliths synthesized in the present study. Ammonium persulfate (APS) and tramethylethylenediamine (TEMED) have been used as a free radical starter and accelerator for the free radical polymerization reaction, respectively. A list of the monomers and other substances used for the polymerization mixture is shown in Tab. 14. The polymerization reaction, and a model of the synthesized polymeric material are shown in Fig. 20.

The nomenclature introduced by Hjerten in 1985 [92] was used to describe the monoliths in terms of the total monomer content (%T) and the cross-linking degree (%C). %T and %C can be calculated as follows,

$$\%T = \frac{\text{total mass of monomer (g)}}{\text{volume of buffer (L)}} * 100$$

$$\%C = \frac{\text{mass of crosslinker (g)}}{\text{total mass of monomers (g)}} * 100$$

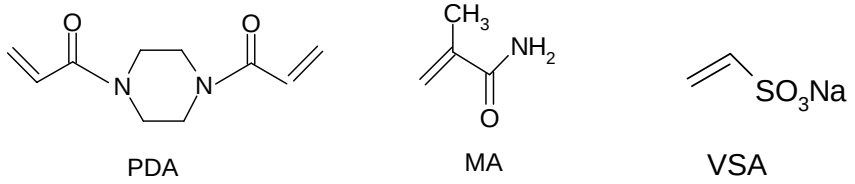

Fig. 18. Structures of the monomers piperazinediacrylamide (PDA), methylacrylamide (MA), and vinylsulfonic acid (VSA).

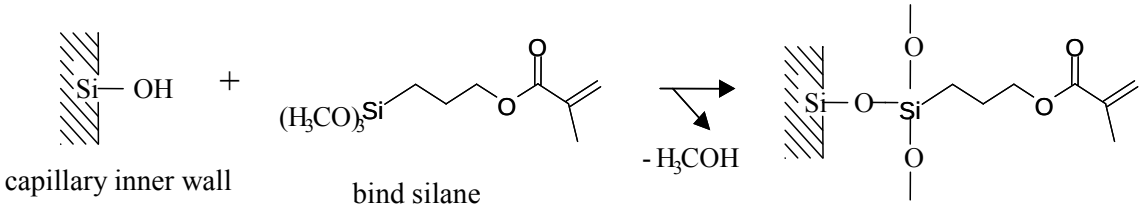

Fig. 19. Pre-treatment of the capillary inner wall with bind silane.

Tab. 14. Monomers and other substances used for the polymerization mixture.

Substance	Use
Methacrylamide	Hydrophilic interaction
Methacrylate monomers	Hydrophobic interaction/separation
Piperazinediacrylamide	Crosslinker
Vinylsulfonic acid	Generation of EOF, ion-exchange site
Methylated-ß-cyclodextrin	Solubilizing agent for hydrophobic monomers
Ammonium sulfate	Pore formation
Ammonium persulfate/ tetramethylethylenediamine	Initiator/accelerator

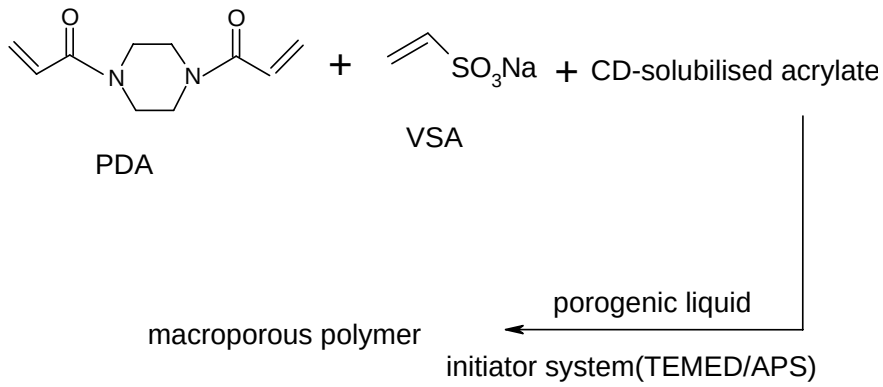

(a)

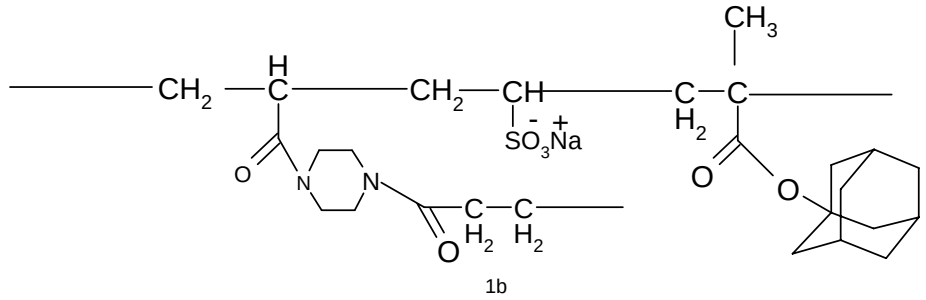

(b)

Fig. 20. The polymerization reaction (a), and a model of the synthesized polymeric material with adamantyl methacrylate as a hydrophobic monomer (b).

4.7 Variation of the content of hydrophobic monomer

Chromatographic properties (retention factors of several analytes) of the monoliths with varied molar fraction of the hydrophobic methacrylate monomers (Monoliths 15-18, for polymerization conditions see Tab. 1) were studied using buffered water/methanol mobile

phase. The retention factors for hydrophobic alkylphenones are increased linearly with increasing molar fraction of the hydrophobic monomer present in the polymerization mixture (Figs. 21-24). Each data point represents the average of triplicate measurements for a given solute. In all cases $r^2 > 0.98$. Standard deviation is represented as an error bar. Hydrophobicity (expressed as methylene selectivity α_{meth} [106]) for the monoliths is also increased with increasing molar fraction of the hydrophobic monomer (Tab. 15). Methylene selectivity α_{meth} was calculated from the slope of the regression line of plotting log k vs. n_{CH2} for alkylphenone series (n = 1-4 for acetophenone, propiophenone, butyrophenone, and valerophenone). Confidence limits for this magnitude were calculated by multiplying the standard deviation of the slope (s_b) with t(95%, f = 2). The increase in the hydrophobicity of the monolith leads to an increase in the retention factors for alkylphenones in the reversed-phase mode. Assuming that these findings reveal the contribution of the hydrophobic monomer in the chromatographic retention, it is demonstrated that with this synthesis procedure the composition of the produced polymer reflects the composition of the monomer solution (similar reactivities of the copolymerized monomers).

The monolith with isobornyl methacrylate monomer had higher methylene selectivity (and so hydrophobicity) compared to monoliths with other monomers using the same mobile phase (Tab. 15). However, it was expected that the monolith with adamantyl group has the highest hydrophobicity since adamantyl group is more hydrophobic compared to the groups of the other monomers (isobornyl, cyclohexyl, and phenyl groups). This unexpected behavior can be explained by the strong complexation between cyclodextrin and adamantyl methacrylate (see section 4.5.2.1) which makes the removal of the remaining cyclodextrin from the monolithic capillary difficult. Therefore, it is expected that some cyclodextrin remains in the monolith which reduces the hydrophobicity of the monolith since cyclodextrin is polar. Ritter et. al. [90] has shown that the polymerization of the complexes methylated-ß-CD/1-adamantylacrylamide and methylated-ß-CD/6-acryloylaminohexanoic acid 1-adamantylamide resulted in the formation of water soluble polymer/methylated-ß-CD- complexes which proves that methylated-ß-CD remains in the polymer. The monolith in which the hydrophobic monomer is replaced with methacrylamide monomer (Monolith 23) showed negligible hydrophobicity.

Tab. 15. Methylene selectivity α_{meth} (± confidence range) for different monoliths with different masses of methacrylate monomers present in the polymerization mixture (for polymerization conditions, see Tab. 2). Mobile phase: methanol/water (60:40, v/v) buffered with triethylamine/acetic acid, pH* = 7.0, electric conductivity = 120 µS cm^{-1}.

Mass of monomer (mg)	phenyl methacrylate	cyclohexyl methacrylate	adamantyl methacrylate	isobornyl methacrylate
10.0	0.05 ± 0.002	0.05 ± 0.003	0.08 ± 0.003	0.09 ± 0.003
20.0	0.08 ± 0.003	0.09 ± 0.002	0.14 ± 0.004	0.18 ± 0.006
30.0	0.14 ± 0.003	0.14 ± 0.004	0.17 ± 0.003	0.22 ± 0.004
40.0	0.15 ± 0.006	0.16 ± 0.004	0.18 ± 0.004	0.23 ± 0.004
50.0	0.18 ± 0.005	0.18 ± 0.004	0.20 ± 0.005	0.25 ± 0.007
50.0[a)]	0.14 ± 0.005	0.14 ± 0.004	0.15 ± 0.004	0.20 ± 0.005

a) Mobile phase: methanol/water (70:30, v/v) buffered with triethylamine/acetic acid, pH* = 7.0, electric conductivity = 120 µS cm^{-1}.

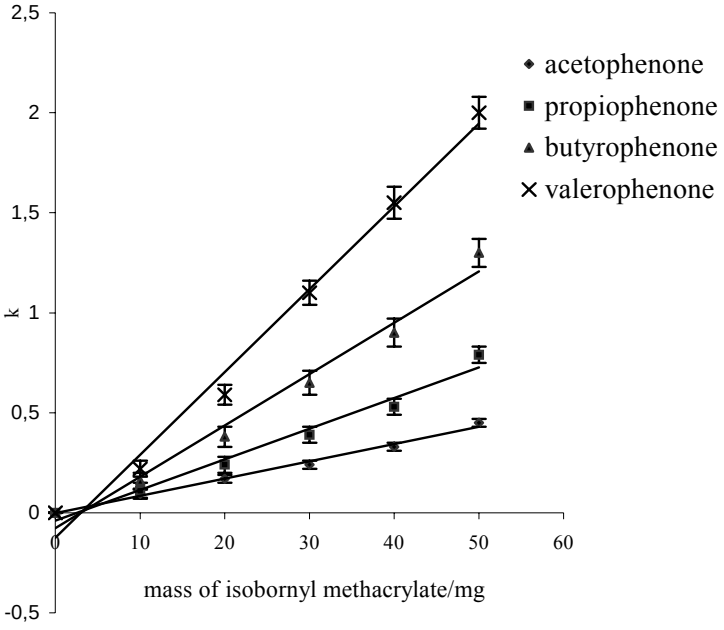

Fig. 21. Retention factors for alkylphenones vs. mass of isobornyl methacrylate monomer present in the polymerization mixture. Mobile phase: methanol/water (60:40, v/v) buffered with triethylamine/acetic acid, pH* = 7.0, electric conductivity = 120 µS cm^{-1}.

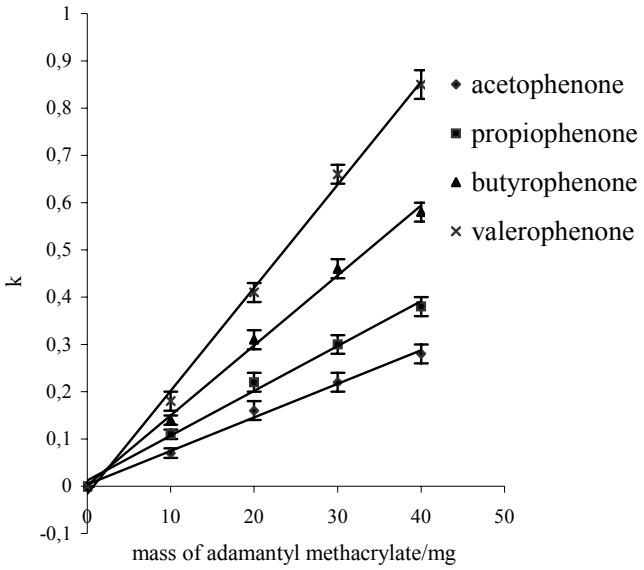

Fig. 22. Retention factors for alkylphenones vs. mass of adamantyl methacrylate monomer present in the polymerization mixture. Mobile phase: methanol/water (60:40, v/v) buffered with triethylamine/acetic acid, pH* = 7.0, electric conductivity = 120 µS cm^{-1}.

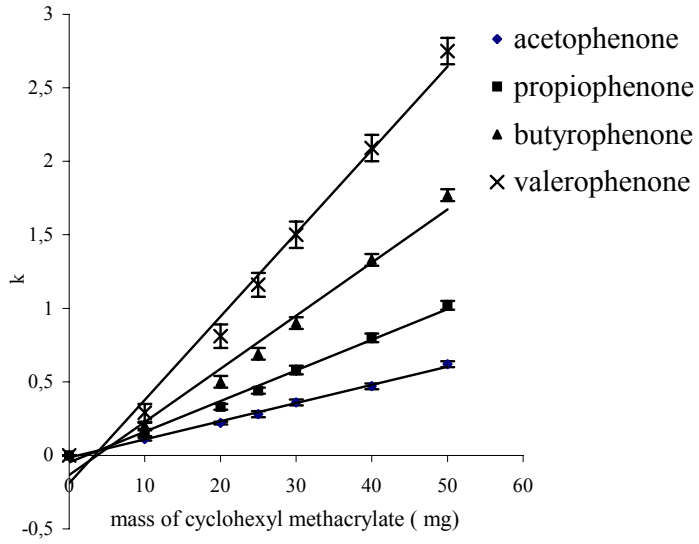

Fig. 23. Retention factors for alkylphenones vs. mass of cyclohexyl methacrylate monomer present in the polymerization mixture. Mobile phase: methanol/water (50:50, v/v) buffered with triethylamine/acetic acid, pH* = 7.0, electric conductivity = 120 µS cm^{-1}.

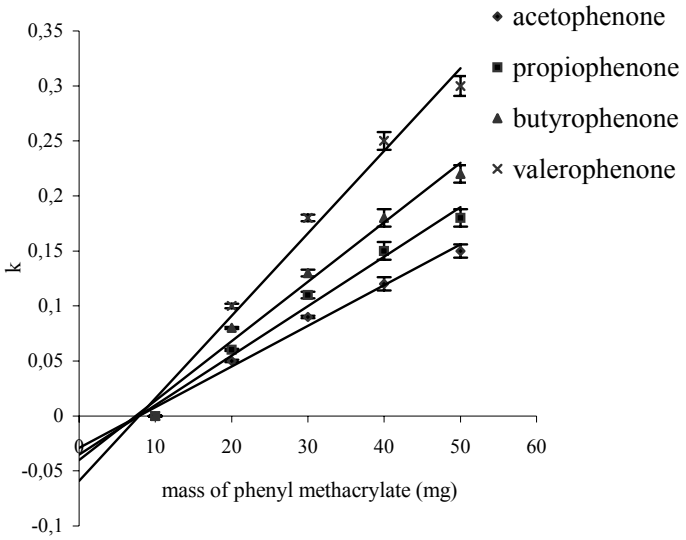

Fig. 24. Retention factors for alkylphenones vs. mass of phenyl methacrylate monomer present in the polymerization mixture. Mobile phase: methanol/water (60:40, v/v) buffered with triethylamine/acetic acid, pH* = 7.0, electric conductivity = 120 µS cm^{-1}.

4.8 Variation of total monomer concentration

The composition of the polymerization mixture: type and total mass of monomers used (%T), mass fraction of crosslinker (%C) with respect to total mass of monomers, type and composition of porogenic liquid present in the polymerization mixture, affect the morphology, chromatographic properties and the performance of the resulting monolithic material.

The influence of total monomer concentration in the polymerization mixture on the retention factors of different alkylphenone analytes, on the specific permeability, on the electroosmotic mobility μ_{eo} (at constant mobile phase composition), and on the porosity of the monolithic stationary phases was studied. Four monoliths with different total monomer concentrations (7.0, 10.0, 14.0, and 18.0 w/v, Monoliths 15-18) were prepared (for polymerization conditions, see Tab. 1).

4.8.1 Effect on the retention factors

The total concentration of the monomers present in the polymerization mixture (%T) affects the volume ratio (stationary phase/mobile phase) of the resulting chromatographic bed. The volume fraction of monolithic stationary phase in the chromatographic bed increases with increasing %T, which in turn increases the retention factor of an analyte according to the definition of retention factor, $k = K\varphi$, where k = retention factor, K = partition coefficient, φ = phase ratio = V_s/V_m, V_s = volume of the stationary phase, V_m = volume of the mobile phase.

Results showed that the retention factors for alkylphenones increase with increasing %T (Fig. 25). In all cases $r^2 > 0.98$. However, as expected the methylene selectivity α_{meth} was not affected by %T (see Tab. 16).

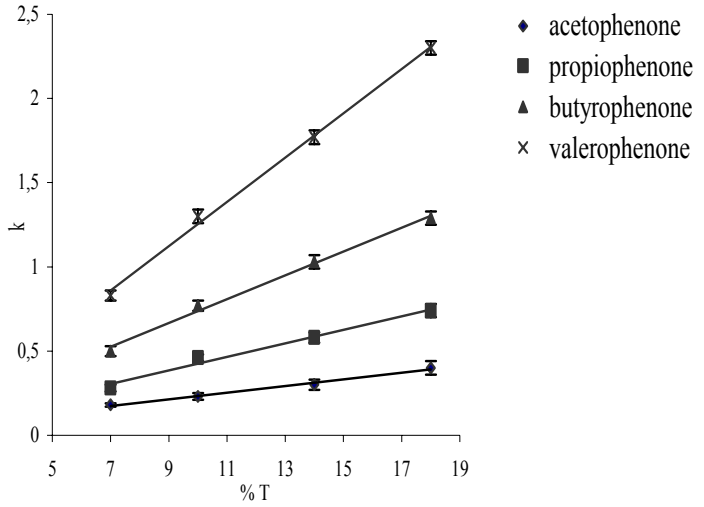

Fig. 25. Retention factors for several alkylphenones vs. percentage of total monomer concentration (composition of stationary phase see Tab. 1). Mobile phase: methanol/water (60:40, v/v) buffered with triethylamine/acetic acid, pH* = 7.0, electric conductivity = 120 µS cm^{-1}.

4.8.2 Effect on permeability and electroosmotic mobility

The ability of a liquid to flow through the network of channel-like pores that traverse the length of the monoliths is essential to all of their applications. The permeability of a monolithic material K_p is defined by the linear velocity u of a liquid streaming through the pores of the monolith normalized on the length of the chromatographic bed L and on the pressure difference between both ends Δp,

$$K_p = \frac{u\,L}{\Delta p} \tag{44}$$

The specific permeability K^o normalized on the viscosity of the liquid η and the total porosity of the filled capillary ε, is defined as follows,

$$K^o = K_p\,\eta\,\varepsilon \tag{45}$$

Using the relationship between linear velocity u and the volume flow rate F,

$$u = \frac{F}{\pi\,r^2\,\varepsilon} \quad \text{, where r: radius of the capillary} \tag{46}$$

and substitution of the value of K into K^o yields,

$$K^o = \frac{L \eta F}{\Delta p \pi r^2} \quad (47)$$

Using this formula, the specific permeability K^o of a monolithic capillary can be measured by determining the volume flow rate using an HPLC pump working at constant pressure with flow splitter employing water as liquid phase (η $H_2O = 10^{-3}$ Pa s at 20 °C).

K^o was determined for monoliths having different %T. Results show that K^o decreases with increasing %T (Tab. 16). This can be explained by the assumption that with increasing %T the mean diameter of the flow-through channels in the monolithic bed will be decreased [37]. As expected, μ_{eo} of these monoliths is not significantly affected by %T (Tab. 16), because it can be assumed that the thickness of the electric double layer is much smaller than the mean channel diameter.

The thickness of the double layer δ can be calculated from Eq. 3 ($\kappa = \frac{1}{\delta} = \sqrt{\frac{2 I F_k^2}{RT\varepsilon_0\varepsilon_r}}$). By substitution the values of F_k (96487 A s mol^{-1}), R (8.314 J $mole^{-1}$ K^{-1}), T (298.15 K), ε_o (8.85 $\times$ 10^{-12} C^2 N^{-1} m^{-2}), and the value of dielectric constant ε_r for methanol/water (60:40, v/v) = 55 (Schwer et al. [107]) in equation 3 yields,

$$\kappa = \frac{1}{\delta} = 3.93 \sqrt{I} \quad (48)$$

The ionic strength can be estimated from the specific conductance of the mobile phase, taking into account the following equation,

$$\Lambda_s = F_k \Sigma c_i z_i \mu_i \quad (49)$$

where F_k is Farady constant, c_i is the molar concentration, z_i is the charge number (valence), and μ_i is the mobility, and Λ_s is the specific conductivity (in $\Omega^{-1}cm^{-1}$) which is defined as $\Lambda_s = \Lambda c$ where Λ is the equivalent conductance (in $\Omega^{-1}cm^2mole^{-1}$) . (50)

Substitution the value of specific conductivity for triethylammonium acetate buffer system (i = 1, 2, z = 1) in Eq. 49 yields,

$\Lambda c = F_k c(\mu_1 + \mu_2)$ or

$$\mu_i = \frac{\Lambda_i}{F_k} \quad (51)$$

where μ_1 and μ_2 are the mobility of triethylammonium ion and acetate ion, respectively.

Equivalent conductance at infinite dilution is called limiting conductance Λ_0. This reduces Eq. 51 to

$$\mu_i = \frac{\Lambda_{0i}}{F_k} \tag{52}$$

For many ions, limiting conductancies have been determined and are listed in [108]. By substitution the value of Λ_0 for triethylammonium and acetate ions (34.3 and 40.9 $\Omega^{-1}cm^2mole^{-1}$ in water at 25°C, respectively [108]) and F_k (96487 A s $mole^{-1}$) in Eq. 52, mobility μ_i was calculated to be 35.5 $\times 10^{-5}$ and 42.4 $\times 10^{-5}$ $cm^2\ V^{-1}\ s^{-1}$ for triethylammonium ion and acetate ion, respectively. These values for mobility, however, were calculated in water while the mobile phase used in this study is a mixture of methanol and water (60:40, v/v). Therefore these values for mobility have to be corrected. Mobility depends on the ratio of dielectric constant to viscosity (ε/η) according to Hückel equation where the charged particle is considered as a point charge ($\mu = 2\varepsilon_0\varepsilon_r\zeta/3\eta$). Schwer et al. [107] has investigated the dependence of ε/η ratio on the solvent composition at 25°C. They have found that the ε/η ratio was decreased by a factor of 2.5 using methanol/water (60:40, v/v) compared to pure water, which in turn decreases the mobility by a factor of 2.5. Accordingly, mobility has calculated to be 14.2 $\times 10^{-5}$ for triethylammonium ion and 17.0 $\times$ 10^{-5} $cm^2\ V^{-1}\ s^{-1}$ for acetate ion.

Concentration of triethylammonium acetate in the mobile phase was calculated by substitution the value of specific conductivity Λ_s of the mobile phase which measured using the conductivity meter (120 $\times$ 10^{-6} Ω^{-1} cm^{-1}), F_k (96487 A s $mole^{-1}$) and the mobility of triethylammonium acetate ($\mu_1 + \mu_2$ = 31.2 $\times 10^{-5}$ $cm^2\ V^{-1}\ s^{-1}$) in Eq. 49 ($\Lambda_s = F_k c(\mu_1 + \mu_2)$). This calculation gave a concentration value of 3.99 $\times 10^{-3}$ mol L^{-1}. Then ionic strength has been calculated (3.99 $\times 10^{-3}$ mole L^{-1}) which enables the calculation of the double layer thickness using Eq. 48. This calculation gave a value of 4.0 nm for the double layer thickness, which is smaller than the mean channel diameter.

Tab. 16. Effect of total monomer concentration (%T) on the total porosity ε, specific permeability K^o, electroosmotic mobility μ_{eo}, and methylene selectivity α_{meth} (± confidence range) of Monoliths 15-18. Mobile phase: methanol/water (60:40, v/v) buffered with triethylamine/acetic acid, pH* = 7.0, electric conductivity = 120 µS cm^{-1}.

Monolith number	%T (w/v)	ε	K^o (m^2)	μ_{eo} ($cm^2\,kV^{-1}\,min^{-1}$)	α_{meth}
15	7.0	0.62	$1.52 * 10^{-12}$	8.02	0.23 ± 0.006
16	10.0	0.58	$1.28 * 10^{-12}$	9.57	0.22 ± 0.007
17	14.0	0.55	$0.78 * 10^{-12}$	8.85	0.23 ± 0.006
18	18.0	0.50	$0.39 * 10^{-12}$	8.67	0.23 ± 0.006

4.8.3 Effect on the total porosity

One major advantage of CEC compared to HPLC is that higher column efficiency can be achieved using identical separation media. For columns packed with beads, the efficiency is generally particle size dependent, and increases as the size of the packing decreases. Since the monolithic capillaries are molded rather than packed, the particle size becomes irrelevant, and instead, the porosity and the pore size distribution within the monolithic material may be expected to affect the chromatographic efficiency.

The porous properties can affect the morphology as well as the chromatographic properties of the monolithic material. Many parameters can affect the porosity of the monolithic material, e.g. the porogenic system used in the polymerization mixture. Hilder et al. [55] has prepared different monoliths with different pore sizes (determined by mercury intrusion porosimetry) with broad range of 250-1300 nm by simply changing the ratio of propanol to butanediol in the porogenic mixture.

The amount of the lyotrophic salt which is dissolved in the porogenic liquid in the polymerization mixture can also affect the porous properties of the monolithic material. It is usually added to promote pore formation (salting out of the polymer chains). The moment of collapse and hence the formation and final structure of the monoliths depends on the nature of the solvent and on the type and concentration of the salting out agent. A study by Hoegger and Freitag showed that the addition of a lyotrophic salt (ammonium sulfate, for example)

favors the formation of small nodules especially at higher monomer concentration, and the pore size of the monoliths can be modulated through the salt concentration [65].

The total monomer concentration affects also the porous properties of the monolithic material. A study by Hoegger and Freitag showed also that the type as well as the percentage of additional functional monomers affect the morphology and the chromatographic properties of acrylamide-based hydrophilic monoliths [65].

In this work, the influence of the total monomer concentration on the total porosity of the monolithic capillaries was studied. Total porosity of a monolith can be determined according to Eq. 46

$u = \frac{F}{\pi r^2 \varepsilon}$, substitution the value of u ($u = L/t_0$) gives,

$$\varepsilon = \frac{F\, t_0}{\pi r^2 L} \qquad (53)$$

Hence the total porosity (macroporous and mesoporous) of a monolithic capillary can be calculated from the elution time of a nonretained marker t_0 and the volume flow rate F. Volume flow rate was determined from CEC experiments using methanol/water (60:40, v/v) buffered with triethylamine/acetic acid, pH* 7.0 as a mobile phase. Total Porosity was decreased with increasing %T (Tab. 16).

4.9 Porosity analysis of the monoliths

Monolithic columns are made of one single piece of an adsorbent material (porous silica or polymer) that fills the entire length and width of the column. This piece of adsorbing material contains two interconnected networks of pores, the macropores and the mesopores. The macropores which also called through-pores, have a pore diameter of > 50 nm. Their network provides flow paths through and along the column and ensures access of the sample molecules to the whole network of mesopores. The density of the macropore network causes monolithic columns to have a high external porosity. This high porosity combined with the relatively large value of the average size of these pores gives to the monolithic columns a high permeability [109]. There is a consistent agreement in the literature suggesting that the macropore network accounts for approximately 80% of the total porosity of a monolith [109]. The mesopore network represents 10-15% of the total porosity. Their pore diameter is between 2 and 50 nm. The specific surface area of the monolith is essentially accounted for

the mesopore network [109]. A small percentage of the total porosity corresponds to micropores [109].

The morphology and the pore structure of a chromatographic bead are important features in the design of broadly useful stationary phase since these aspects influence directly the hydrodynamic properties (e.g. flow properties), thermodynamic properties (e.g. loadability) and the mass transfer kinetics (e.g. efficiency [110]). The investigation of the properties of monolithic columns is complicated due to the characteristics of the macropore network. This network does not have a scale that is determined by the size (radius) of the packing material. The external porosity of the column or porosity of the macropore network is no longer close to 0.40 as it is in a packing formed from particulate beads [109].

Direct and indirect techniques can be used in order to analyze porous materials. Direct techniques provide actual images of the surface but no significant quantitative characterization of the surface area or pore volume. Examples of this technique are electron microscopy (scanning electron microscopy (SEM), and transmission electron microscopy (TEM)) and X-ray analysis. Indirect techniques which measure the macroscopic effects of phenomena occurring in the pore volume and on the pore surface are gas adsorption and mercury penetration. In addition, a chromatographic method, as inverse size-exclusion chromatography (ISEC), could be a powerful method to quantitatively characterize the pore morphology of a monolithic material [110].

Monolithic columns could be studied with the same theoretical and experimental methods used for conventional chromatographic columns. In principle, their porosity can be determined by measuring the amount of nitrogen sorbed on the monolith at the temperature of its atmospheric boiling point as a function of the partial pressure of nitrogen [111]. In this method, adsorption and desorption isotherms are used to measure the pore size distribution of a material (micro-, meso-, and macropores). Total surface area (BET surface area, BET is the abbreviation of the names Brunauer, Emmet, and Teller) as well as total volume of mesopores and the mesopore size distribution according to the BJH method (BJH is the abbreviation of the names Barrett, Joyner, and Halenda) can also be measured for an adsorbent material. Unfortunately, the monolith has dimensions that are not compatible with those of conventional nitrogen-sorption instruments. Mercury porosimetry could also give the size distribution of the mesopore and macropore networks [111]. Using this method, it is able to detect pore diameters of porous materials from 3.6 to 15000 nm. The theory of this method is

based on the physical principle that a non-reactive, non-wetting liquid e.g. mercury will not penetrate pores until sufficient pressure is applied to force its entrance. The relationship between the applied pressure P and the pore size r into which mercury will intrude is given by the Washburn equation ($P\ r = -2\ \gamma \cos\theta$), where r is the diameter of the pore, γ is the surface tension of mercury (480×10^{-3} N/m) and θ is the contact angle between mercury and the pore wall which is usually near 140^{o}. This reduces Washburn equation to $P\ r = 0.736$. The column tubing, however, can not withstand the required pressure and the monolith is not compatible with the sample holder of available instruments. In fact, the monolith can be synthesized in bulk and investigated using gas adsorption or mercury intrusion porosimetry. However, such pore size measurements in bulk and in the dry state are not always representative of the actual pore size in the column filled with mobile phase.

Among the conventional methods of determination of the column porosities, only inverse size-exclusion chromatography (ISEC) [109-110] can be used conveniently with monolithic columns in the wet state (column filled with the mobile phase). In ISEC, information on the structure of the pores of a packing material is obtained from the retention data of a series of known probe compounds, e.g., samples of polymers of narrow molecular mass distribution and known average molecular mass [109]. Retention data are used to determine external (macroporous), internal (mesoporous), and total porosity of the packing material. These data provide also information on the pore-size distribution of the adsorbent material. In ISEC, tetrahydrofuran (THF) is usually used as a mobile phase. The monoliths prepared in this work, however, can not withstand THF. Therefore, ISEC can not be used to investigate the porosity of the monoliths.

Pore size distribution and total surface area were determined for one of the monolithic stationary phases in bulk and dry state using the nitrogen-adsorption method and mercury intrusion porosimetry. The monolith synthesized with isobornyl methacrylate was used (Monolith 1). 1 g of this polymeric monolith was synthesized in bulk, washed with water and methanol, then dried in oven (40 ^{o}C) and kept in a dessicator over silica gel. Results show that this monolith has a total specific surface area (BET surface area) of 7.6 m^2/g. Compared to conventional packing material, this monolith has very low specific surface. This can be attributed to the lower mesoporosity of the monolith compared to sorbents like C18 silica gel, because the internal surface of a porous material reflects its mesoporosity. It is described in section 4.11.3, that the retention factors of alkylphenones are indeed higher on a C18-packed column compared to the monolithic stationary phases which confirms that specific surface

area of the mesoporous C18 silica gel material is higher compared to that of the monolithic stationary phases employed in this study.

An investigation of the pore size distribution was also performed using mercury intrusion porosimetry. Results show that 72% of the pore volume is in the range of 1500-20000 nm (macroporous), 27% in the range of 7-150000 nm (macroporous and mesoporous) and only 1% in the range of 7-0 nm (Tab. 17). These results show that the monolith is macroporous with an average pore diameter of 3045 nm and a total cumulative volume of 1478 mm^3/g. If we consider the density of the monolithic material to be 1 g/mol, the total cumulative volume of 1478 mm^3/g corresponds to 0.15 total porosity. This total porosity is lower than the value obtained for the monoliths in section 4.8.3 (see Tab. 16). In this study, the porosity is determined in bulk for a portion of dry monolithic material, while in section 4.8.3 it is determined for the monolithic capillary using methanol/buffer mobile phase, which may explain the different results obtained.

Tab. 17. Pore size distribution of Monolith 1 performed by mercury intrusion porosimetry.

Pore diameter ranges (nm)	Specific volume (mm^3/g)	Relative volume (mm^3/g)	Relative volume (%)
1500-20000	1065	1065	72
7-1500	1461	396	27
7-0	1478	17	1

4.10 Scanning electron microscopy

SEM is used to study the structure of a polymer-filled capillary and its uniformity, as well as the bonding of the polymeric support to the silanized capillary wall. The use of the electron microscopy for morphological investigation of the monolithic materials is rather common but requires dry samples [37]. However, drying may change dramatically the morphological features of the porous material. The roughness of the continuous bed surface and the channels in the polymeric matrix change when the bed is dried [37].

Two monolithic capillaries (Monolith 2, for polymerization conditions, see Tab. 1) were synthesized at different days with identical polymerization mixtures to study the reproducibility of synthesis. Three different segments from each capillary (one segment from the end of the capillary close to the detection window, segment from the middle of the

capillary, and another segment from the end of the capillary) were tested to study the uniformity of packing over the length of the capillary.

SEM images of the capillaries synthesized at different days reveal that the morphology of these capillaries is reproducible (Fig. 26, SEM photos of a sector of the polymer cross section in a filled capillary). For all capillaries typical macroporous polymers with interconnected microgloubules were obtained (Fig. 26). The microglobular or nodular structure is homogenous over both the cross section (I.D 100 μm) and the length of the capillary (Fig. 26).

The attachment of the polymeric monolith to the silanized capillary wall is also clear for all the investigated capillaries. SEM photographs reveal also that these polymeric monoliths are homogeneously filled over the entire of the capillary. This demonstrates that the procedure for synthesis renders a highly reproducible morphology and uniform monoliths.

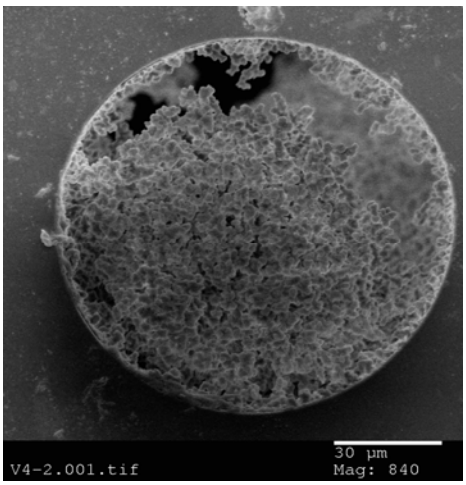

(a)

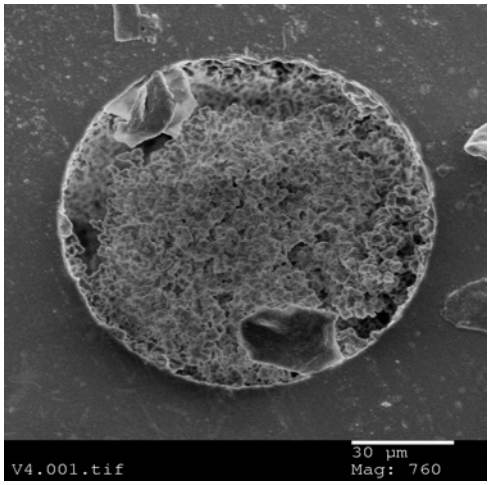

(b)

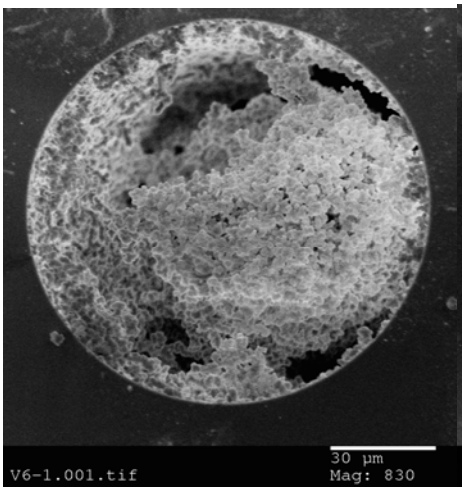

(c)

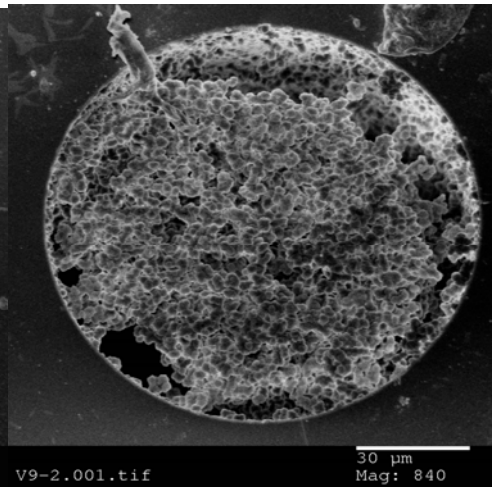

(d)

Fig 26. Continued on next page.

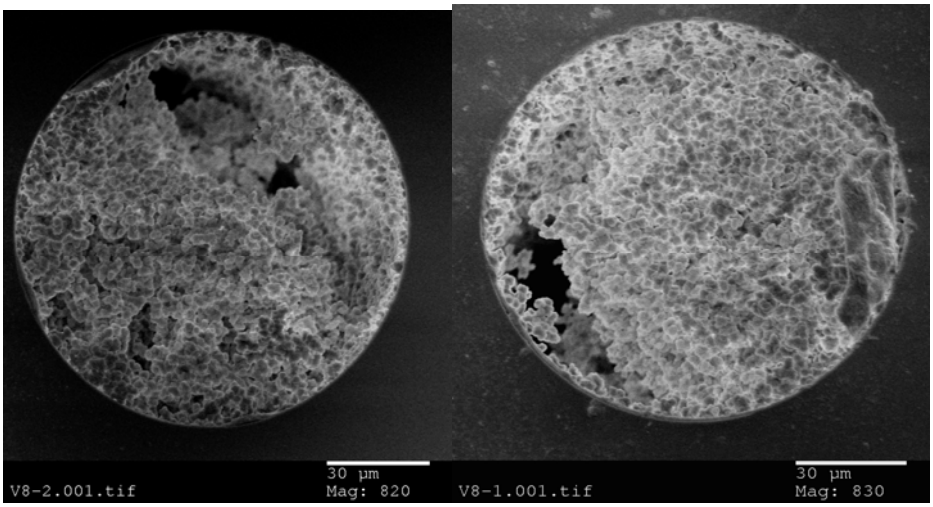

(e) (f)

Fig. 26. SEM photographs of Monolith 2 synthesized at two different days (a) first day, cross section from the end of the capillary close to the detection window (b) second day, cross section from the end of the capillary close to the detection window (c) first day, cross section from the middle of the capillary (d) second day, cross section from the middle of the capillary (e) first day, cross section from the other end of the capillary (f) second day, cross section from the other end of the capillary.

4.11 Chromatographic properties of the monoliths

4.11.1 Efficiency (Van Deemter plots)

A plot of plate height H against average linear velocity of the mobile phase u (Van Deemter plot) is used to determine the optimum mobile phase velocity through a column at which the plate height is a minimum and the separation efficiency is at a maximum (Fig. 27). Below the optimum velocity, the plate height H is large due to the contribution of longitudinal diffusion of the analyte (B term in Van Deemter equation) as this term increases with decreasing mobile phase velocity ($H = A + B/u + C_m u + C_s u$). Beyond the optimum velocity, an increase in the velocity of the mobile phase results in an increase in the plate height (decrease in the separation efficiency) due to the increase in resistance to mass transfer in the mobile- and stationary phase (C_m and C_s terms in Van Deemter equation, respectively).

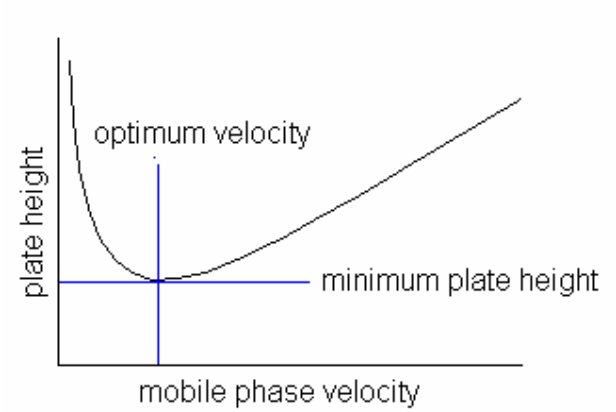

Fig. 27. A typical Van Deemter plot [29].

The Van Deemter curves for Monolith 1 were determined for DMF as unretained marker and for different alkylphenones as retained solutes. The plate number N was calculated according to the formula $N = 5.54 (t_r / w_{0.5})^2$, where t_r is the retention time and $w_{0.5}$ is the peak width at half height of a peak. Accordingly, the plate height H was calculated as $H = L_{eff} / N$, where L_{eff} is the effective capillary length. The range of linear velocities corresponds to an applied voltage between 5 and 17 kV. Using these plots, efficiencies of 180.000 m^{-1} for DMF, and about 100.000-120.000 m^{-1} for acetophenone and propiophenone (with a range of retention factors of 0.4-1.0) were obtained at optimum velocity of the mobile phase (Fig. 28). The plots obtained do not show a clear minimum due to the limited range of mobile phase velocity investigated. With the home built CEC instrument, there is a limitation of a maximum voltage of 20 kV due to the formation of bubbles within the capillary at higher voltage. In all cases, a decrease in the efficiency was observed with increasing retention factor. This observation can be explained by an increase in the resistance to mass transfer in the stationary phase C_s with increasing retention factor due to a significant length of distance to be passed by diffusion. Bruin et. al. [29] have also observed a decrease in the efficiency (increase in plate height) with increasing retention factors using open tubular CEC. They have attributed this observation to the dependence of C_s on the retention factor.

Retention factors and efficiencies of alkylphenones (acetophenone, propiophenone, butyrophenone, and valerophenone) separated using methanol/aqueous buffer (reversed-phase mode), nitrotoluenes (4-nitrotoluene, 2,4-dinitrotoluene, 2,4,6-trinitrotoluene) separated using methanol/aqueous buffer (mixed-mode), and phenolic solutes (vanillin, 4-hydroxybenzaldehyde, resorcinol) separated using both methanol/aqueous buffer (mixed-mode) and buffered nonpolar mobile phase methanol/acetonitrile (normal-phase mode) are

shown in Tab. 18. Plots of N vs. k for these analytes were drawn. The slope of such plot gives information about the change in the efficiency with increasing retention factor. The decrease in the efficiency for alkylphenones separated by reversed-phase with increasing retention factors is found to be higher (with a slope of –599,329) compared to the decrease in the efficiency for phenolic solutes (slope –396,154) or nitrotoluenes (slope –115,714), which have been separated by mixed-mode. However, this decrease in the efficiency was not observed for the phenolic solutes separated by normal-phase mode where the slope of the plot of N vs. k was found to be positive (1×10^6) indicating an increase in the efficiency with increasing retention factor. One explanation of these behaviors might be the difference in the retention mechanism of these analytes i.e. reversed-phase, mixed-mode and normal-phase.

Comparing the typical Van Deemter curve for HPLC-columns with that for CEC-columns, higher mobile phase velocity can be used (to reduce the analysis time) using CEC-monolithic capillaries without decrease in the separation efficiency. This can be explained by the fact that the resistance to mass transfer in the mobile phase (C_m term) and the A term of the Van Deemter equation using CEC are reduced due to the flat flow-velocity profile in EOF compared to the parabolic flow profile in pressure-driven μ-LC.

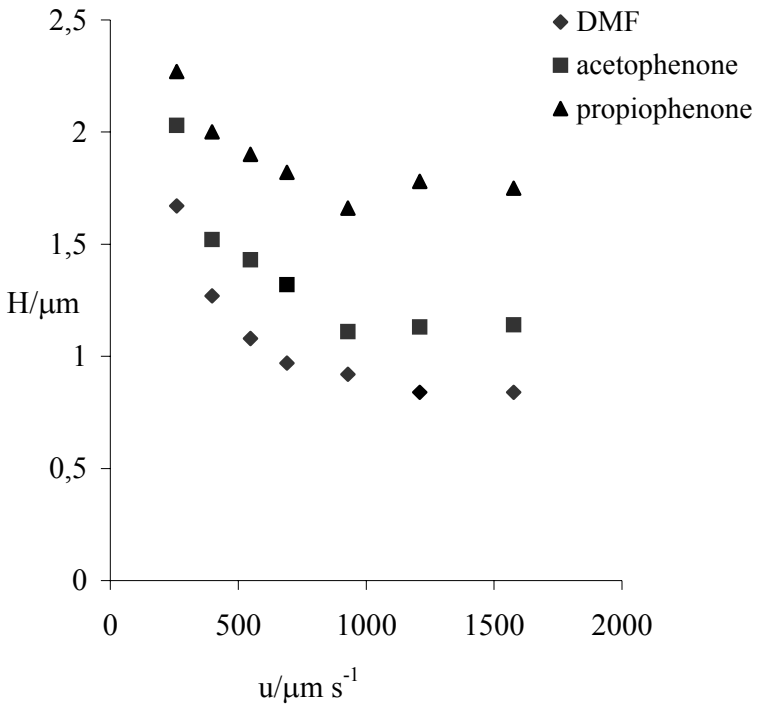

Fig. 28. Van Deemeter curve for DMF, acetophenone (k = 0.22), and propiophenone (k = 0.30) for Monolith 1. Mobile phase: methanol/water (60:40, v/v) buffered with triethylamine/acetic acid, pH* = 7.0, electric conductivity = 120 μS cm^{-1}.

Table 18. Retention factors and efficiencies of alkylphenones (acetophenone, propiophenone, butyrophenone, valerophenone), phenolic solutes (vanillin, 4-hydroxybenzaldehyde, resorcinol), and nitrotoluenes (4-nitrotoluene, 2,4-dinitrotoluene, 2,4,6-trinitrotoluene).

Separation mode	Analyte	Retention factor	Efficiency
Reversed-phase mode [a)]	acetophenone	0.11	195000
	propiophenone	0.16	120000
	butyrophenone	0.23	70000
	valerophenone	0.34	48000
Mixed-mode [a)]	vanillin	0.17	158000
	4-hydroxybenzaldehyde	0.22	148000
	resorcinol	0.28	115000
Mixed-mode [b)]	4-nitrotoluene	0.17	42000
	2,4-dinitrotoluene	0.27	29000
	2,4,6-trinitrotoluene	0.47	7000
Normal-phase mode [c)]	vanillin	0.08	55000
	4-hydroxybenzaldehyde	0.12	139000
	resorcinol	0.17	169000

[a)] Mobile phase: methanol/aqueous buffer (70:30,v/v), pH* = 7.0, electric conductivity = 120 μS cm^{-1}.

[b)] Mobile phase: methanol/water (80:20, v/v) buffered with triethylamine/acetic acid, pH* = 7.0, electric conductivity = 120 μS cm^{-1}.

[c)] Mobile phase: methanol/acetonitrile (60:40, v/v) buffered with triethylamine/acetic acid, pH* = 7.0, electric conductivity = 120 μS cm^{-1}.

4.11.2 Selectivity for noncharged analytes

Several neutral hydrophobic and hydrophilic analytes have been tested on these monoliths using both aqueous mobile phase and nonaqueous mobile phase.

4.11.2.1 Aqueous mobile phase

Hydrophobic alkylphenones follow the ideal reversed-phase elution mode on these monolithic stationary phases using a buffered aqueous mobile phase; they elute in the order of increasing hydrophobicity (Fig. 29a-d), their retention factors also decrease with increasing volume fraction of methanol in the mobile phase (Fig. 30). Using a buffered aqueous mobile phase, nitrotoluenes and phenolic solutes, on the other hand, follow neither a reversed- nor a normal-

phase mode, but a mixed-mode; their retention factors are decreased with increasing volume fraction of methanol in the mobile phase as in RP-LC (Fig. 31-32), while their elution order follows what would be expected in the normal-phase mode, i.e. they are eluted in the order of increasing polarity (Fig. 33-34). The behavior of these polar analytes can be attributed to the polar interactions e.g. dipole-dipole between the mixed-mode monolith and these polar analytes. This leads to conclude that both solvophobic and polar interactions contribute to the retention of polar analytes on the mixed-mode monoliths prepared in this study as these monoliths have both nonpolar and polar structure units.

The effect of mobile phase composition on the electroosmotic mobility was also investigated. Results show that there was only a small change in the electroosmotic mobility with increasing the volume fraction of methanol in the mobile phase (range of μ_{eo} 8.33-8.75 cm^2 $kV^{-1}min^{-1}$). It should be noted that the electroosmotic mobility depends on the ratio of dielectric constant to viscosity of the mobile phase, and on the temperature. However, the capillary is not temperature-controlled.

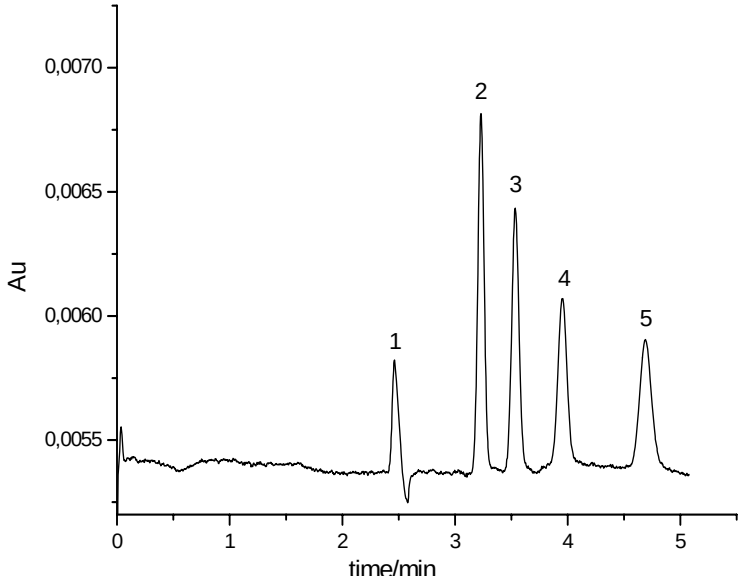

(a)

Fig 29. Continued on next page.

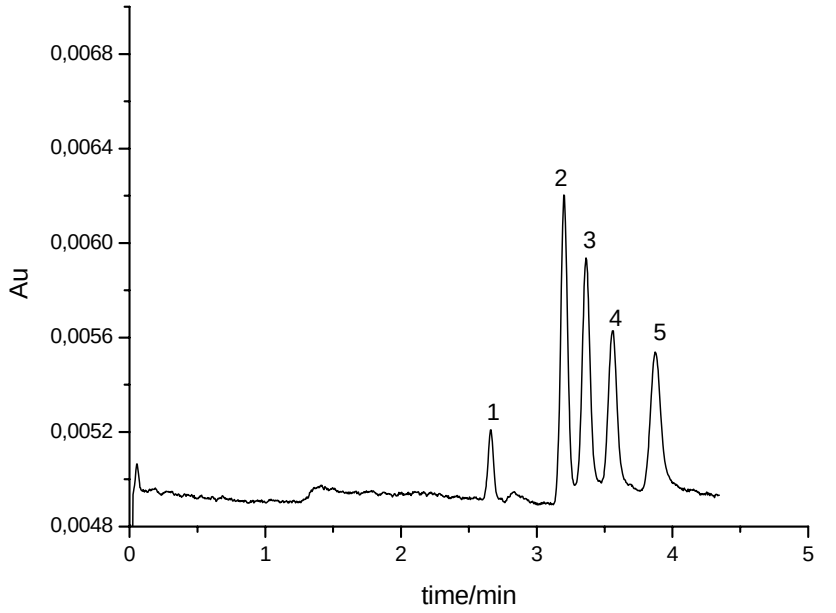

(b)

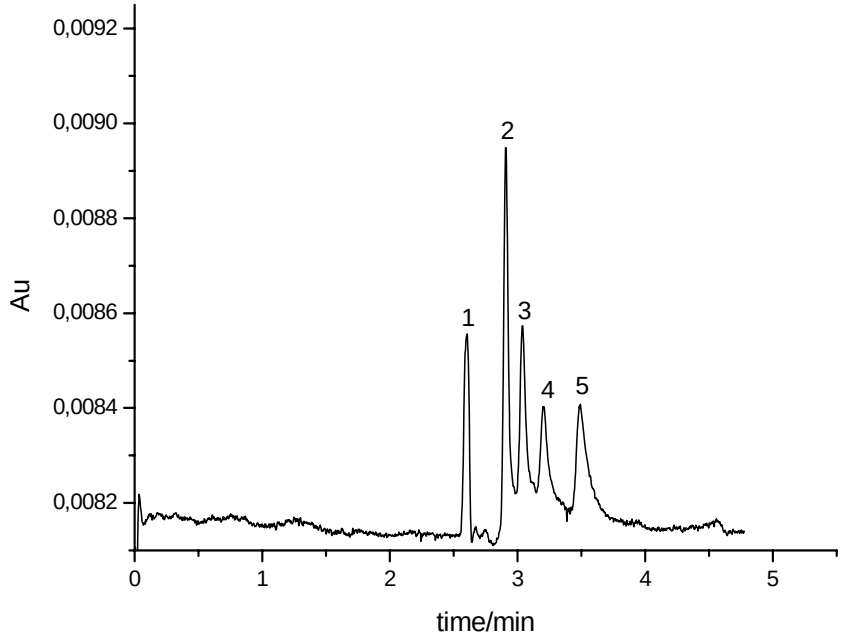

(c)

Fig 29. Continued on next page.

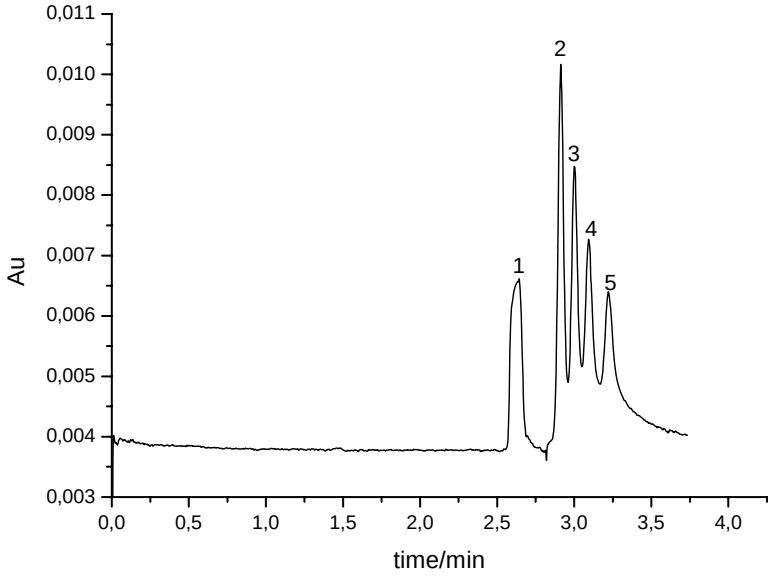

(d)

Fig. 29. Reversed phase separation of different alkylphenones on the Monoliths 1-4 (a-d). Solutes: (1) DMF (2) acetophenone (3) propiophenone (4) butyrophenone (5) valerophenone. Mobile phase: methanol/water (70:30, v/v) buffered with triethylamine/acetic acid, pH* = 7.0, electric conductivity = 120 µS cm^{-1}. Monolithic capillary used: total length 21.0 (corresponds to effective length 15.0) cm ×100 µm I.D.

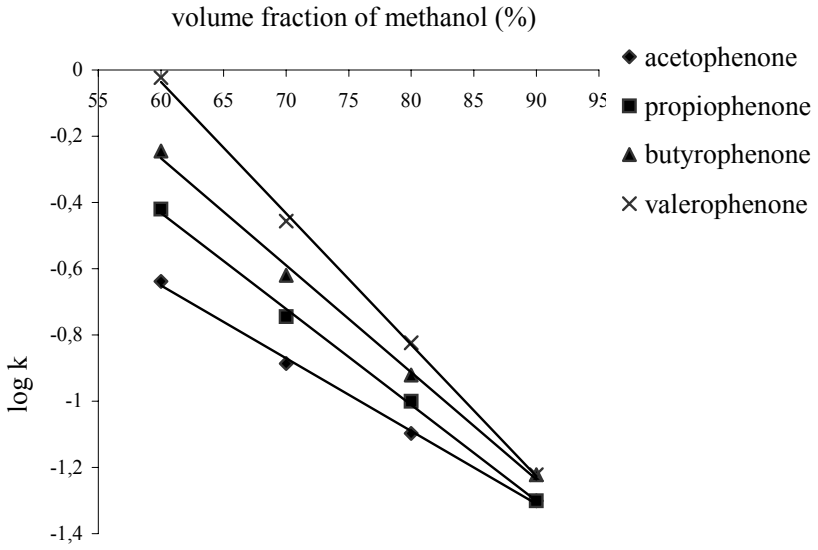

Fig. 30. Log k of alkylphenones on Monolith 2 vs. volume fraction of methanol in the mobile phase. Mobile phase: methanol/water, buffered with triethylamine/acetic acid, pH* 7.0, electric conductivity = 120 µS cm^{-1}.

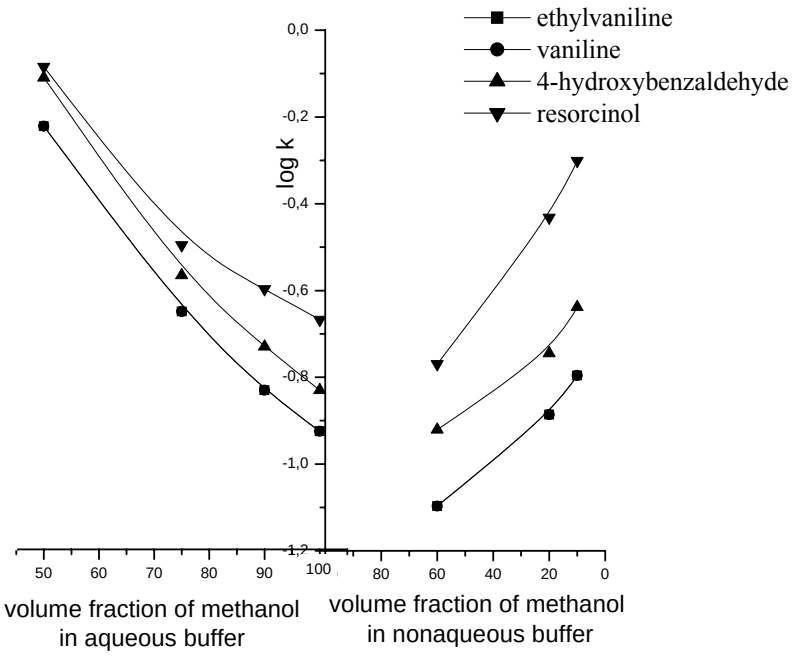

Fig. 31. Log k of several phenolic solutes on Monolith 2 vs. volume fraction of methanol in both aqueous and nonaqueous mobile phases.
Aqueous mobile phase: methanol/water, buffered with triethylamine/acetic acid, pH* 7.0, electric conductivity = 120 µS cm^{-1}.
Nonaqueous mobile phase: methanol/acetonitrile, buffered with triethylamine/acetic acid, pH* = 7.0, electric conductivity = 150 µS cm^{-1}.

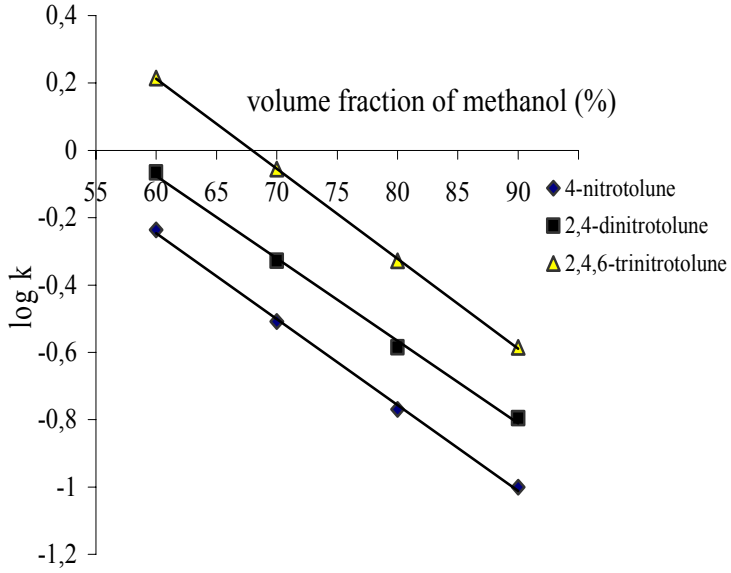

Fig. 32. Log k of nitrotoluenes on Monolith 2 vs. volume fraction of methanol in the mobile phase. Mobile phase: methanol/water, buffered with triethylamine/acetic acid, pH* 7.0, electric conductivity = 120 µS cm^{-1}.

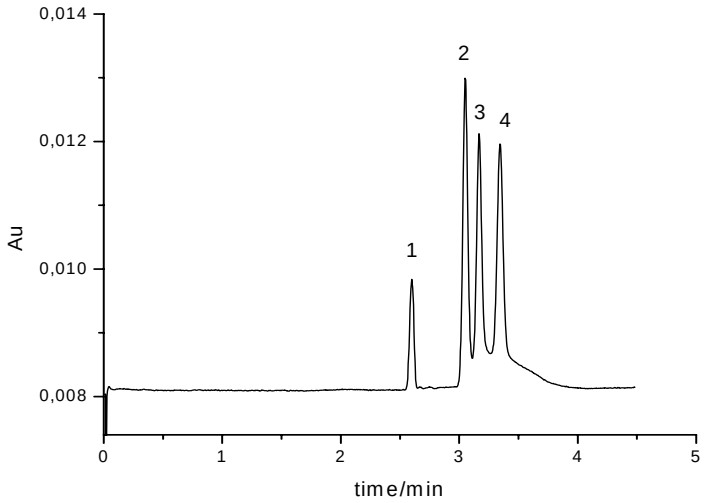

Fig. 33. Mixed-mode separation of phenolic solutes on Monolith 2. Solutes: (1) DMF (2) vanillin (3) 4-hydroxybenzaldehyde (4) resorcinol. Mobile phase: methanol/water (70:30, v/v) buffered with triethylamine/acetic acid, pH* = 7.0, electric conductivity = 120 μS cm^{-1}. Monolithic capillary used: total length 21.0 (corresponds to effective length 15.0) cm ×100 μm I.D.

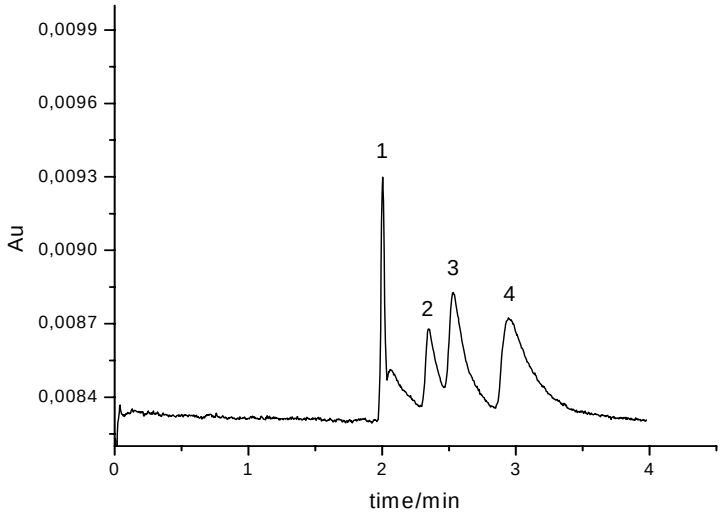

Figure 34. Mixed-mode separation of nitrotoluenes on Monolith 2. Solutes: (1) DMF (2) 4-nitrotoluene (3) 2,4-dinitrotoluene (4) 2,4,6-trinitrotoluene. Mobile phase: methanol/water (80:20, v/v) buffered with triethylamine/acetic acid, pH* = 7.0, electric conductivity = 120 μS cm^{-1}. Monolithic capillary used: total length 21.0 (corresponds to effective length 15.0) cm ×100 μm I.D.

4.11.2.2 Nonaqueous mobile phase

The monoliths employed in this study have both hydrophobic and hydrophilic structure units, such monoliths are called amphiphilic stationary phases. Therefore, they can be used in the reversed- and in the normal-phase mode [37]. I employed these monoliths for the analysis of polar analytes in the normal phase mode using different methanol/acetonitrile mixtures

buffered with 0.01% triethylamine and 0.06% acetic acid as the mobile phase. Polar phenolic compounds elute under these conditions in the order of increasing polarity (Fig. 35) and their retention factors increase with increasing volume fraction of acetonitrile in the mobile phase (Fig. 31). As expected for hydrophobic analytes in the normal-phase mode, alkylphenones and nitrotoluenes are weakly retained and have very low retention factors (0.0 in most cases).

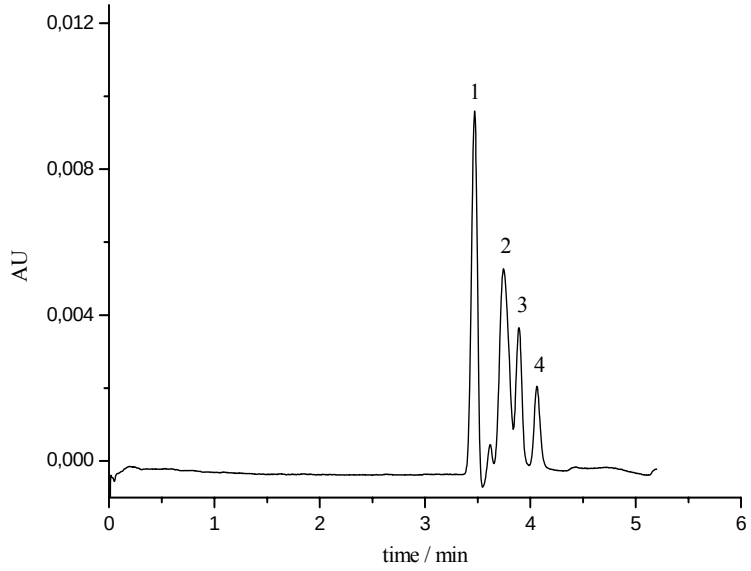

Fig. 35. Normal-phase separation of phenolic solutes on Monolith 3. Solutes: (1) DMF (2) vanilline (3) 4-hydroxy-benzaldehyde (4) resorcinol. Mobile phase: methanol/acetonitrile (60:40, v/v) buffered with triethylamine/acetic acid, pH* = 7.0, electric conductivity = 120 μS cm^{-1}. Monolithic capillary used: total length 21.0 (corresponds to effective length 15.0) cm ×100 μm I.D.

4.11.3 Comparison of CEC-monoliths with LC-columns packed with C18-silica gel

It was interesting to compare chromatographic properties (retention factors, and methylene selectivity) of the synthesized mixed-mode monolithic stationary phases with an octadecyl silica gel (Kromasil 5 C18) usually employed for packing reversed-phase HPLC-columns. Alkylphenones, alkylanilines, phenolic compounds, and nitrotoluenes were used for this study. It should be noted here that alkylanilines are neutral using methanol/aqueous buffer at pH* 7.0. Results showed that the hydrophobic alkylphenones (acetophenone, propiophenone, butyrophenone, valerophenone) have much higher retention factors on the C18-silica gel packed column compared to the monolithic stationary phases at identical composition of the mobile phase (Fig. 36). This observation was attributed to the higher intra-particle porosity (mesoporosity) of the alkylated silica gel. It is remarkable that C18-silica gel exhibited only a slightly higher hydrophobicity (expressed as methylene selectivity α_{meth}) than the monoliths synthesized in this work (0.28 for the C18-silica gel column, and 0.25, 0.20, 0.18, 0.18 for the

Monoliths 1-4, respectively, keeping the composition of the mobile phase constant; methanol/water, 60:40, v/v, buffered with triethylamine/acetic acid).

Results showed also that 4-butylaniline, 4-pentylaniline, and 4-hexylaniline followed the same behavior of alkylphenones, i.e. higher retention factors on the C18-silica gel packed column compared to the monolithic stationary phases (Fig. 36). 4-ethylaniline and 4-propylaniline, on the other hand, showed contradictory results i.e. higher retention factors on the monolithic stationary phase. The behavior for 4-ethylaniline and 4-propylaniline can be attributed to the polar interactions e.g dipole-dipole with the monolithic stationary phase as the monoliths prepared in this study have polar structure units, which can interact with the polar amine group of the alkylanilines (form hydrogen bonding, for example). These polar interactions are stronger for 4-ethylaniline and 4-propylaniline compared to hydrophobic interactions, therefore, their retention factors are higher on the monolithic stationary phase compared to the C18 silicag gel packed column. While the other alkylanilines with long alkyl chain groups (4-butylaniline, 4-pentylaniline, and 4-hexylaniline) have stronger hydrophobic interactions compared to polar interactions.

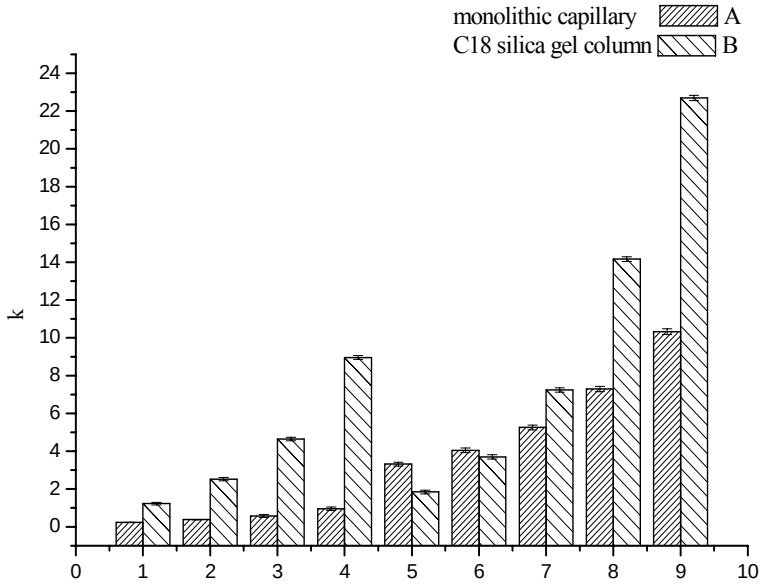

Fig. 36. Retention factors for alkylphenones and alkylanilines determined by HPLC with octadecyl silica gel as stationary phase and by CEC with Monolith 2 (standard deviation for three consecutive runs given as error bar). Solutes: (1) acetophenone (2) propiophenone (3) butyrophenone (4) valerophenone (5) 4-ethylaniline (6) 4-propylaniline (7) 4-butylaniline (8) 4-pentylaniline (9) 4-hexylaniline. Mobile phase: methanol/water (60:40, v/v) buffered with triethylamine/acetic acid, pH* = 7.0, electric conductivity = 120 μS cm^{-1}.

All the studied analytes; alkylphenones, phenolic compounds, nitrotoluenes, and alkylanilines are eluted in the order of increasing hydrophobicity from the packed C18-silica gel column using methanol/aqueous buffer as mobile phase as expected for the reversed-phase elution order (Fig. 36-37). Alkylphenones and alkylanilines follow the same retention mechanism on the monolithic stationary phase and on the C18-silica gel packed column (i.e. reversed-phase mode), Fig 36. On the other hand, the phenolic compounds and nitrotoluenes show different elution orders on the two types of stationary phases compared in this study (Fig. 37), which can be explained by a pure reversed-mode retention by C18- silica gel and a mixed-mode retention (hydrophobic interaction plus van der Waals interactions) by the monolith synthesized.

Hydrophobicity of the studied analytes can be compared using the results of HPLC study. The alkyl anilines (4-hexyl and 4- pentylaniline) have the highest retention factors, and consequently a higher hydrophobicity. The polar phenolic analytes as expected have the lowest retention factors. Nitrotoluenes have intermediate values.

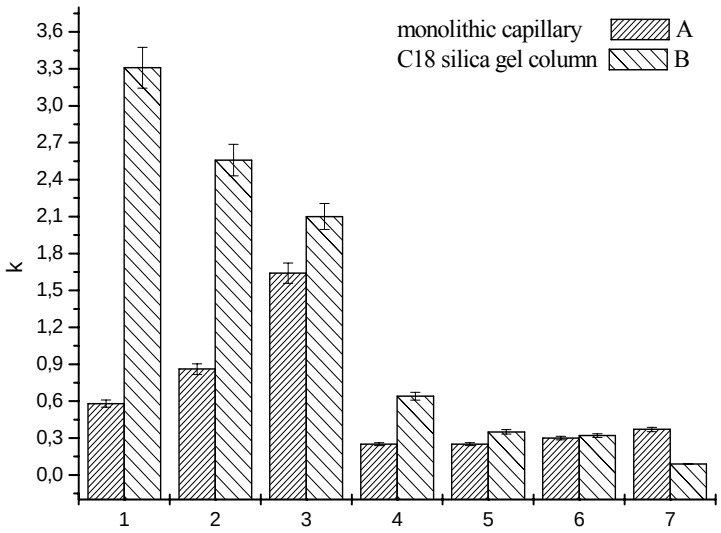

Fig. 37. . Retention factors for nitrotoluenes and phenolic analytes determined by HPLC with octadecyl silica gel as stationary phase and by CEC with Monolith 2 (standard deviation for three consecutive runs given as error bar). Solutes: (1) 4-nitrotoluene (2) 2,4-dinitrotoluene (3) 2,4,6-trinitrotoluene (4) ethylvanillin (5) vanillin (6) 4-hydroxybenzaldehyde (7) resorcinol. Mobile phase: methanol/water (60:40, v/v) buffered with triethylamine/acetic acid, pH* = 7.0, electric conductivity = 120 µS cm^{-1}.

4.11.4 Comparison of the separation on monoliths using CEC and µ-LC

It is interesting to compare the separation on these monolithic stationary phases using CEC and µ-LC. Same monolithic capillary (Monolith 1) was used for the separation using CEC and µ-LC. Results show that the efficiency for amino acids using µ-LC is lower compared to CEC (Fig. 38, Table 19), while the efficiency for alkylphenones is almost identical (Fig. 39, Table 19). The decrease in efficiency for amino acids might be attributed to the difference in the mobile phase flow mechanism; pressure-induced flow in µ-LC compared to EOF-induced flow in CEC, where this decrease in efficiency using LC compared to CEC has been observed by Freitag [66] and by Szucs et al. [112]. In the current study, however, this decrease in efficiency was not observed for alkylphenones with µ-LC using the same experimental conditions used for the amino acids. This behavior proves that the difference in the flow mechanism is not the reason of the lower efficiency obtained for amino acids.

Extra column band-broadening contributions also have to be taken into consideration, e.g. sample injection volume, detection volume, and data processing. Using CEC compared to LC, no significant band broadening due to injection, detection, and data processing because of on-column injection and on-column detection used in CEC. This can not, however, be the reason of the lower efficiency of amino acids using µ-LC because this decrease was not observed for alkylphenones using same experimental conditions. Therefore it can be concluded that the reason for the observed decrease in efficiency for amino acids must be the difference in the retention mechanism of the amino acids on CEC and µ-LC.

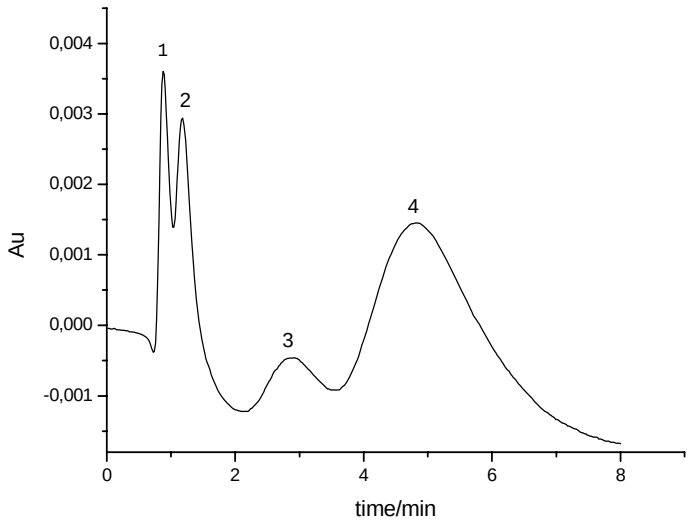

(a)

Fig 38. Continued on next page.

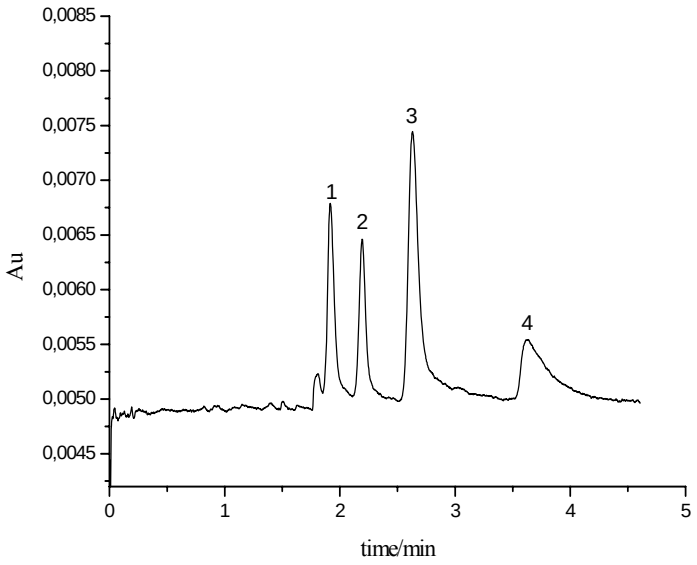

(b)

Fig. 38. Separation of amino acids on Monolith 1 by by μ-LC (a) and by CEC (b). Solutes: (1) DMF (2) phenylalanine (3) tryptophan (4) histidine. Mobile phase: methanol/20 mmol L^{-1}ammonium acetate buffer (70:30, v/v), pH* 4.0, electric conductivity = 120 μS cm^{-1}.

Monolithic capillary used for CEC: total length 21.0 (corresponds to effective length 15.0) cm ×100 μm I.D. Electrokinetic injection (7 Kv for 3 s), UV detection at 213 nm.

Monolithic capillary used for μ-LC: total length 15.0 cm ×100 μm I.D. Hydrodynamic injection (injection volume 1μL), flow rate 0.20 mL min^{-1}, UV detection at 213 nm.

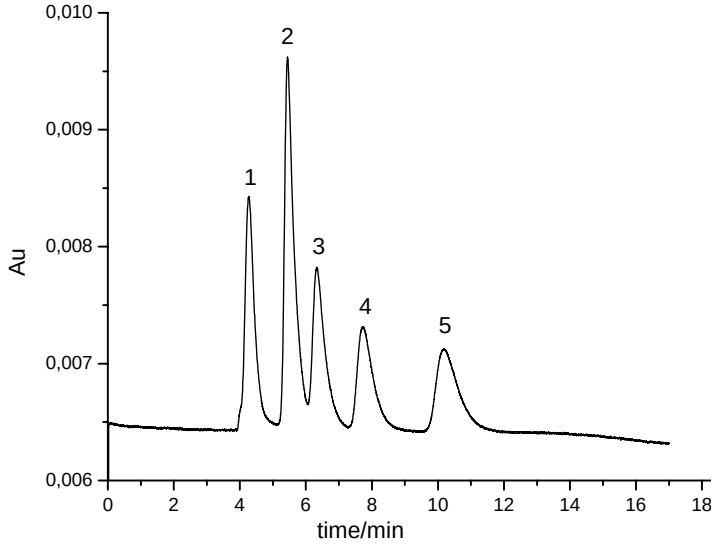

(a)

Fig 39. Continued on next page.

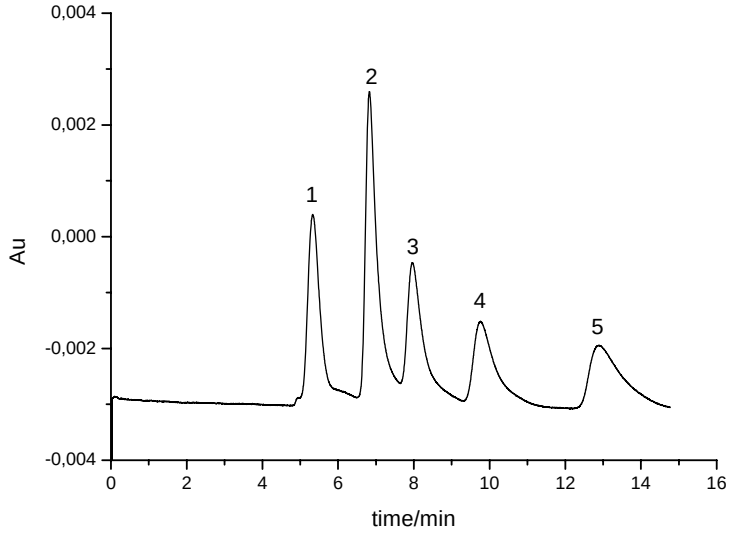

(b)

Fig. 39. Separation of alkylphenones on Monolith 1 by μ-LC (a) and by CEC (b). Solutes: (1) DMF (2) acetophenone (3) propiophenone (4) butyrophenone (5) valerophenone. Mobile phase methanol/water (70:30, v/v) buffered with triethylamine/acetic acid pH* 6.47, electric conductivity = 120 μS cm^{-1}. For other conditions, see Fig 38.

Table 19. Efficiencies of amino acids and alkylphenones separated by CEC and μ-LC. For other conditions, see Figs. 38 and 39.

Analyte	μ-LC	CEC
phenylalanine	700	47000
tryptophan	500	29000
histidine	400	11000
acetophenone	13000	19000
propiophenone	10000	14000
butyrophenone	9000	11000
valerophenone	8000	8000

4.11.5 Selectivity of weak electrolytes

The prepared mixed-mode monolithic stationary phases were applied for the separation of different charged analytes with basic amine groups: alkylanilines (4-ethylaniline, 4-propylaniline, 4-butylaniline, 4-pentylaniline, and 4-hexylaniline), different amino acids having absorption bands in the UV range (phenylalanine (p*I* 5.49), tryptophan (p*I* 5.89), and histidine (p*I* 7.60)), and several di- and tripeptides (Phe-Phe-Phe (p*I* 6.02), Phe-Phe (p*I* 6.02),

Phe-Tyr (p*I* 5.93), Phe-Arg (p*I* 11.05), and Phe-Glu (p*I* 3.29)). This set of peptides was chosen according to differences in their hydrophobicity and their isoelectric point. These analytes are charged depending on the pH of the mobile phase. Amino acids and peptides are positively charged at a pH lower than their p*I* while they are negatively charged at a pH higher than their p*I*. Buffered water/methanol mobile phase was used for this study with acidic pH* (4.0) in which these analytes have a positive effective charge, which was proven by studies with open-tubular CE (see Figs. 43, 47, and 51). It should be noted here that dissociation constants (especially acid dissociation constants) are heavily influenced in pure organic solvents, however they are not dramatically influenced in mixed aqueous-alcoholic solvents [113] like the mobile phases used in this study (aqueous-methanol). pK_a values in mixed-alcoholic solvents agree comparably well with thermodynamic pK_a ones, while large deviations are detected in pure organic solvents [113].

4.11.5.1 Determination of corrected retention factors

Charged analytes separated by CEC have an electrophoretic mobility μ_{ep} in addition to the retention due to chromatographic interactions. The studied analytes with basic amino groups (alkylanilines, amino acids, and oligopeptides) have an effective electric charge depending on the pH of the mobile phase, and therefore they have an electrophoretic mobility μ_{ep}, which affects the elution time (it is decreased if the electrophoretic mobility μ_{ep} is positive, while it is increased if μ_{ep} is negative). The corrected retention factor k_c of a charged analyte (corresponding to the definition of the retention factor k as it is used in the chromatographic nomenclature) is different from the apparent value k_{app}, which reflects both chromatographic interaction and electrophoretic migration. In order to calculate the corrected retention factor k_c, it is necessary to take into consideration the electrophoretic mobility μ_{ep} of the analyte. The electrophoretic mobility μ_{ep} can be determined from open-tubular CE experiments. Following equations are valid:

$$k_{app} = \frac{t_r - t_0}{t_0} \tag{54}$$

where k_{app} = apparent retention factor of a charged analyte in CEC, t_r = retention time of the analyte, t_0 = hold-up time.

$$k_c = \frac{t_r - t_0'}{t_0'} \tag{55}$$

where t_0' is the corrected hold-up time, which can be calculated as follows:

$$v_{eo} + v_{ep} = \frac{L_D}{t_0'} \tag{56}$$

where v_{eo} = electroosmotic flow velocity, v_{ep} = electrophoretic velocity, L_D = effective length of the capillary (CEC experiments). While v_{eo} is determined with the monolithic capillary via CEC, v_{ep} is determined by open-tubular CE with a separation buffer being identical to the mobile phase employed in CEC.

Rearrangement of this equation gives

$$t_0' = \frac{L_D}{(v_{eo} + v_{ep})} \tag{57}$$

v_{eo} and v_{ep} are determined as follows,

$$v_{eo} = \frac{L_D}{t_0} \tag{58}$$

$$v_{ep} = \mu_{ep} \frac{U}{L_{tot}} \tag{59}$$

where U = voltage, L_{tot} = total length of capillary, and μ_{ep} = electrophoretic mobility which can be determined from open-tubular CE experiments from the following equation,

$$\mu_{ep} = \frac{L_D L_{tot}}{U}\left(\frac{1}{t_M} - \frac{1}{t_0}\right) \tag{60}$$

where t_M = migration time.

Substitution the value of t_0' (Eq. 57) in equation 55 gives the value of k_c,

$$k_c = \frac{t_r - \frac{L_D}{(v_{eo} + v_{ep})}}{\frac{L_D}{(v_{eo} + v_{ep})}} \tag{61}$$

$$k_c = \frac{t_r (v_{eo} + v_{ep})}{L_D} - 1 \tag{62}$$

Using this method for the calculation of the corrected retention factor, the same equation was obtained as that derived by Rathore and Horvath [114] for the so-called electrochromatographic retention factor k''. The derived equation for k'' by Rathore and Horvath is [114],

$$k'' = \frac{t_r\left(1 + \frac{\mu_{ep}}{\mu_{eo}}\right) - t_0}{t_0} \tag{63}$$

The derived equation for corrected retention factor in this work (Eq. 62) can be transformed into k'' obtained by Rathore and Horvath as follows:

Substitution the values of v_{eo} and v_{ep} by μ_{eo} E and μ_{ep} E in equation 62 yields,

$$k_c = \frac{t_r\ (\mu_{eo} + \mu_{ep})E}{L_D} - 1 \qquad (64)$$

Substitution the value of L_D by $v_{eo}\ t_0$ in Eq. 64 yields,

$$k_c = \frac{t_r\ (\mu_{eo} + \mu_{ep})E}{v_{eo}\ t_0} - 1 \qquad (65)$$

Substitution the value of v_{eo} by μ_{eo} E in Eq. 65 yields,

$$k_c = \frac{t_r\ (\mu_{eo} + \mu_{ep})}{\mu_{eo} t_0} - 1 \qquad (66)$$

By dividing the first term of Eq. 66 by μ_{eo} yields,

$$k_c = \frac{t_r\ (1 + \frac{\mu_{ep}}{\mu_{eo}})}{t_0} - 1 \qquad (67)$$

$$k_c = \frac{t_r\ (1 + \frac{\mu_{ep}}{\mu_{eo}}) - t_0}{t_0} \qquad (68)$$

which is the same as the equation derived by Rathore and Horvath (Eq. 63).

4.11.5.2 Separation of charged analytes

The positively charged alkylanilines follow a reversed-phase elution order; they elute in the order of increasing hydrophobicity (increased length of alkyl chain) (Fig. 40). Their corrected retention factors k_c are decreased with increasing volume fraction of methanol in the mobile phase as expected for the reversed-phase mode (Fig. 41). However, their corrected retention factors are also increased with decreasing pH of the mobile phase (Fig. 42) which clearly shows the additional presence of electrostatic (ion-exchange) interaction between these positively charged analytes and the negatively charged monolithic stationary phase. This dependence would be expected for an ion-exchange retention mechanism because the degree of protonation (the effective charge) for analytes with basic amino groups (e.g. anilines, amino acids, peptides, and proteins) is increased with lower pH. Selectivity, however, was not affected by the pH* of the mobile phase. In Fig. 43 the (effective) electrophoretic mobility μ_{ep}

calculated according to Eq. (60) determined by open-tubular CE is plotted against the pH*. While at pH* = 7 the electrophoretic mobility μ_{ep} and the degree of protonation $\rightarrow$ 0, at pH* = 4 the degree of protonation $\rightarrow$ 1. Comparison of Fig. 42 and Fig. 43 clearly shows that the observed increase in k_c with decreasing pH* can clearly be ascribed to the increase in the effective charge.

The apparent and corrected retention factors of alkylanilines were compared at different pH* (Tab. 20). The apparent retention factors and corrected retention factors are identical at pH* 7.0 i.e. alkylanilines are neutral, while the corrected retention factor is higher than the apparent at pH* $\leq$ 5.90 i.e. they are positively charged. Furthermore, the difference between the corrected and the apparent retention factors increases as the pH* decreases due to the larger impact of the positive electrophoretic mobility with lower pH*, see Tab. 20.

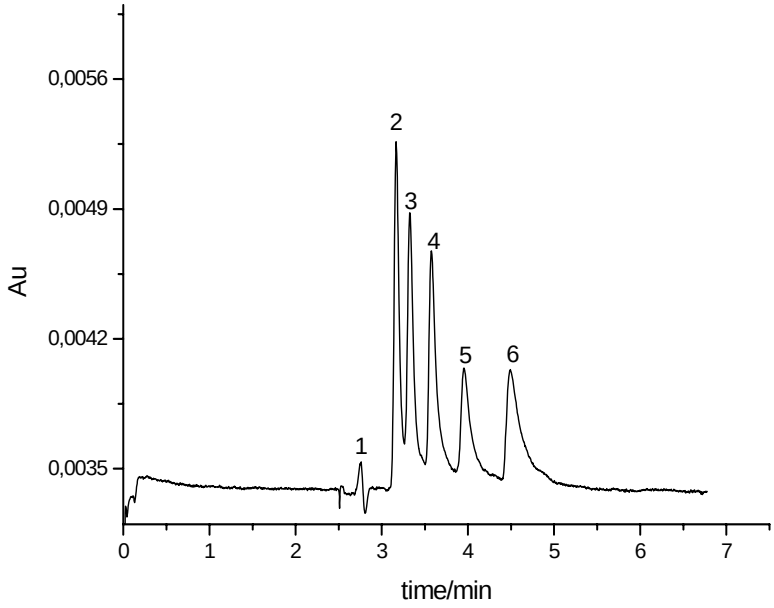

Fig. 40. CEC separation of different alkylanilines on Monolith 1. Solutes: (1) DMF (2) 4-ethylaniline (3) 4-propylaniline (4) 4-butylaniline (5) 4-pentylaniline (6) 4-hexylaniline. Mobile phase: methanol/water (80:20, v/v) buffered with triethylamine/acetic acid, pH* 4.0, electric conductivity = 120 µS cm^{-1}. Monolithic capillary used: total length 21.0 (corresponds to effective length 15.0) cm ×100 µm I.D.

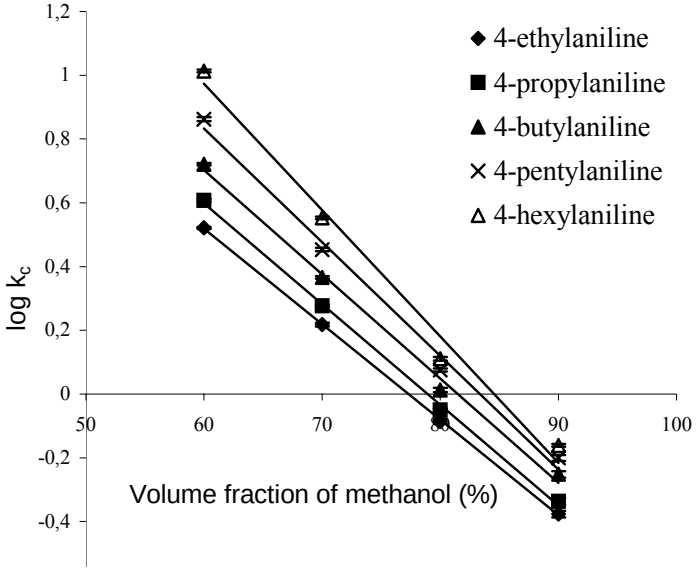

Fig. 41. Log k_c of alkylanilines on Monolith 1 vs. volume fraction of methanol in the mobile phase. Mobile phase: methanol/water, buffered with triethylamine/acetic acid, pH* 4.0, electric conductivity = 120 µS cm^{-1}. Each data point is the mean of three replicate measurements, standard deviations are represented as error bars.

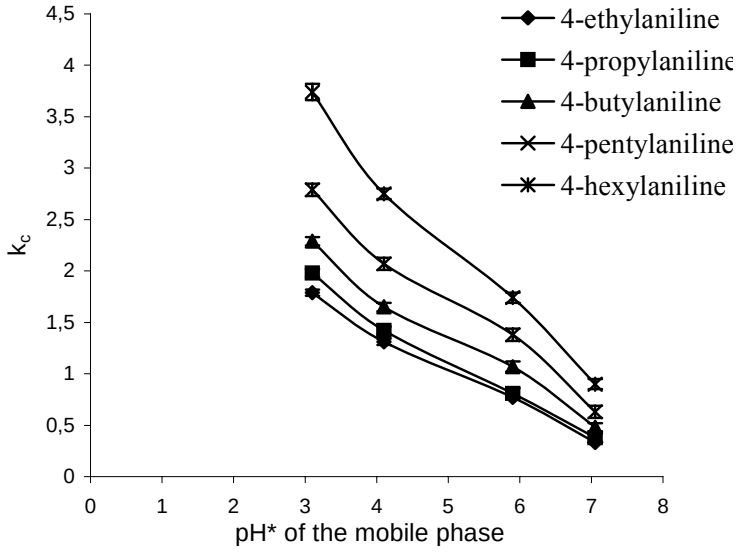

Fig. 42. Corrected retention factors of alkylanilines vs. pH* of the mobile phase on Monolith 1. Mobile phase: methanol/water (70:30, v/v) buffered with triethylamine/acetic acid, electric conductivity = 120-200 µS cm^{-1}. Each data point is the mean of three replicate measurements, standard deviations are represented as error bars.

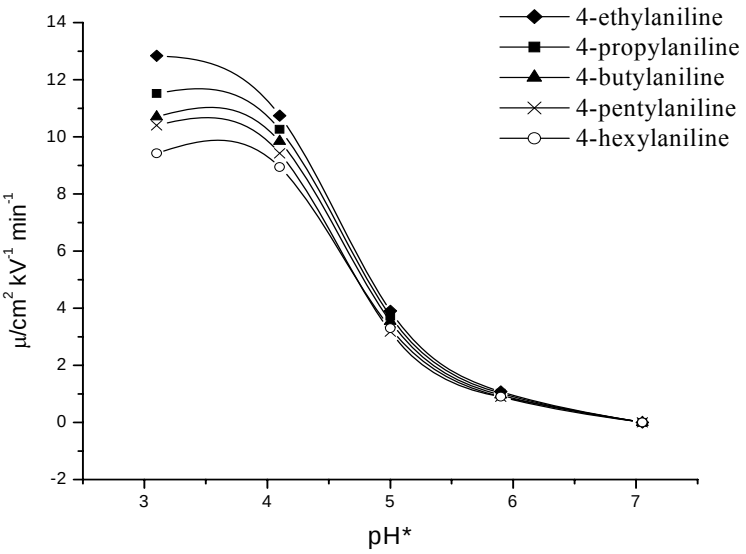

Fig. 43. Effective electrophoretic mobility μ_{ep} of different alkylanilines dependent on pH* obtained via open-tubular CE. Separation buffer: methanol/water (70:30, v/v), buffered with triethylamine/acetic acid, electric conductivity = 120-200 μS cm^{-1}. Capillary 28.0 (20.4) cm ×50 μm I.D., separation voltage 25 kV, UV detection at λ = 214 nm.

Table 20. Apparent and corrected retention factors of alkylanilines on Monolith 1 at different pH*. Mobile phase: methanol/water (70:30, v/v) buffered with triethylamine/acetic acid, electric conductivity = 120-200 μS cm^{-1}.

pH*	k values	4-ethylaniline	4-propylaniline	4-butylaniline	4-pentylaniline	4-hexylaniline
3.10	k_{app}	0.68	0.81	1.01	1.20	1.72
	k_c	1.79	1.98	2.29	2.79	3.74
4.10	k_{app}	0.48	0.54	0.78	0.91	1.28
	k_c	1.31	1.42	1.65	2.07	2.75
5.90	k_{app}	0.65	0.69	0.95	1.25	1.64
	k_c	0.77	0.81	1.07	1.38	1.74
7.05	k_{app}	0.33	0.38	0.48	0.63	0.90
	k_c	0.33	0.38	0.48	0.63	0.90

The amino acids are eluted in the increasing order of phenylalanine, tryptophan, histidine with an aqueous buffer/methanol mobile phase at both pH* 7.0 where the amino acids are neutral and at pH* 4.0 (pH* < p*I*) where the amino acids are positively charged (Fig. 44). The corrected retention factor k_c is increased with decreasing pH* of the mobile phase (Fig. 45) which indicates the contribution of electrostatic interaction since the effective charge for amino acids increases with decreasing pH*. This is shown in Fig. 46 where the (effective) electrophoretic mobility μ_{ep} calculated according to Eq. (60) determined by open-tubular CE is plotted against the pH*. While at pH* = 7 the electrophoretic mobility μ_{ep} and the degree of protonation $\rightarrow$ 0, at pH* = 4 the degree of protonation $\rightarrow$ 1. Comparison of Fig. 45 and Fig. 46 clearly shows that the observed increase in k_c with decreasing pH* can clearly be ascribed to the increase in the effective charge.

The corrected retention factors of these amino acids, however, are decreased with increasing methanol content in the mobile phase at pH* 4.0 which is in accordance with a reversed-phase retention mechanism (Fig. 47). These results show that both hydrophobic interactions (reversed-phase) and electrostatic interactions (ion-exchange) contribute to the retention of positively charged amino acids. The net effective charge of the amino acids reflected by their isoelectric points is responsible for their electrostatic interactions with the monolithic stationary phase. The basic amino acid histidine which has the highest net effective charge (isoelectric point 7.60) interacts more strongly (has higher retention factor) compared to phenylalanine or tryptophan, which have lower effective charges (isoelectric point 5.49, and 5.89, respectively). This elution order indicates that electrostatic interactions is predominant compared to hydrophobic interactions for these amino acids.

The apparent and corrected retention factors of amino acids were compared at different pH* (Tab. 21). The apparent retention factors and corrected retention factors are identical at pH* 7.0 i.e. amino acids are neutral. At pH* 5.90 corrected and apparent retention factors for phenylalnine and tryptophan are identical i.e. they are neutral while histidine is positively charged (its corrected retention factor is higher that the apparent). The corrected retention factors for amino acids are higher than the apparent at pH* $\leq$ 4.10 i.e. they are positively charged.

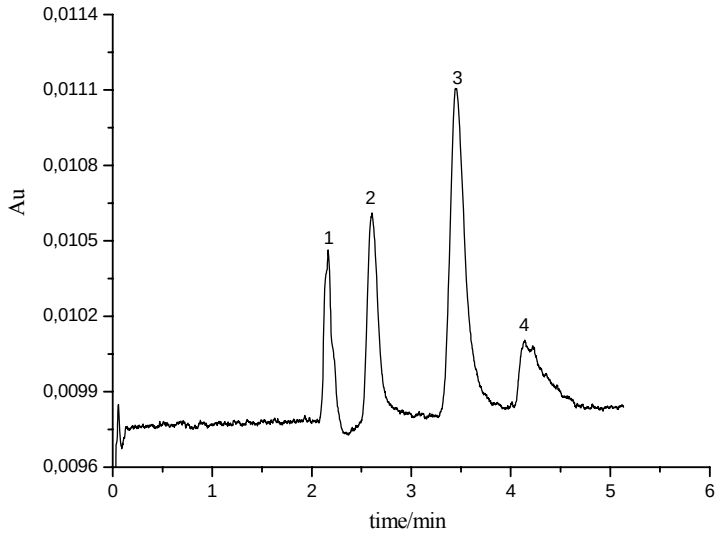

(a)

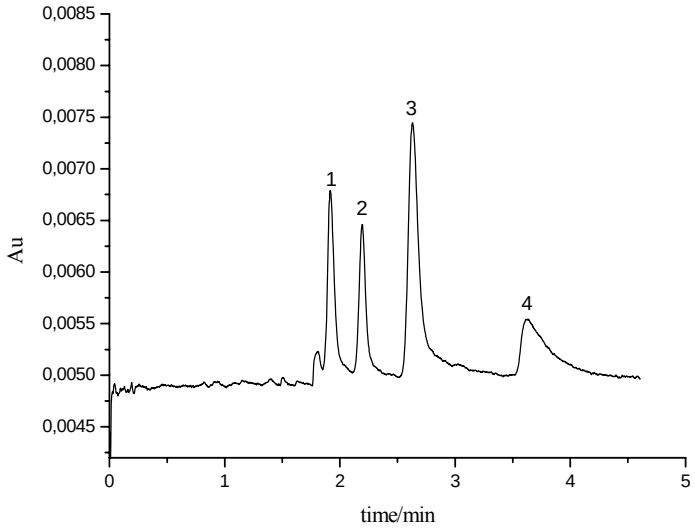

(b)

Fig. 44. CEC Separation of amino acids on Monolith 1. Solutes: (1) DMF (2) phenylalanine (3) tryptophan (4) histidine. Mobile phase: methanol/water buffer (70:30, v/v) buffered with triethylamine/acetic acid, pH* 4.0 (a) pH* 7.00 (b).

Monolithic capillary used: total length 21.0 (corresponds to effective length 15.0) cm ×100 µm I.D.

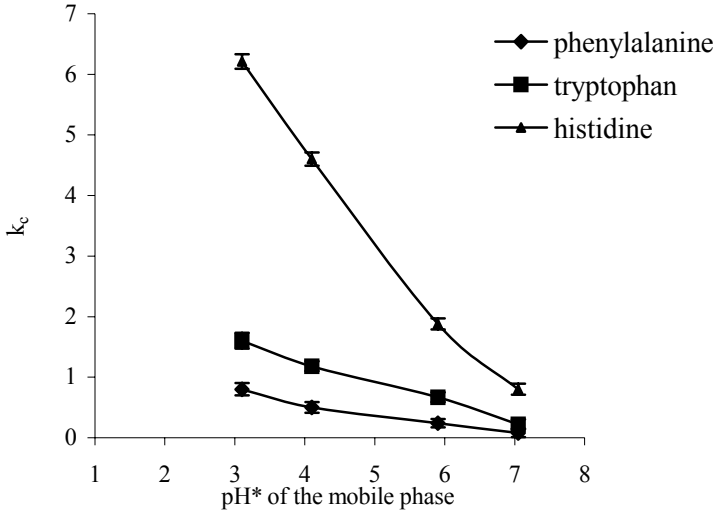

Fig. 45. Corrected retention factors of amino acids vs. pH* of the mobile phase on Monolith 1. Mobile phase: methanol/water (70:30, v/v) buffered with triethylamine/acetic acid, electric conductivity = 120-200 µS cm^{-1}.

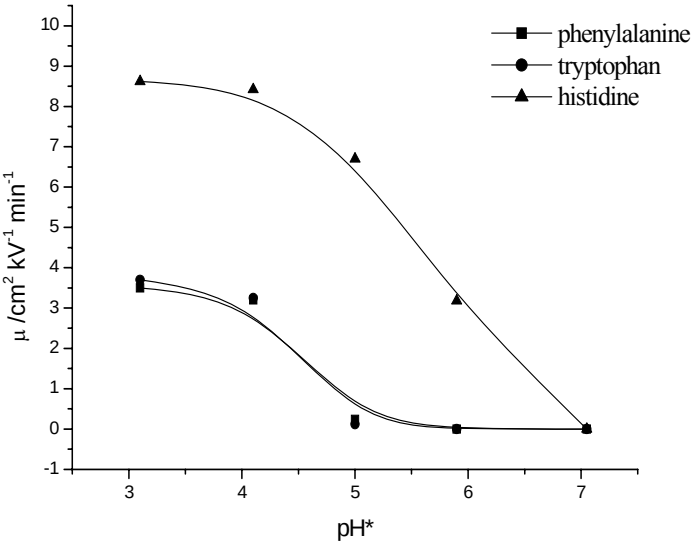

Fig. 46. Effective electrophoretic mobility μ_{ep} of different amino acids dependent on pH* obtained via open-tubular CE. Separation buffer: methanol/water (70:30, v/v) buffered with triethylamine/acetic acid, electric conductivity = 120-200 µS cm^{-1}. Capillary 28.0 (20.4) cm ×50 µm I.D., separation voltage 25 kV, UV detection at λ = 214 nm.

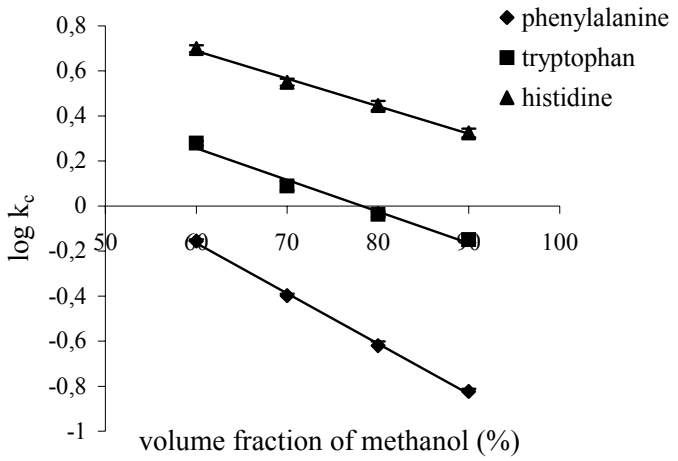

Fig. 47. log k_c of amino acids on Monolith 1 vs. volume fraction of methanol in the mobile phase. Mobile phase: methanol/water, buffered with triethylamine/acetic acid, pH* 4.0, electric conductivity = 120 µS cm^{-1}.

Table 21. Apparent and corrected retention factors of amino acids on Monolith 1 at different pH*. Mobile phase: methanol/water (70:30, v/v) buffered with triethylamine/acetic acid, electric conductivity = 120-200 µS cm^{-1}.

pH*	k values	phenylalanine	tryptophan	histidine
3.10	k_{app}	0.42	0.99	4.27
	k_c	0.80	1.60	6.21
4.10	k_{app}	0.31	0.83	2.33
	k_c	0.50	1.18	4.60
5.90	k_{app}	0.24	0.67	1.29
	k_c	0.24	0.67	1.88
7.05	k_{app}	0.08	0.22	0.80
	k_c	0.08	0.22	0.80

The monolithic capillary was also applied for the CEC separation of several short-chain peptides. These peptides are eluted with an aqueous buffer/methanol mobile phase at pH* 4.0 (pH* < p*I*) in the order of increasing net effective charge reflected by their isoelectric points (Fig. 48). Phe-Arg which has the highest net effective charge (isoelectric point 10.76) has the highest corrected retention factor compared to other analytes, while Phe-Glu which has the

lowest net effective charge (isoelectric point 3.15) has the lowest corrected retention factor. The corrected retention factor of Phe-Arg (pH* = 4.0) is decreased with increasing concentration of the ion-pairing agent 1-pentanesulfonic acid in the mobile phase which was needed for elution of this peptide (Fig. 49). The peptides Phe-Phe-Phe, Phe-Phe, and Phe-Tyr have almost identical net effective charge and p*I*. They are eluted in the order of Phe-Phe, Phe-Tyr, Phe-Phe-Phe. The tri-peptide Phe-Phe-Phe has a higher corrected retention factor than the dipeptides Phe-Phe and Phe-Tyr due to the stronger solvophobic interaction with the stationary phase. However the hydrophilic peptide Phe-Tyr has a higher corrected retention factor than the more hydrophobic peptide Phe-Phe. This phenomenon can be attributed to the contribution of Van der Waals interactions (dipole-dipole) between the stationary phase and the analyte. It is interesting to note here that polar phenolic solutes are also eluted in the order of increasing polarity using an aqueous buffer/methanol mobile phase (pH* = 7.0) (section 4.11.2.1). The observed selectivity for neutral phenolic solutes resulted in the conclusion that with this type of stationary phase both solvophobic and Van der Waals interactions (dipole-dipole) are involved in the retention of analytes with hydrophobic and polar sites (mixed-mode retention).

The corrected retention factors of the peptides selected were increased with decreasing pH* of the mobile phase (Fig. 50) which would be expected for retention by ion-exchange. In Fig. 51 the (effective) electrophoretic mobility μ_{ep} calculated according to Eq. (60) determined by open-tubular CE is plotted against the pH*. As expected, Phe-Glu has a negative mobility while Phe-Arg has a positive mobility at all studied pH* since the former is acidic with pI 3.15 while the later is basic with pI 11.05. For all peptides, the effective electrophoretic mobility increases with decreasing pH* of the mobile phase. In accordance with the results obtained for the amino acids, corrected retention factors of the peptides are also decreased with increasing methanol content in the mobile phase at pH* 4.0 as expected for a solvophobic interaction retention (Fig. 52).

The apparent retention factors of the peptides were compared with the calculated corrected retention factors at different pH* (Tab. 22). The corrected retention factors for Phe-Arg is higher than the apparent retention factors at all pH* studied as this peptide is basic with high isoelectric point (10.76) while for the acidic peptide Phe-Glu with low isoelectric point (3.15) the apparent retention factors are higher than the corrected retention factors at all studied pH*. Additionally, the apparent retention factor for Phe-Glu is 2.25 and 1.47 at pH* 6.52 and 7.05, respectively while its corrected retention factor is zero indicating that the apparent retention of

this acidic peptide on CEC is due to the negative electrophoretic mobility and not chromatographic interactions. Same behavior was also observed for Phe-Phe and Phe-Tyr at pH* 7.05 as they are negatively charged at this pH*, see Tab. 22. This behavior, however, was not observed for the hydrophobic peptide Phe-Phe-Phe as it is neutral at this pH*. This behavior can be explained by the effect of methanol present in the mobile phase on the ionization constants of these peptides. The influence of methanol content on the ionization constant of the hydrophobic peptide (Phe-Phe-Phe) might be different from the influence on the less hydrophobic peptides: Phe-Tyr and Phe-Phe.

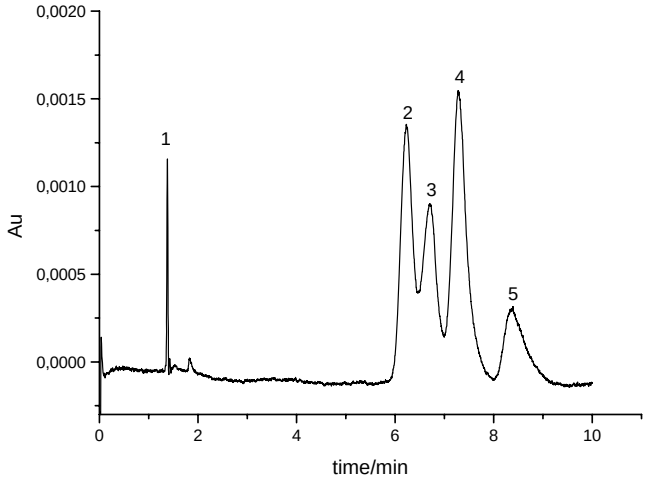

Fig. 48. CEC separation of di- and tripeptides on Monolith 1. Solutes: (1) DMF (2) Phe-Glu (3) Phe-Phe (4) Phe-Tyr (5) Phe-Phe-Phe. Mobile phase: methanol/water (90:10, v/v) buffered with triethylamine/ acetic acid, pH* 4.0, electric conductivity = 120 µS cm^{-1}. Monolithic capillary used: total length 21.0 (corresponds to effective length 15.0) cm ×100 µm I.D.

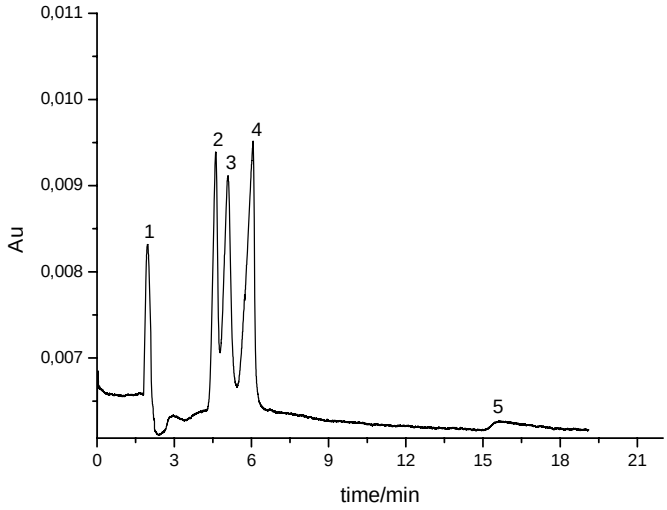

Fig. 49. CEC separation of di- and tripeptides on Monolith 1. Solutes: (1) DMF (2) Phe-Phe (3) Phe-Phe-Phe (4) Phe-Glu (5) Phe-Arg. Mobile phase: methanol/ water (90:10, v/v) buffered with triethylamine/acetic acid in the presence of 5 mmol L^{-1} 1-pentanesulfonic acid sodium salt, pH* 6.72, electric conductivity = 150 µS cm^{-1}. Monolithic capillary used: total length 21.0 (corresponds to effective length 15.0) cm ×100 µm I.D.

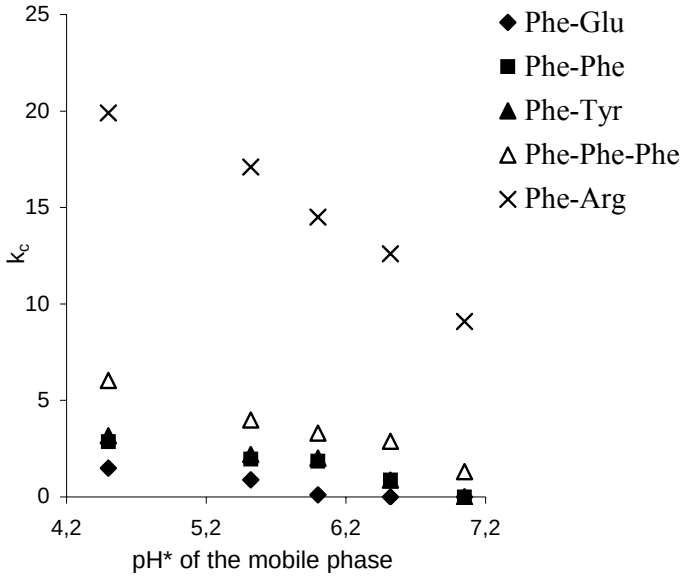

Fig. 50. Corrected retention factors of peptides vs. pH* of the mobile phase on Monolith 1. Mobile phase: methanol/water (70:30, v/v) buffered with triethylamine/acetic acid, electric conductivity = 120-200 µS cm^{-1}.

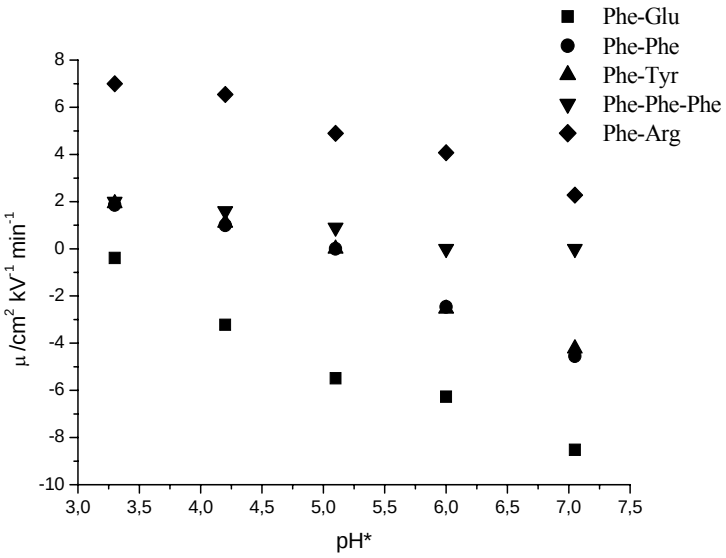

Fig. 51. Effective electrophoretic mobility μ_{ep} of different peptides dependent on pH* obtained via open-tubular CE. Separation buffer: methanol/water (70:30, v/v) buffered with triethylamine/acetic acid, electric conductivity = 120-200 µS cm^{-1}. Capillary 28.0 (20.4) cm × 50 µm I.D., separation voltage 25 kV, UV detection at λ = 214 nm.

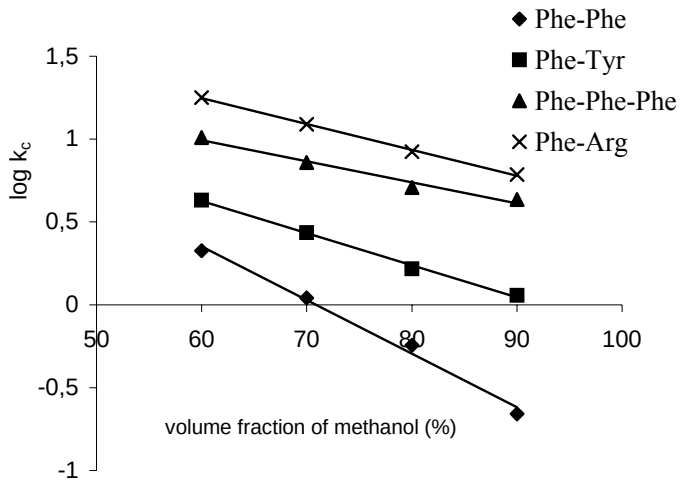

Fig 52. log k_c of peptides on Monolith 1 vs. volume fraction of methanol in the mobile phase. Mobile phase: methanol/water, buffered with triethylamine/acetic acid, pH* 4.0, electric conductivity = 120 μS cm^{-1}.

Table 22. Apparent and corrected retention factors of the peptides on Monolith 1 at different pH*. Mobile phase: methanol/water (70:30, v/v) buffered with triethylamine/acetic acid, electric conductivity = 120-200 μS cm^{-1}.

pH*	k values	Phe-Glu	Phe-Phe	Phe-Tyr	Phe-Phe-Phe	Phe-Arg
4.50	k_{app}	1.62	2.20	2.44	4.49	10.7
	k_c	1.50	2.87	3.16	6.04	19.9
5.52	k_{app}	1.72	1.96	2.20	3.78	10.4
	k_c	0.89	1.96	2.20	4.00	17.1
6.00	k_{app}	1.83	1.85	2.01	3.30	8.9
	k_c	0.11	1.85	2.01	3.30	14.5
6.52	k_{app}	2.25	1.66	1.81	2.88	7.47
	k_c	0.0	0.88	0.87	2.88	12.6
7.05	k_{app}	1.47	0.78	0.75	1.31	5.50
	k_c	0.0	0.0	0.0	1.31	9.1

4.11.6 Comparison of separation selectivity obtained by CEC and by CE

Using CEC, the charged analytes were eluted after DMF (the neutral polar EOF marker) even at acidic pH where these analytes bear a positive effective charge, which indicates that their separation is mainly achieved via differences in their corrected retention factors (solvophobic and electrostatic interactions), while their electrophoretic migration plays a minor role. In order to demonstrate that the selectivity obtained in CEC is dominated by the chromatographic process, separation selectivity of these analytes in CEC was compared with the separation selectivity obtained via open-tubular CE.

Alkylanilines are separated by CE at optimized conditions with very low resolution and with comigration of 4-pentylaniline and 4-hexylaniline (Fig. 53a). Amino acids are separated by CE at optimized conditions with comigration of phenylalanine and tryptophan (Fig. 54a). Peptides were separated by CE at optimum pH* (7.05) with comigration of the EOF marker DMF and Phe-Phe-Phe (Fig. 55a), and at pH* 4.0 with comigration of Phe-Phe, Phe-Tyr, and Phe-Phe-Phe (Fig. 55b). In contrast to these results, in CEC good peak resolutions were obtained for all solutes selected (see Figs. 53b, 54b, 55c).

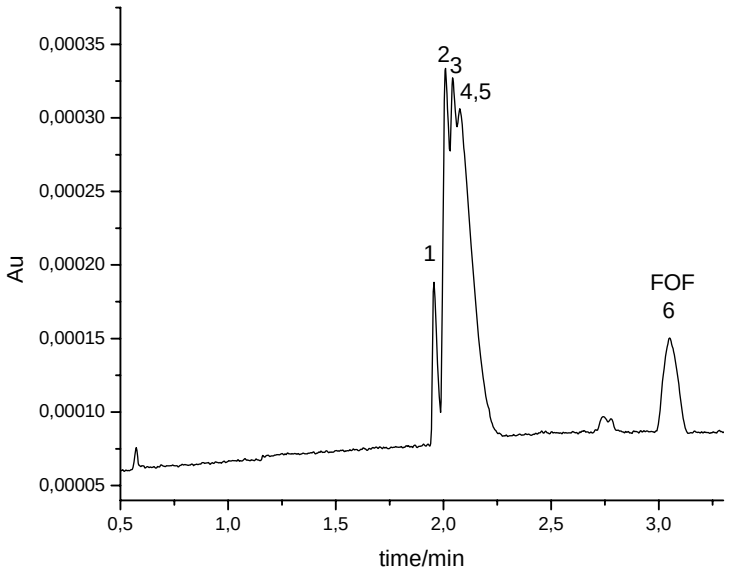

(a)

Fig 53. Continued on next page.

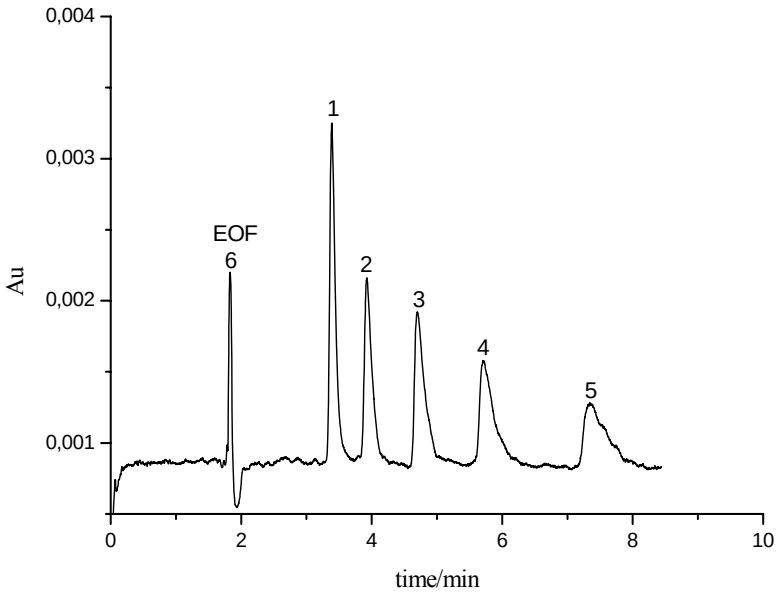

(b)

Fig. 53. Separation of alkyanilines by (a) Open tubular CE (b) CEC on Monolith 1. Solutes: 4-ethylaniline (1) 4-propylaniline (2) 4-butylaniline (3) 4-pentylaniline (4) 4-hexylaniline (5) DMF (6). Mobile phase: methanol/30 mmol L^{-1} ammonium acetate buffer (70:30, v/v), pH* 4.10, electric conductivity = 150 μS cm^{-1}. Monolithic capillary used for CEC: total length 21.0 (corresponds to effective length 15.0) cm ×100 μm I.D. Capillary used for CE 28.0 (20.4) cm × 50 μm I.D.

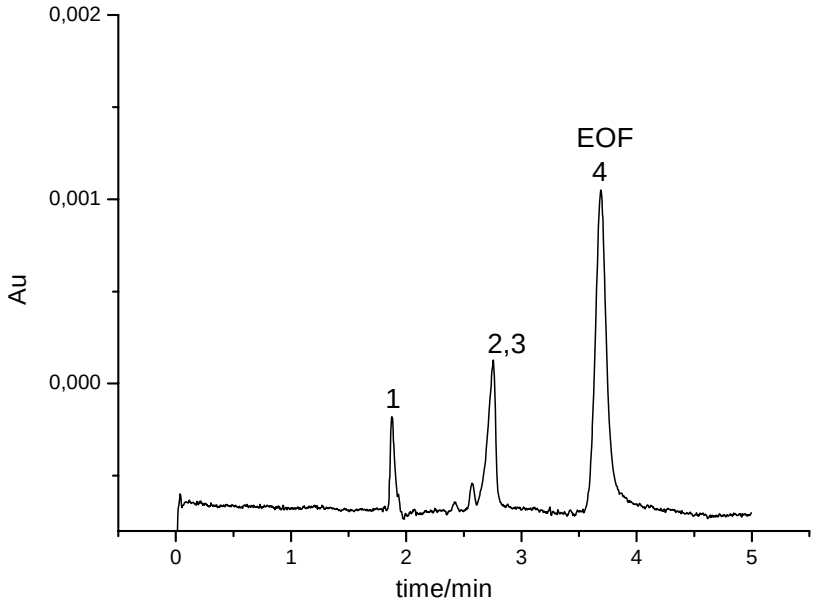

(a)

Fig 54. Continued on next page.

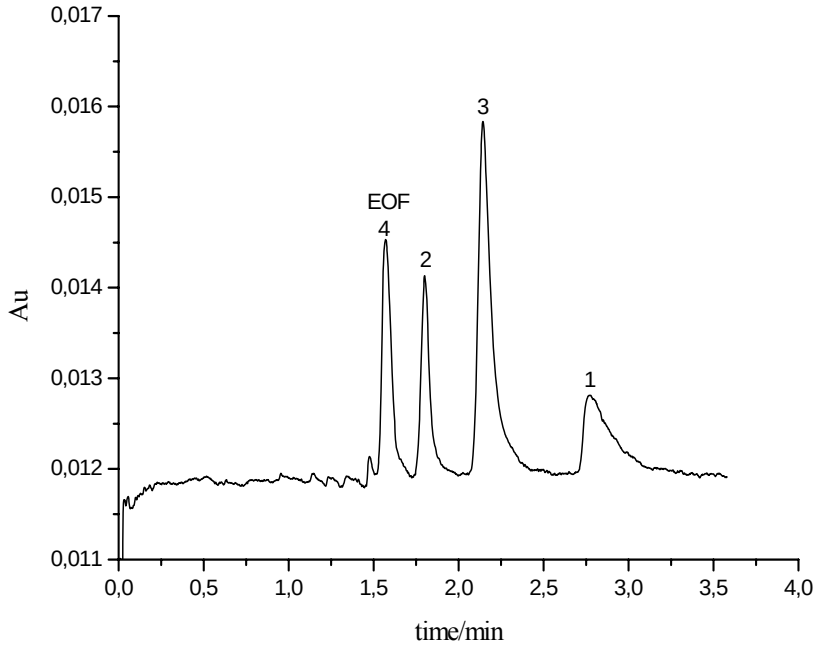

(b)

Fig. 54. Separation of amino acids by (a) Open tubular CE (b) CEC on Monolith 1. Solutes: histidine (1), phenylalanine (2), tryptophan (3), DMF (4). Mobile phase: methanol/30 mmol L^{-1} ammonium acetate buffer (70:30, v/v), pH* 4.68, electric conductivity = 120 µS cm^{-1}. Monolithic capillary used for CEC: total length 21.0 (corresponds to effective length 15.0) cm ×100 µm I.D. Capillary used for CE 28.0 (20.4) cm × 50 µm I.D.

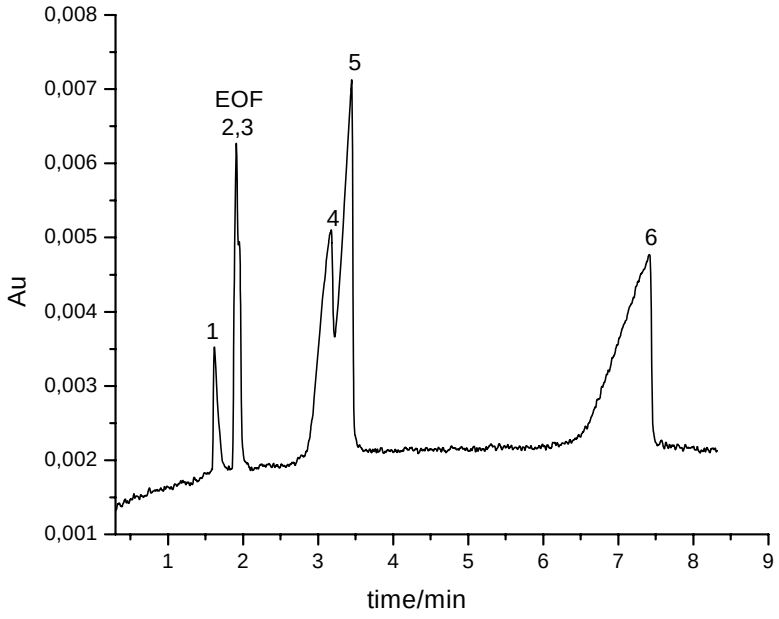

(a)

Fig 55. Continued on next page.

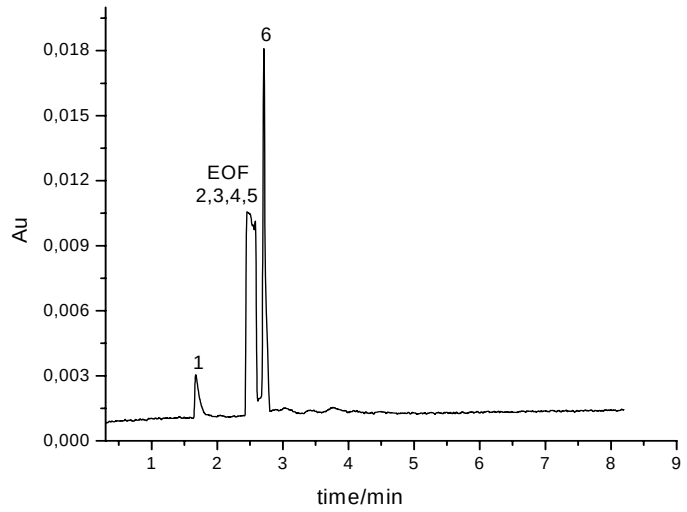

(b)

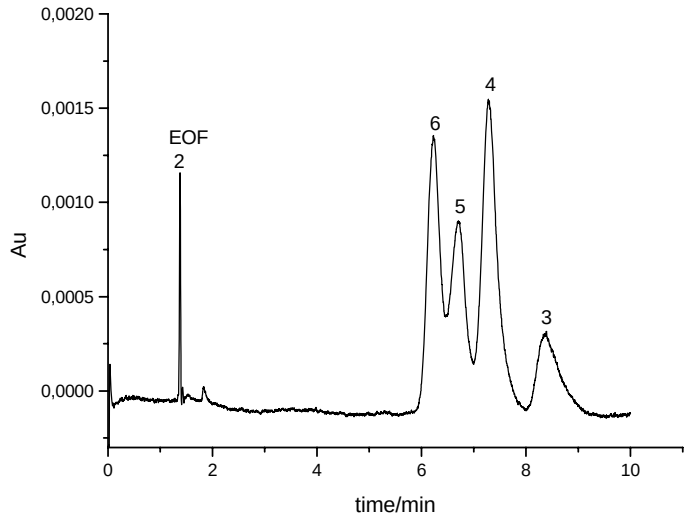

(c)

Fig. 55. Separation of peptides by (a-b) Open-tubular CE. Mobile phase: methanol/15 mmol L^{-1} ammonium acetate buffer (70:30, v/v), pH* 7.05 (a) and 4.0 (b). Capillary used: 28.0 (20.4) cm × 50 µm I.D. (c) CEC on Monolith 1. Mobile phase: methanol/water (90:10, v/v) buffered with triethylamine/acetic acid, pH* 4.50, electric conductivity = 120 µS cm^{-1}. Solutes: (1) Phe-Arg (2) DMF (3) Phe-Phe-Phe (4) Phe-Tyr (5) Phe-Phe (6) Phe-Glu. Monolithic capillary used: total length 21.0 (corresponds to effective length 15.0) cm ×100 µm I.D.

4.12 Investigation of the retention mechanism of charged analytes

The results obtained show that the retention mechanism for basic and amphoteric analytes (alkylanilines, amino acids, and peptides) is a combination of electrostatic and solvophobic interactions. It is interesting to investigate this mixed-mode retention mechanism more in detail. Therefore, the effect of the counter ion (ammonium ion) concentration in the mobile phase, the effect of the concentration of vinylsulfonic acid (VSA) in the polymerization

mixture (variation of the ion-exchange capacity), and the effect of the concentration of the hydrophobic monomer in the polymerization mixture (variation of the hydrophobicity of the stationary phase) on the corrected retention factors k_c of the charged analytes were studied.

4.12.1 Effect of counter ion concentration

In this section a methanol/aqueous solution of ammonium acetate was used as buffered mobile phase (70:30, v/v) with varied concentration of the ammonium ion, which acts as displacing cation regarding the ion-exchange process. According to Figs. 43, 47, and 51 at pH* = 4.0 (methanol/aqueous buffer (70:30, v/v)) the effective charge of the analytes investigated is close to +1.00 (except for Phe-Glu which is negatively charged at this pH, therefore it is excluded from this study). In the ion-exchange mode, the retention factor for a protonated solute HR^+ is not only determined by the ion-exchange capacity of the stationary phase, but also by the molar concentration and the type of counter-ion C^+ present in the mobile phase according to the following chemical equilibrium,

$$SO_3^-C^+ + HR^+ \rightleftharpoons SO_3^-HR^+ + C^+ \quad (69)$$

For this ion exchange reaction, the ion exchange equilibrium constant K_{IEX} can be written as,

$$K_{IEX} = \frac{[SO_3^-HR^+]_s\,[C^+]_m}{[SO_3^-C^+]_s\,[HR^+]_m} \quad (70)$$

where $[SO_3^-C^+]_s$ is the amount of substance of accessible (available) sulfonic acid sites normalized on the volume of the stationary phase, $[HR^+]_m$ is the molar concentration of the charged analyte in the mobile phase, $[SO_3^-HR^+]_s$ is the molar concentration of the analyte in the stationary phase, and $[C^+]_m$ is the molar concentration of the counter ion in the mobile phase. The retention factor k_{IEX} due to the ion-exchange process is defined as:

$$k_{IEX} = \varphi \frac{[SO_3^-HR^+]_s}{[HR^+]_m} = \varphi\, K_{IEX}\, \frac{[SO_3^-C^+]_s}{[C^+]_m} \quad (71)$$

where φ is the phase ratio (volume of stationary phase divided by volume of mobile phase). According to this equation, increasing the concentration of the counter ion $[C^+]_m$ will decrease the retention factor k_{IEX}, which is in agreement with the experimental results for alkylanilines, amino acids, and peptides (Figs. 56-58).

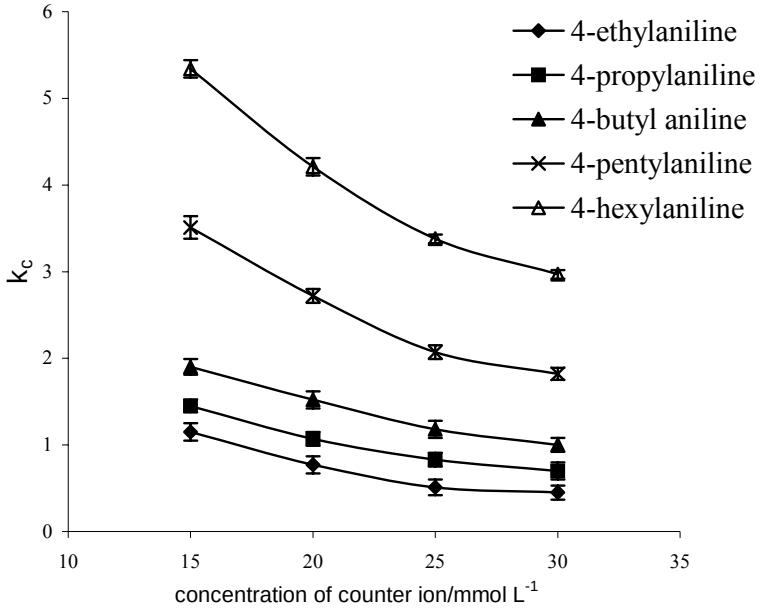

Fig. 56. Corrected retention factors k_c for alkylanilines on Monolith 1 vs. concentration of ammonium in the mobile phases. Mobile phases: methanol/ammonium acetate buffer with different concentration of ammonium (70:30, v/v), pH* 4.0, electric conductivity = 120-200 µS cm^{-1}. Each data point is the mean of three replicate measurements, standard deviations are represented as error bars.

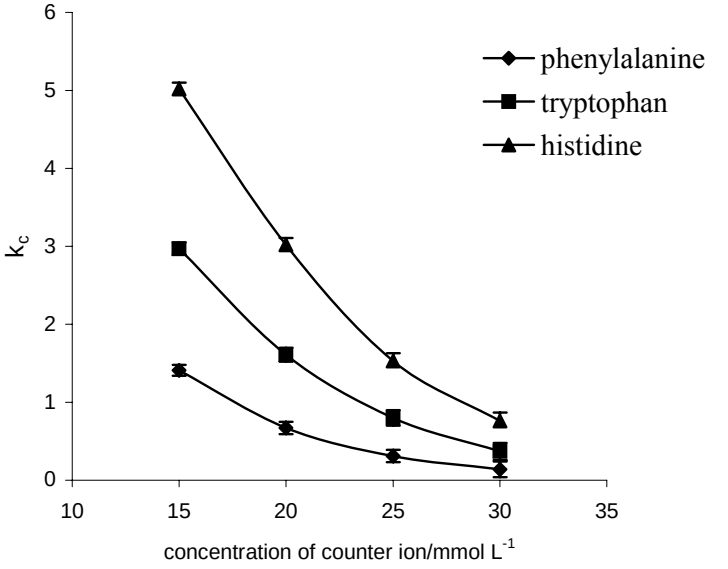

Fig. 57. Corrected retention factors of amino acids on Monolith 1 vs. concentration of ammonium in the mobile phases. Mobile phases: methanol/ammonium acetate buffer with different concentration of ammonium (70:30, v/v), pH* 4.0, electric conductivity = 120-200 µS cm^{-1}. Each data point is the mean of three replicate measurements, standard deviations are represented as error bars.

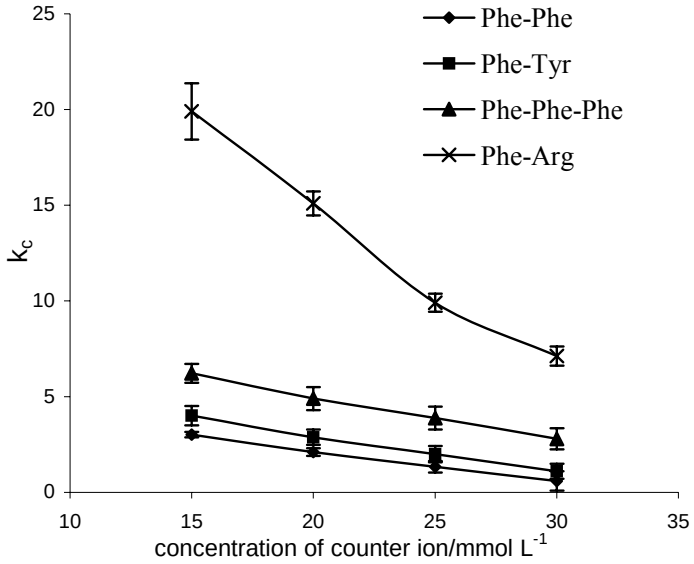

Fig. 58. Corrected retention factors of peptides on Monolith 1 vs. concentration of ammonium in the mobile phase. Mobile phases: methanol/ammonium acetate buffer with different concentrations (70:30, v/v), pH* 4.0, electric conductivity = 120-200 µS cm^{-1}. Each data point is the mean of three replicate measurements, standard deviations are represented as error bars.

4.12.2 Effect of vinylsulfonic acid concentration

The effect of the concentration of the charged monomer vinylsulfonic acid (VSA) in the polymerization mixture on the corrected retention factors for protonated analytes was investigated. According to Eq. (71) the retention factor of a positively charged analyte k_{IEX} is expected to increase with increasing number of amount of substance of accessible (available) sulfonic acid sites normalized on the volume of the stationary phase $[SO_3^-C^+]_s$ (increase in the ion-exchange capacity). In order to investigate the impact of the ion-exchange capacity on the corrected retention factors of the charged analytes, different monoliths with varied concentration of VSA in the polymerization mixture were prepared, for polymerization mixture, see Tab. 1.

As expected from Eq. (71) the corrected retention factors k_c of alkylanilines, amino acids, and the peptides are linearly correlated with the volume of VSA in the polymerization mixture (Figs. 59-61). This correlation corresponds to a linear increase in k_{IEX} with increasing $[SO_3^-C^+]_s$. It would also be interesting to note here that the y-intercepts of the plot k_c vs. volume of VSA, which are the corrected retention factors for alkylanilines without VSA in the monoliths, are different from zero (0.25, 0.56, 0.84, 1.03, 1.48 for 4-ethylaniline, 4-propylaniline, 4-butylaniline, 4-pentylaniline, and 4-hexylaniline, respectively). This observation proves that hydrophobic interactions, in addition to electrostatic interactions, play

a role in the retention of alkylanilines on the monolithic stationary phases. The y-intercepts for peptides are also higher than zero (0.51, 0.84, 1.50, 2.30 for Phe-Phe, Phe-Tyr, Phe-Phe-Phe, and Phe-Arg, respectively). The y-intercepts of the amino acids, on the other hand, are not different from zero, which indicates that hydrophobic interactions play a negligible role in their retention compared to electrostatic interactions.

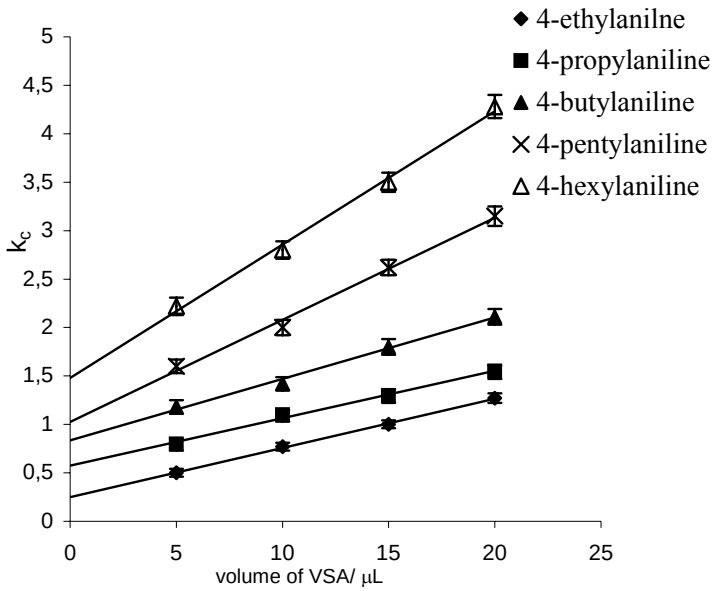

Fig. 59. Corrected retention factors of alkylanilines on Monoliths 6-9 vs. volume of VSA monomer present in the polymerization mixture. Mobile phase: methanol/30 mmol L^{-1} ammonium acetate buffer (70:30, v/v), pH* 4.0, electric conductivity = 120 µS cm^{-1}. Each data point is the mean of three replicate measurements, standard deviations are represented as error bars.

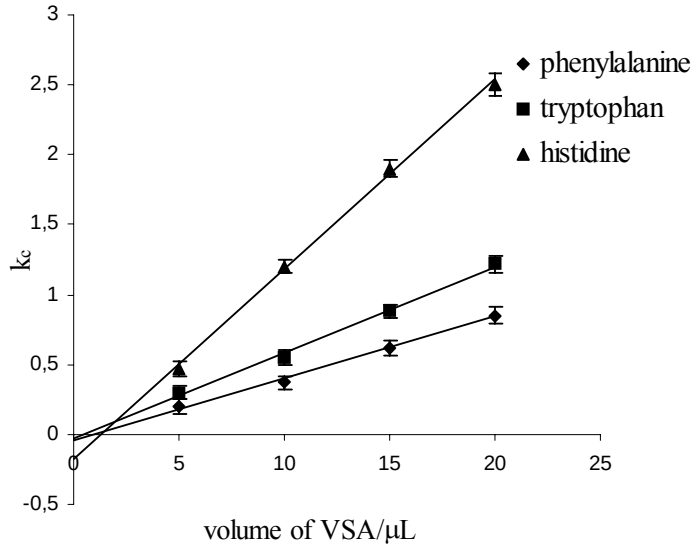

Fig. 60. Corrected retention factors of amino acids on Monoliths 6-9 vs. volume of VSA present in the polymerization mixture. Mobile phase: methanol/30 mmol L^{-1} ammonium acetate buffer (70:30, v/v), pH* 4.0, electric conductivity = 120 µS cm^{-1}. Each data point is the mean of three replicate measurements, standard deviations are represented as error bars.

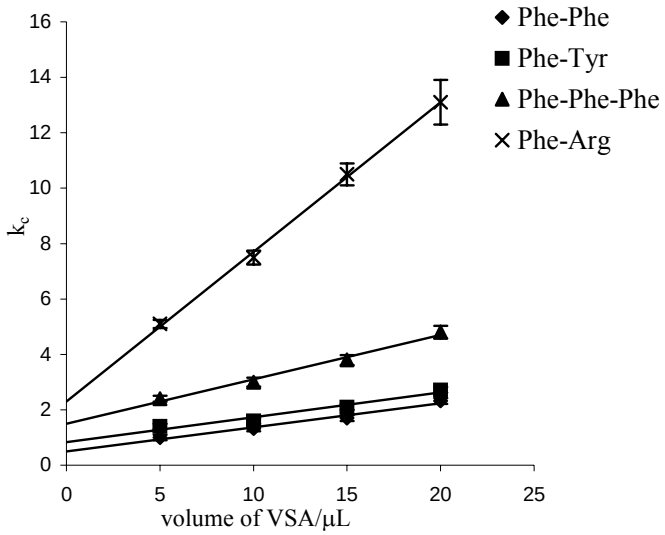

Fig. 61. Corrected retention factors of peptides on Monoliths 6-9 vs. volume of VSA present in the polymerization mixture. Mobile phase: methanol/30 mmol L^{-1} ammonium acetate buffer (70:30, v/v), pH* 4.0, electric conductivity = 120 µS cm^{-1}. Each data point is the mean of three replicate measurements, standard deviations are represented as error bars.

VSA has a hydrophilic structure unit, therefore the increase of its molar concentration in the polymerization mixture will decrease the hydrophobicty of the monolithic stationary phase which in turn decreases the retention factors of noncharged analytes (reversed-phase mode). Retention factors of neutral alkylphenones were decreased with increasing volume of VSA present in the polymerization mixture (Fig. 62).

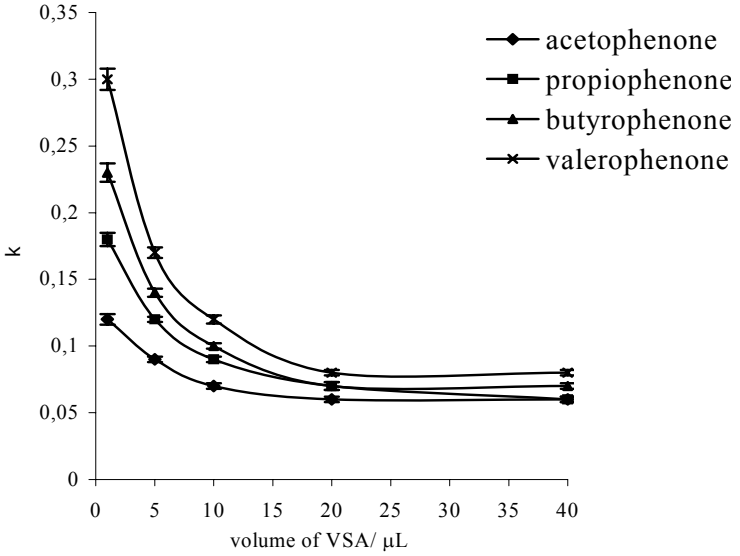

Fig. 62. Retention factors of alkylphenones on Monoliths 10-14 vs. volume of VSA present in the polymerization mixture. Mobile phase: methanol/water (80:20, v/v) buffered with triethylamine/acetic acid, pH* 6.80, electric conductivity = 120 µS cm^{-1}. Each data point is the mean of three replicate measurements, standard deviations are represented as error bars.

Electroosmotic mobility depends on the surface charge density, therefore it is expected that the electroosmotic mobility increases with increasing amount of substance of accessible (available) sulfonic acid sites normalized on the volume of the stationary phase $[SO_3^-C^+]_s$. Results show that electroosmotic mobility was increased with increasing volume of VSA in the polymerization mixture from 5 to 10 µL, when increasing further the content of VSA in the polymerization mixture only a slight increase in the electroosmotic mobility was observed with increasing the concentration of VSA from 10 to 20 µL (Fig. 63) due to charge condensation taking place at higher surface charge density where the major parts of covalently attached negatively charged sulfonic acid groups will be neutralized by fixed counter ions.

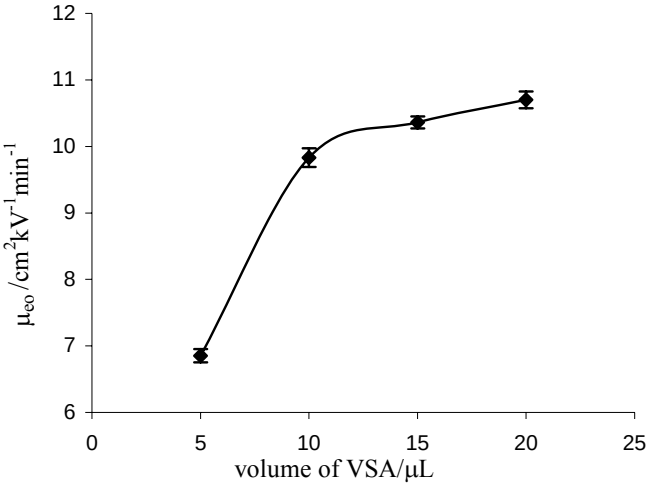

Fig. 63. Electroosmotic mobility of Monoliths 6-9 vs. volume of VSA present in the polymerization mixture. Mobile phase: methanol/ammonium acetate buffer (70:30, v/v), pH* 5.0, electric conductivity = 120 µS cm^{-1}. Each data point is the mean of three replicate measurements, standard deviations are represented as error bars.

4.12.3 Effect of isobornyl methacrylate concentration

It was also interesting to study the effect of the mass fraction of the hydrophobic monomer e.g. isobornyl methacrylate present in the polymerization mixture on the retention factors of charged analytes. Previous investigations have shown that the hydrophobicity of the monolithic stationary phase is increased by increasing the mass fraction of the hydrophobic monomer in the polymerization mixture, see section 4.7. Accordingly, different monoliths were synthesized varying the mass fraction of isobornyl methacrylate monomer in the polymerization mixture. In these experiments different mass ratios of isobornyl methacrylate to methacrylamide (keeping the sum of masses constant) were copolymerized, for polymerization conditions, see Tab. 2. With this procedure it is possible to vary the total number of isobornyl groups per unit mass of copolymer. Methacrylamide is a very polar

monomer, which is expected not to enable solvophobic interaction of the solutes with the stationary phase.

The experimental results support the postulation that also in case of protonated analytes solvophobic interactions cannot be neglected. The corrected retention factors k_c for the protonated analytes were increased with increasing mass fraction of isobornyl methacrylate in the polymerization mixture (Figs. 64-66), which is in accordance with an increase in k_c with increasing hydrophobicity of the stationary phase.

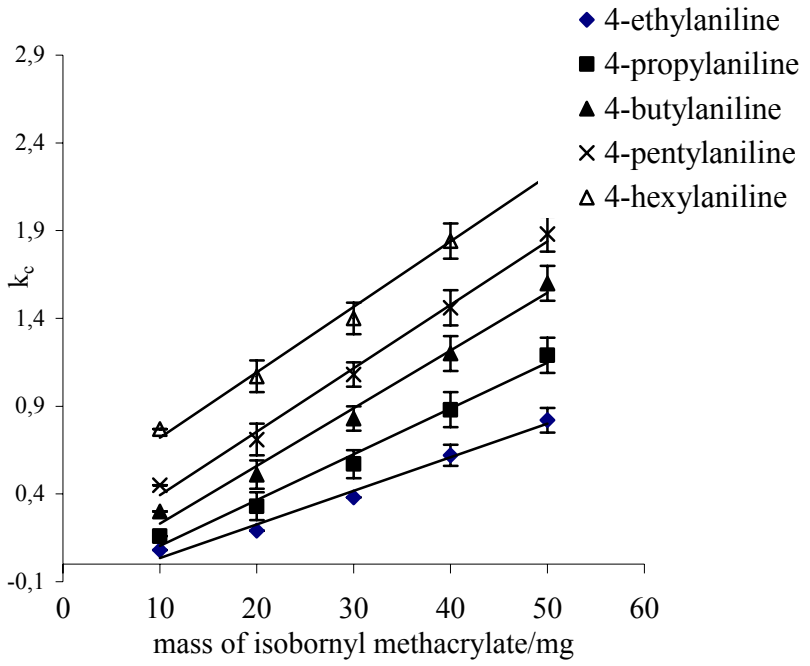

Fig. 64. Corrected retention factors of alkylanilines vs. mass of isobornyl methacrylate monomer present in the polymerization mixture. Mobile phase: methanol/30 mmol L^{-1} ammonium acetate buffer (70:30, v/v), pH* 4.0, electric conductivity = 120 µS cm^{-1}. Each data point is the mean of three replicate measurements, standard deviations are represented as error bars.

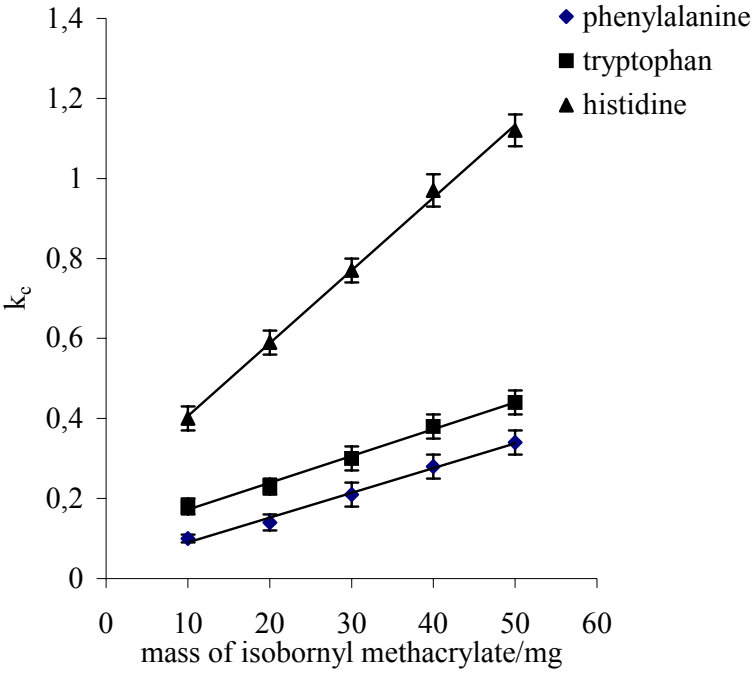

Fig. 65. Corrected retention factors of amino acids vs. mass of isobornyl methacrylate monomer present in the polymerization mixture. Mobile phase: methanol/30 mmol L^{-1} ammonium acetate buffer (70:30, v/v), pH* 4.0, electric conductivity = 120 µS cm^{-1}. Each data point is the mean of three replicate measurements, standard deviations are represented as error bars.

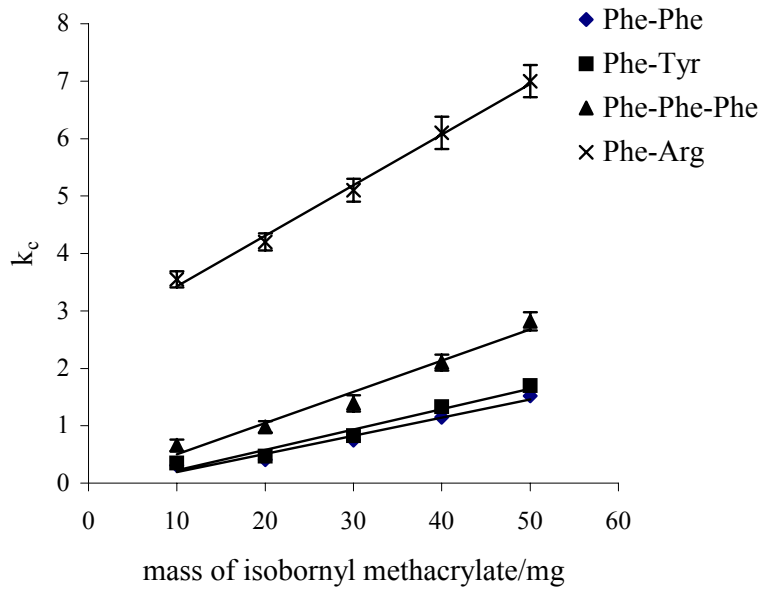

Fig. 66. Corrected retention factors of peptides vs. mass of isobornyl methacrylate monomer present in the polymerization mixture. Mobile phase: methanol/30 mmol L^{-1} ammonium acetate buffer (70:30, v/v), pH* 4.0, electric conductivity = 120 µS cm^{-1}. Each data point is the mean of three replicate measurements, standard deviations are represented as error bars.

4.13 Investigation of the quantitative relationship between solvophobic and ion-exchange interactions

In view of the results obtained from the previous studies, the major modes of retention of the charged analytes on the monolithic stationary phases by CEC are hydrophobic and ion-exchange (electrostatic) interactions which can be denoted as a mixed-mode mechanism. The influence of reversed-phase and ion-exchange interactions on the chromatographic retention of positively charged analytes is qualitatively well recognized, however, the quantitative relationship between hydrophobic and ion-exchange interaction is not clear. A study by Yang and coworkers [115] has developed a quantitative measure of the relative amount of reversed-phase and ion-exchange interaction regarding a given solute, stationary phase and mobile phase composition. They have also compared several retention models for mixed-mode retention on silica-based and coated zirconia phases, which correspond to distinctly different physical interpretations of the retention process: the one site and the two-site model. It is assumed that the same principles of investigation are applicable to the mixed-mode monolithic stationary phases prepared in this study. Therefore, these models were applied to the monoliths in this work in order to analyze qualitatively and quantitatively the contributions of ion-exchange and reversed-phase interactions to the overall retention of the positively charged analytes.

The one-site model of mixed-mode retention of basic solutes in RPLC was illustrated by Neue and coworkers [116]. For a cationic solute, Neue and coworkers have assumed that both reversed-phase and ion-exchange interactions take place simultaneously at a single type of site (Fig. 67). They combined the retention effects of cation-exchange and reversed-phase interaction (regarding one analyte) by summing up the free energies ΔG° for the phase transition of both types of interactions:

$$\ln k_c = \ln j + \left(\frac{\Delta G_{RP}^{o}}{RT} + \frac{\Delta G_{IEX}^{o}}{RT}\right) \qquad (72)$$

where ΔG_{RP}^{o} and ΔG_{IEX}^{o} are the free energy contributions from the reversed-phase and ion-exchange interaction, respectively. It is important to note that according to this model the overall corrected retention factor k_c results from the product $k_{RP}\, k_{IEX}$.

Taking into account the dependence of the ion-exchange retention factor k_{IEX} on the counter ion concentration $[C^+]_m$ (Eq. 71), the following expression is obtained.

$$k_c = k_{RP} \frac{j\ K_{IEX}\ [SO_3^-\ C^+]_s}{[C^+]_m} \quad (73)$$

Where k_{RP} is the reversed-phase retention factor.

According to this equation, the only interaction that a positively charged solute undergoes is a simultaneous interaction with both the hydrophobic group and the ionized sulfonic acid group (see Fig. 68) [115]. This site is called, according to Neue and coworkers [116], hydrophobically assisted ion-exchange site.

Taking the decadic logarithm of Eq. 73 results in:

$$\log k_c = A' + \log k_{RP} - \log[C^+]_m \quad (74)$$

where A´ is a constant equal to $\log(j\ K_{IEX}\ [SO_3^-\ C^+]_s)$. Following the Martin equation [117] (Eq. 75) $\log k_{RP}$ can be replaced by an expression containing the methylene group number n_{CH2} [115].

$$\log k_{RP} = A + B\ n_{CH2} \quad (75)$$

$$\log k_c = A'' + B\ n_{CH2} - \log[C^+]_m \quad (76)$$

where A´´ = A + A´. This equation predicts that the slope of $\log k_c$ vs. $\log [C^+]_m$ for a cationic solute with an effective charge $\rightarrow$ +1 having a displacing cation of charge +1 in the mobile phase must be close to -1. Taking the molar concentration instead of the activity small deviations from the ideal value are expected. However, these deviations will be low with a low maximum concentration of the counter ion of 30 mmol L^{-1}. Simultaneously, for a homologous series of cationic analytes (e.g. protonated alkyl anilines) there will be a linear dependence of $\log k_c$ on n_{CH2} and the slope of this plot (which corresponds to the methylene selectivity) must be the same as for a nonpolar, non-ionic homologous series [115].

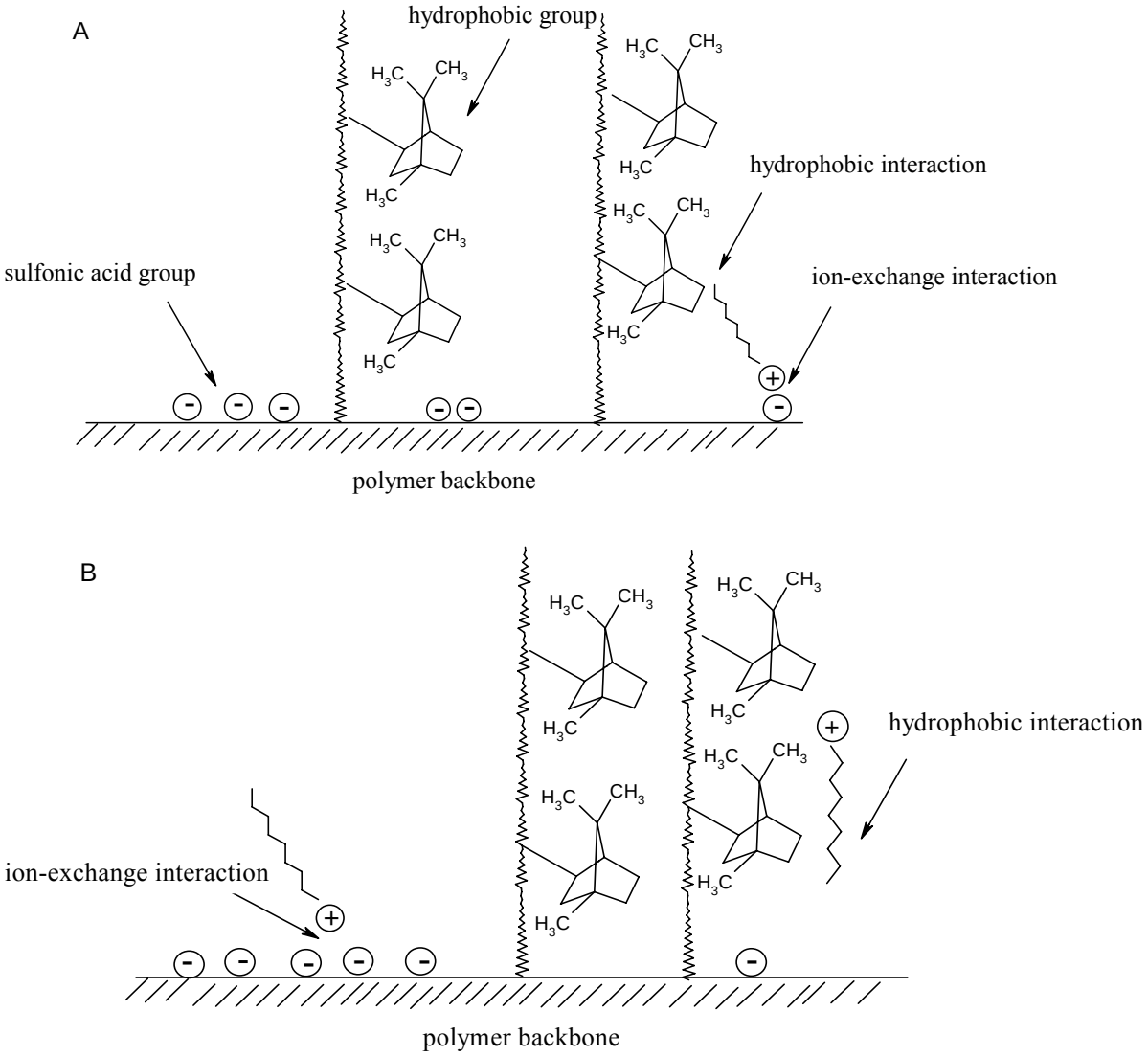

Fig. 67. Schematic illustration of the interaction of a cationic solute binding on the mixed-mode polymeric stationary phase prepared in this study according to the one site model (A) and to the two-site model (B) (according to [115]).

Retention of charged solutes on a mixed-mode stationary phase may also take place according to the two-site model, which has been originally proposed by Sokolowski and Wahlund [118] and was further elaborated by Nahum and Horvath [119]. In this model, solutes are assumed to bind to the surface having distinct reversed-phase and sulfonic acid sites (Fig. 67b). The key assumption of this model is that the two different binding sites (the hydrophobic moieties and the sulfonic acid groups) are locally separated and independent. Therefore, solute molecules interact independently with the two types of sites, and retention is the sum of two independent processes [115]:

$$k_c = j_{RP} K_{RP} + j_{IEX} K_{IEX} = k_{RP} + k_{IEX} \quad (77)$$

Thus, according to this model, retention is treated as if two different stationary phases are mixed; retention by one of the stationary phases is pure reversed-phase retention, while retention by the other stationary phase other is pure ion-exchange interaction.

Substitution of k_{IEX} with $\frac{\varphi\ K_{IEX}\ [SO_3^-\ C^+]_s}{[C^+]_m}$ (Eq. 71) in Eq. 77 yields:

$$k_c = k_{RP} + \frac{\varphi\ K_{IEX}\ [SO_3^-\ C^+]_s}{[C^+]_m} \tag{78}$$

Taking the decadic logarithm of Eq. 78 results in:

$$\log k_c = \log \left(k_{RP} + \frac{\varphi\ K_{IEX}\ [SO_3^-\ C^+]_s}{[C^+]_m} \right) \tag{79}$$

Because k_{RP} is only very weakly dependent on the counter-ion concentration in the mobile phase, the first term inside parenthesis of the logarithm on the right hand side of Eq. 79 can be regarded to be constant, whereas the second term is inversely proportional to the eluent counter ion concentration (the term $\varphi\ K_{IEX}\ [SO_3^-C^+]_s$ is constant). If k_{RP} is much larger than k_{IEX}, the two-site model results in a slope close to zero for the plot of log k_c vs. log $[C^+]_m$. On the other hand, if k_{IEX} is much larger than k_{RP}, the slope will be -1. Regarding the relation between n_{CH2} and k_c, a straight line with the same slope as for a homolog series of nonpolar solutes will be obtained only, if the contribution of solvophobic interaction to retention is much larger than the ion-exchange contribution ($k_{RP} >> k_{IEX}$) [115]. If the retention process is due to solvophobic and ion-exchange interaction, nonlinearity of the function $\log k_c = f([C^+]_m)$ is expected.

Other valuable information regarding the contribution of ion-exchange and reversed-phase to the retention can be obtained from the plot of k_c vs. $1/[C^+]_m$ (see Eq. (78)). If there is only one type of site (one-site model), the intercept of this plot will be zero, while the y-intercept will be finite if there are two types of sites (two-site model, ion-exchange site and hydrophobic site). Moreover, a large slope relative to the intercept indicates that ion-exchange interactions predominate [115].

On the basis of these two models, the contributions of solvophobic interaction and ion-exchange to the overall retention of the charged analytes on the monolithic stationary phase prepared in this study were analyzed. A plot of log k_c vs. log $[NH_4^+]$ for alkylanilines is linear with a slope close to -1 (Fig. 68). Simultaneously, there is a linear dependence of log k_c on n_{CH2} with regression coefficient of 0.99 (Fig. 69). Additionally, the slope of this plot (0.20) is the same as for a homolog series of nonpolar non-ionic alkylphenones (here B = 0.20, using

methanol/aqueous buffer, 70:30, v/v, pH* 7.0), see Tab. 15. These observations clearly indicate that the experimental results are best described with a hydrophobically assisted ion-exchange one-site model.

For the peptides Phe-Phe, Phe-Tyr, and Phe-Phe-Phe, a slope of about -1 is obtained for the plot of log k_c vs. log [NH_4^+] (Fig. 70), which is also according to the hydrophobically assisted ion-exchange one-site model. Plots of log k_c vs. log [NH_4^+] for the Phe-Arg peptide and the amino acids (phenylalanine, tryptophan, histidine), on the other hand, resulted in a slope having an absolute value >> |-1|, which is expected neither for the one-site nor for the two-site model (Figs. 70-71). One explanation of this unexpected result could be that the proposed models and equations do not apply to these analytes as they can be assumed to have an effective charge >> 1 and to possess structure units with high local dipole moment being able to undergo hydrogen bonding with the stationary phase. Likewise, the amino acids, which are very polar can have multiple positive charges depending on the pH. For instance, tryptophan and histidine can be doubly protonated resulting in an effective charge of +2 as they have two amine groups that can be protonated. Additionally, this applies for the basic peptide Phe-Arg which has multiple (four) amine groups that could be protonated resulting in multiple charges. Furthermore, the shape of alkylanilines could be envisaged as a linear structure having amine group on one side and alkyl group at the opposite side, which suits well the proposed models of a (hydrophobic) cationic solute binding on the mixed-mode polymeric stationary phase. However, amino acids (and peptides) do not have this property.

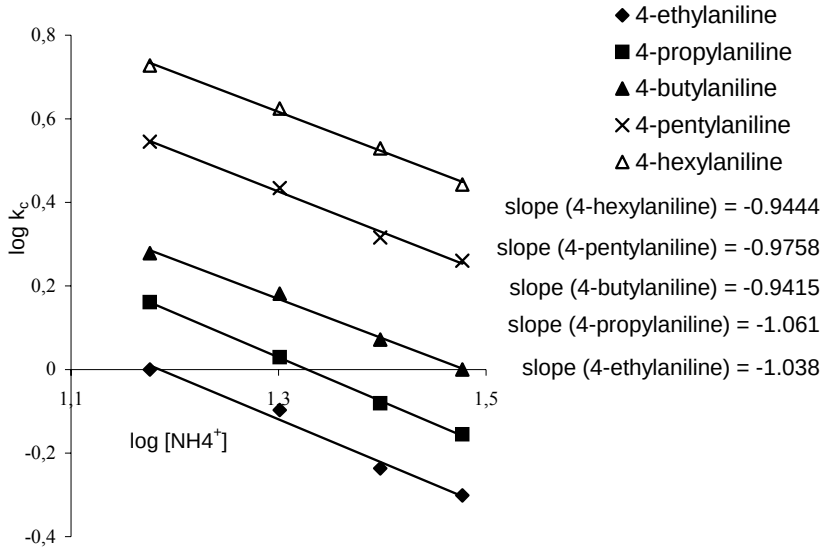

Fig. 68. Log k_c vs. log [NH_4^+] of different alkylanilines on Monolith 1. Mobile phases: methanol/ammonium acetate buffer with different concentration of ammonium (70:30, v/v), pH* 4.0, electric conductivity = 120-200 μS cm^{-1}.

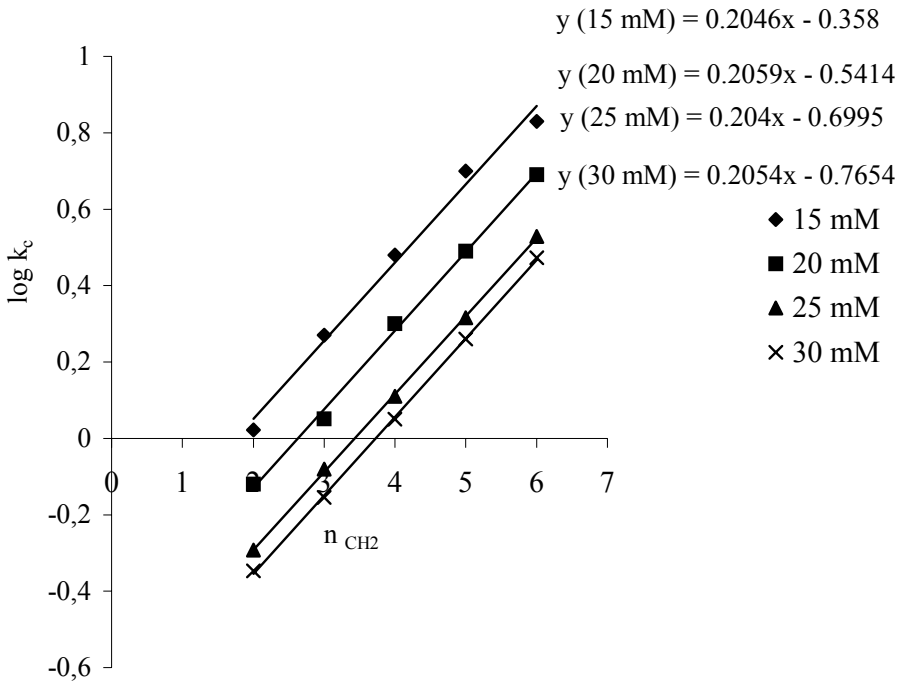

Fig. 69. Log k_c vs. number of methylene groups for a series of alkylanilines. Mobile phases: methanol/ammonium acetate buffer with different concentration of ammonium (70:30, v/v), pH* 4.0, electric conductivity = 120-200 μS cm^{-1}.

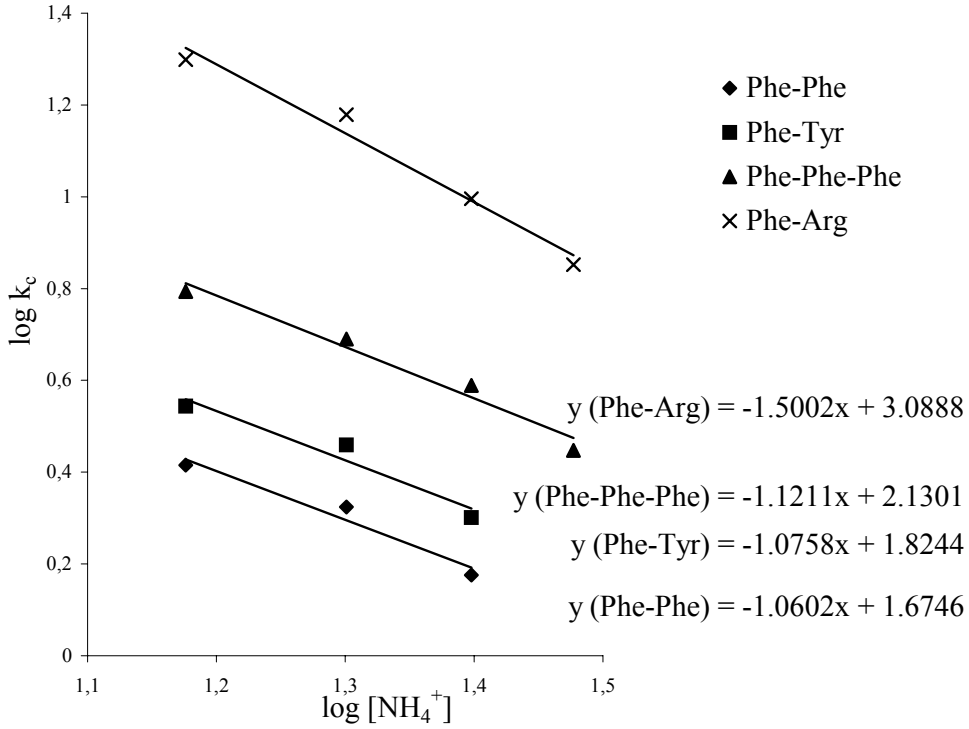

Fig. 70. Log k_c vs. log [NH_4^+] of different peptides on Monolith 1. Mobile phases: methanol/ammonium acetate buffer with different concentration of ammonium (70:30, v/v), pH* 4.0, electric conductivity = 120-200 μS cm^{-1}.

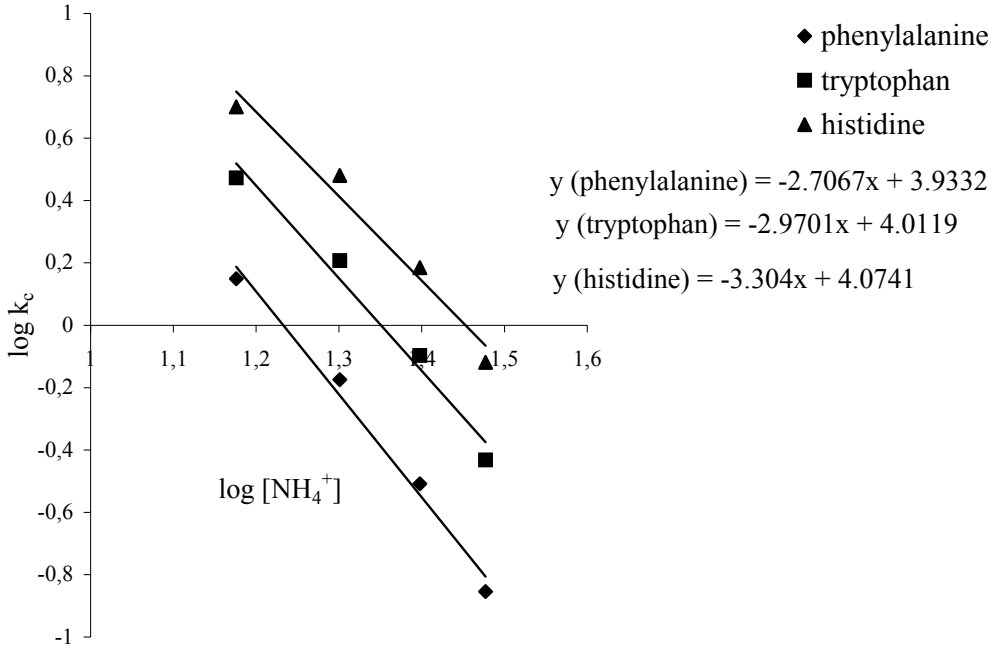

Fig. 71. Log k_c vs. log [NH_4^+] of amino acids on Monolith 1. Mobile phases: methanol/ammonium acetate buffer with different concentration of ammonium (70:30, v/v), pH* 4.0, electric conductivity = 120-200 μS cm^{-1}.

For the two-site model, the plot of k_c vs. $1/[NH_4^+]_m$ permits access to the quantification of the relative contributions of solvophobic and ion-exchange interactions to the overall retention of charged analytes (see Eq. (78)). Additionally the plot of k_c vs. $1/[NH_4^+]_m$ is a valuable tool to decide whether the retention process can be regarded as hydrophobically assisted ion-exchange (see Eq. (73)) or as two-site mixed-mode retention. According to Eq. (73), which is based on the one-site model, the y-intercept of the plot k_c vs. $1/[C^+]_m$ will be zero. According to Eq. (78), which is based on the two-site model, the y-intercept of the plot k_c vs. $1/[C^+]_m$ will be finite. For protonated alkylanilines the intercepts of this plot are close to zero with the exception of 4-hexylaniline (Fig. 72), which has a slightly higher intercept value. This observation is consistent with Eq. (73) (hydrophobically assisted ion-exchange). To check if the y-intercepts are significantly different from zero (if zero is included in the confidence interval), the confidence intervals for the y-intercepts for alkylanilines were calculated by multiplying the standard error of the y-intercept with the tabulated t-value 2.92 t (95%, f = n-2). The confidence intervals were found to be: -0.57/-0.007 (4-ethylaniline), -0.129/0.00 (4-propylaniline), -0.136/0.344 (4-butylaniline), -0.33/0.45 (4-pentylaniline), 0.22/0.88 (4-hexylaniline). Regarding the plot of 4-hexylaniline, which has a significant intercept, the slope is much larger than the y-intercept, which indicates that hydrophobically assisted ion-

exchange interaction can be regarded as a predominant type of interaction. Additional observation is that the slopes increase as the solute chain length is increased. This increase in slope with solute hydrophobicity is predicted (see Eq. 73) by Neue's model of hydrophobically assisted ion-exchange [115-116]. Interestingly, Rahman and Hoffman [120] observed a similar phenomenon with a polymeric ion-exchange phase. Plots of the retention factor versus the reciprocal of the alkali metal ion (here: the counter ion) molar concentration in the mobile phase were linear: the intercepts and the slopes of plots of k vs. $1/[C^+]_m$ were increased with an increase in alkyl chain length for a series of phenyl alkylammonium ions [120]. They concluded that reversed-phase and ion-exchange interactions showed synergistic behavior in a mixed-mode type retention process. Conversely, plot of k_c vs. $1/[C^+]_m$ for amino acids and peptides resulted in negative intercepts, which is according to neither one-site nor two-site models of retention (Figs. 73-74). The confidence intervals for the y-intercepts for amino acids and peptides were found to be: -1.59/-0.83 (phenylalanine), -2.61/-2.00 (tryptophan), -4.15/-3.0 (histidine), -2.70/-0.50 (Phe-Phe), -2.8/-0.26 (Phe-Phe-Phe), -1.83/1.29 (Phe-Tyr), -10.7/-0.03 (Phe-Arg). The slopes of these plots, however, are much larger than the absolute values of the y-intercepts, which indicates that the hydrophobically assisted ion-exchange mechanism is predominant.

In the next step, it was of worth while to see if the significant difference of the y-intercepts from zero for 4-hexylaniline, amino acids and peptides is due to the use of corrected retention factors k_c instead of apparent retention factors k_{app}. Therefore, k_{app} vs. $1/[NH_4^+]$ was plotted for alkylanilines, amino acids, and peptides (Figs. 75-77). It was observed that the y-intercepts of the plot k_{app} vs. $1/[NH_4^+]$ were smaller than the intercepts for k_c vs. $1/[NH_4^+]$, however, the calculations of the confidence intervals of the y-intercepts for amino acids and peptides showed that they were significantly different from zero. The confidence intervals of the y-intercepts were calculated to be: -1.00/-0.5 (phenylalanine), -1.68/-1.36 (tryptophan), -2.11/-1.41 (histidine), -2.1/-0.38 (Phe-Phe), -2.18/-0.04 (Phe-Phe-Phe), -1.37/0.97 (Phe-Tyr), -5.7/-0.037 (Phe-Arg). This proves that taking k_c is not the reason for this deviation. It is therefore concluded that the same reasons which are responsible for the deviation of the slope of log k_c vs. log $[NH_4^+]$ have to be taken, see the previous discussion. The y-intercepts of the plot k_{app} vs. $1/[NH_4^+]$ for alkylanilines, on the other hand, are not significantly different from zero (except 4-hexylaniline), which is the same as using the plot k_c vs. $1/[NH_4^+]$.

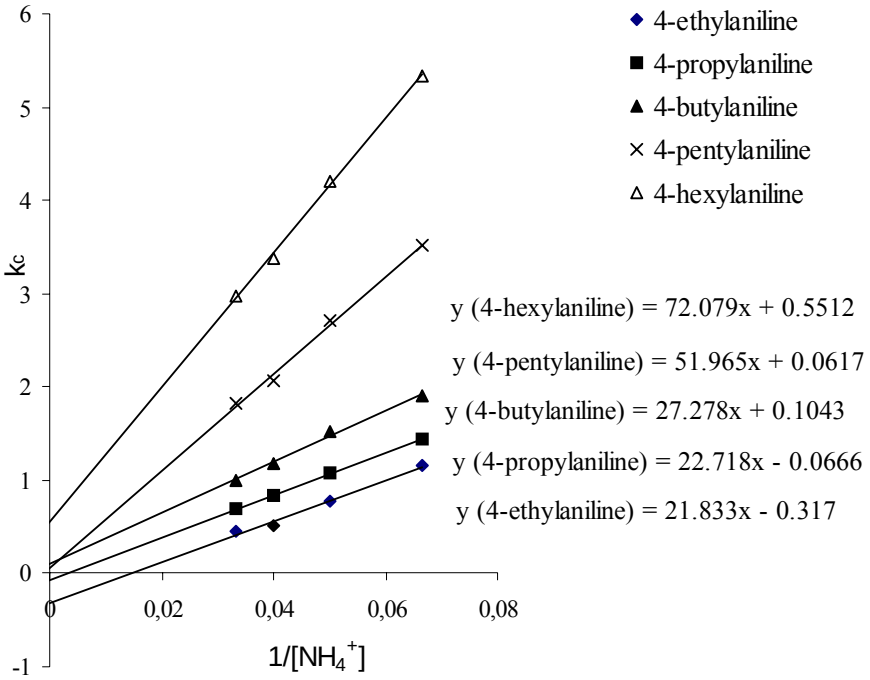

Fig. 72. k_c vs. $1/[NH_4^+]$ for alkylanilines on Monolith 1. Mobile phases: methanol/ammonium acetate buffer with different concentration of ammonium (70:30, v/v), pH* 4.0, electric conductivity = 120-200 µS cm^{-1}.

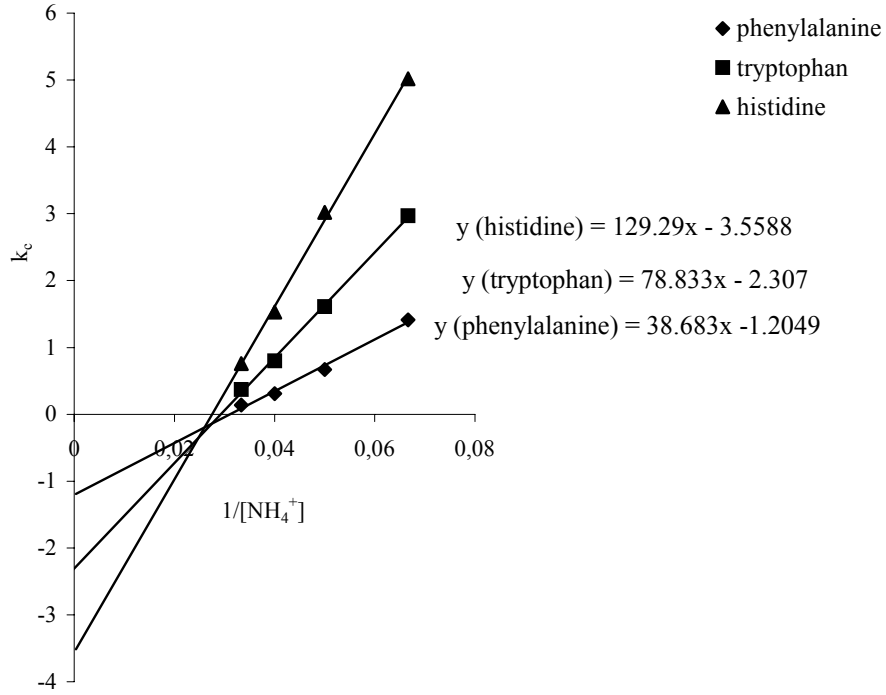

Fig. 73. k_c vs. $1/[NH_4^+]$ for amino acids on Monolith 1. Mobile phases: methanol/ammonium acetate buffer with different concentration of ammonium (70:30, v/v), pH* 4.0, electric conductivity = 120-200 µS cm^{-1}.

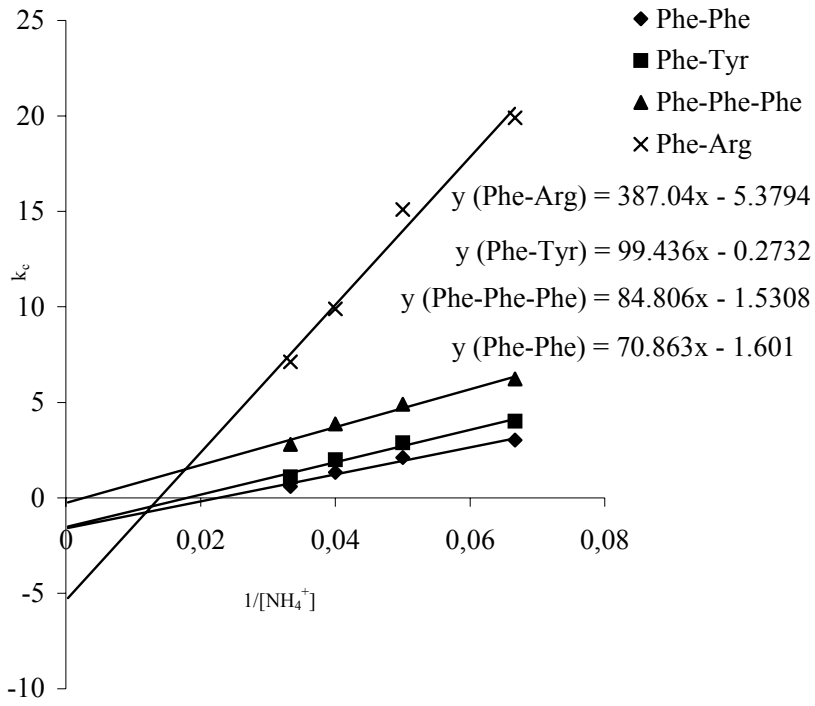

Fig. 74. k_c vs. $1/[NH_4^+]$ for peptides on Monolith 1. Mobile phases: methanol/ammonium acetate buffer with different concentration of ammonium (70:30, v/v), pH* 4.0, electric conductivity = 120-200 μS cm^{-1}.

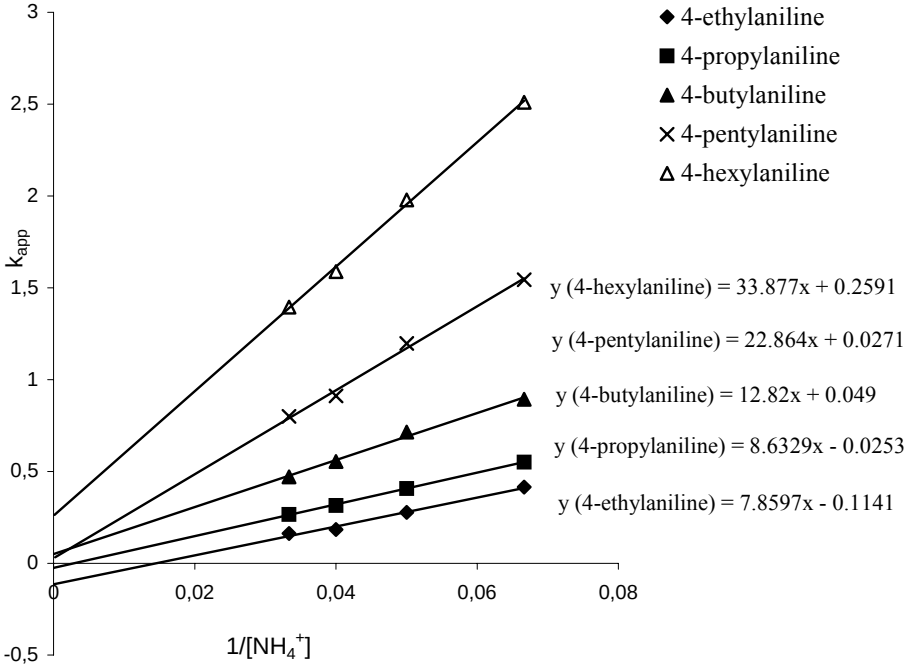

Fig. 75. k_{app} vs. $1/[NH_4^+]$ for alkylanilines on Monolith 1. Mobile phases: methanol/ammonium acetate buffer with different concentration of ammonium (70:30, v/v), pH* 4.0, electric conductivity = 120-200 μS cm^{-1}.

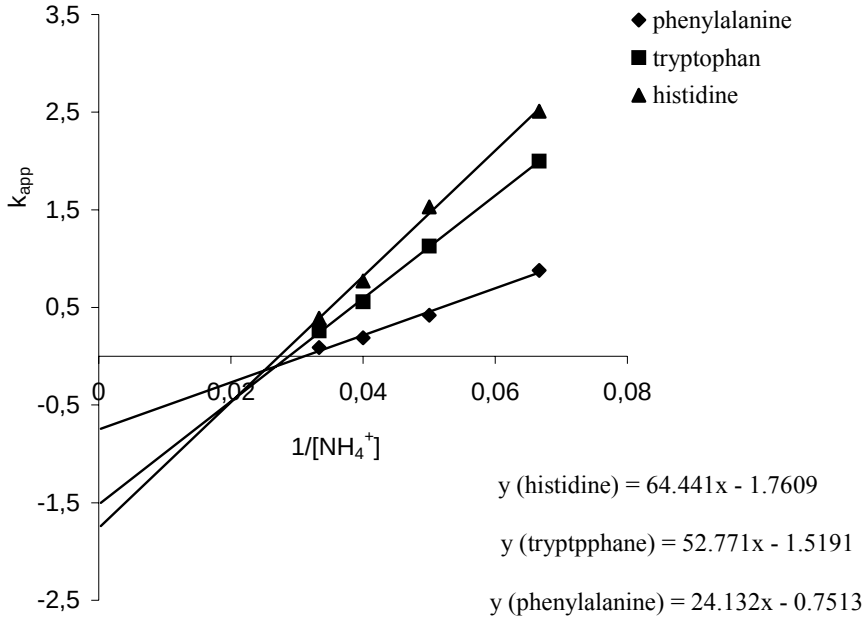

Fig. 76. k_{app} vs. 1/[NH_4^+] for amino acids on Monolith 1. Mobile phases: methanol/ammonium acetate buffer with different concentration of ammonium (70:30, v/v), pH* 4.0, electric conductivity = 120-200 μS cm^{-1}.

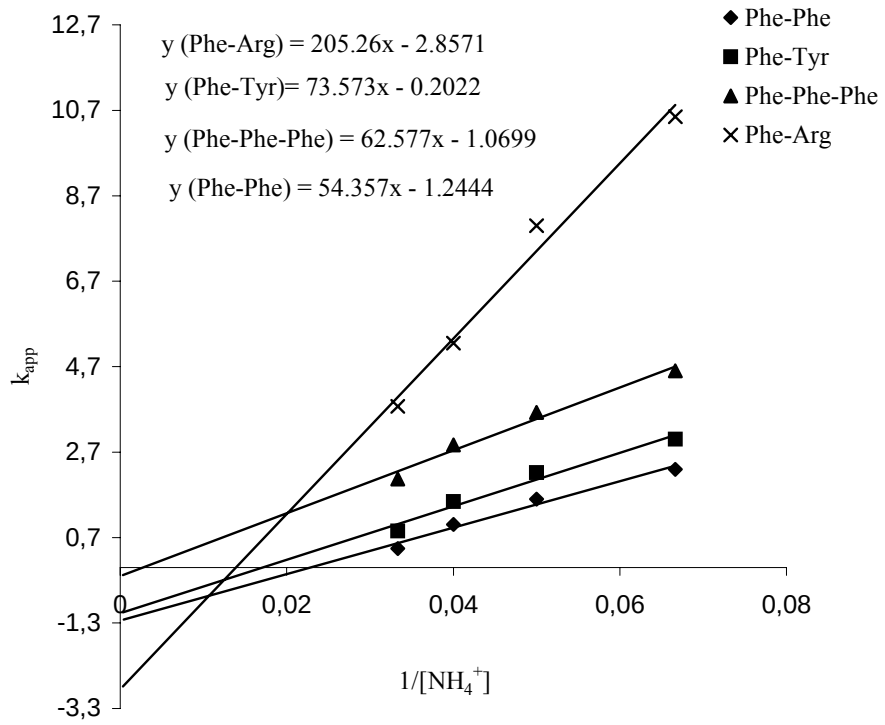

Fig. 77. k_{app} vs. 1/[NH_4^+] for peptides on Monolith 1. Mobile phases: methanol/ammonium acetate buffer with different concentration of ammonium (70:30, v/v), pH* 4.0, electric conductivity = 120-200 μS cm^{-1}.

4.14 Reproducibility and stability of the monolithic capillaries

In order to investigate whether the CEC instrument employed and the synthesis procedure of the monoliths can be used for routine analysis, the reliability and reproducibility of this system for achieving the separation of a test mixture of alkylphenones were determined. Four monolithic capillaries prepared from the same polymerization composition (Monolith 1) were synthesized and tested for the separation of alkylphenones under identical chromatographic conditions (capillary to capillary reproducibility). For each capillary, six runs were performed measuring the elution time of the unretained marker DMF t_0, and the retention factors for several alkylphenones (Tab. 23). The relative standard deviations obtained were compared to each other employing ANOVA (analysis of variance) [121]. In another study, the day to day reproducibility was studied by calculating the relative standard deviation for the magnitudes named above for 24 runs performed with one monolith (Monolith 1) (6 runs each for 4 days). In the same fashion the run to run reproducibility was studied by calculating the relative standard deviation for these magnitudes for 10 runs performed at one day with one monolith (Monolith 1). The results are listed in Tab. 23.

Analysis of variance (ANOVA) [121] was used to test whether the values for t_o, and retention factors, which were obtained in 4 days (day to day reproducibility) or for 4 capillaries (capillary to capillary reproducibility) are differing significantly from day to day or from capillary to capillary. The variances between the 4 groups (4 days or 4 capillaries) and within the groups (every day, every capillary) were calculated (S_1^2, S_2^2). The variance between m groups (S_1^2) can be calculated as follows [121],

$$S_1^2 = \frac{\sum_{j=1}^{m} p(\bar{X}_j - \bar{X}_g)^2}{m-1} \tag{80}$$

where $\bar{X}_j$ is the arithmetic average within a group, $\bar{X}_g$ is the total average, p is the number of values within one group.

The variance within the groups (S_2^2) can be calculated as follows,

$$S_2^2 = \frac{\sum_{j=1}^{m}\sum_{i=1}^{p}(X_{ji} - \bar{X}_j)^2}{n-m} \tag{81}$$

where X_{ji} is the single value, n is the total number of the measurements = m p.

The ratio of variances (S_1^2/S_2^2, always ≥ 1) is compared to the tabulated F-value 3.10 (95%, f_1 = m-1 = 3, f_2 = n-m = 20). Results show (Tab. 24) that regarding four different capillaries or four different days, the within groups and between groups variances differ significantly from each other for t_0, and the retention factor for alkylphenones ($F_{calculated} > F_{tabulated}$), i.e. these values obtained for 4 capillaries or four days are not homogeneous and belong to 4 groups. This inhomogeneity of the data material shows that changing the capillary or measuring at different days introduces a second source of variation, which can clearly be distinguished from the source of variation being responsible for the standard variation measured when repeating injections during one day. For the day to day reproducibility, the major source of variation is variation of the room temperature as the separation capillary is not temperature-controlled. Variation in the temperature has impact on μ_{eo}, via change in the viscosity of the mobile phase and impact on k via change in the distribution coefficient. For the capillary to capillary reproducibility obviously the major source of variation is also the variation in the room temperature, because the four capillaries were tested at different days. An additional source of variation are differences in the monoliths tested, e.g. variation in the zeta potential at the liquid/solid-interface, variation in the phase ratio or variation in the hydrophobicity of the solid material.

It is remarkable that the between groups variances for the capillary to capillary (S_1^2 for capillary to capillary) reproducibility are insignificantly higher than the between groups variances for the day to day reproducibility (S_1^2 for day to day) ($F_{calculated} < F_{tabulated}$, see Tab. 25), which shows that the synthesis parameters can be very well controlled. It is therefore demonstrated that the synthesis procedure, as well as the homebuilt-CEC instrument can be used to achieve reproducible and reliable separations.

Tab. 23. Capillary to capillary, day to day, and run to run reproducibility of Monolith 1; overall relative standard deviation for t_0 (min), and retention factors of different alkylphenones.

RSD, %	t_0	k acetophenone	k propiophenone	k butyrophenone	k valerophenone
Capillary to capillary (N = 24)	2.43	3.16	2.66	3.00	3.44
Day to day (N = 24)	1.65	3.05	2.38	2.71	2.76
Run to run (N = 10)	0.13	0.10	0.13	0.21	0.30

Mobile phase: methanol/water (60:40, v/v) buffered with triethylamine/acetic acid, pH* = 7.0, electric conductivity = 120 µS cm^{-1}.

Tab. 24. Between groups variance (S_1^2), within groups variance (S_2^2), and the ratio of variances (S_1^2/S_2^2) for t_0 (min), and retention factors of different alkylphenones determined for capillary to capillary and day to day reproducibility.

	Capillary to capillary			day to day		
	S_1^2	S_2^2	S_1^2/S_2^2	S_1^2	S_2^2	S_1^2/S_2^2
t_0	0.021	0.00023	91.3	0.0082	0.00018	45.6
k (acetophenone)	0.0004	0.00005	8.0	0.0004	0.00007	5.71
k (propiophenone)	0.002	0.000065	30.8	0.0014	0.000095	14.7
k (butyrophenone)	0.0028	0.00058	4.83	0.0038	0.000275	13.3
k (valerophenone)	0.0178	0.00156	11.4	0.0124	0.000585	21.2

Tab. 25. Between groups variances for the capillary to capillary reproducibility (S_1^2 for capillary to capillary), between groups variances for the day to day reproducibility (S_1^2 for day to day), and the ratio of variances (S_1^2 (capillary to capillary)/ S_1^2 (day to day)) for t_0 (min), and retention factors of different alkylphenones.

	S_1^2 (capillary to capillary)	S_1^2 (day to day)	S_1^2 (capillary to capillary)/ S_1^2 (day to day)
t_0	0.021	0.0082	2.56
k (acetophenone)	0.0004	0.0004	1.00
k (propiophenone)	0.002	0.0014	1.43
k (butyrophenone)	0.0028	0.0038	0.74
k (valerophenone)	0.0178	0.0124	1.43

5. Conclusions

A new method for the preparation of monolithic stationary phases for CEC has been evaluated. Cyclodextrin can be successfully employed for the solubilization of hydrophobic monomers in aqueous solution. This method makes it possible to synthesize continuous chromatographic beds for reversed-phase chromatographic separations employing synthesis mixtures dissolved in aqueous solution. Electrophoretic and spectroscopic methods complement each other when studyig complex formation between hydrophobic methacrylate and cyclodextrin. Different modes of separation (reversed-phase, normal-phase, and ion-exchange mode) can be achieved with the prepared monolithic stationary phases by including simply different types of monomers (polar, nonpolar, charged, and noncharged) into the polymerization mixture, enabling hydrophobic, electrostatic and polar interactions with the analytes. Accordingly, different types of analytes (polar, nonpolar, neutral, and charged) can be separated on these mixed-mode stationary phases. Solvophobic interactions are responsible for the separation of neutral hydrophobic analytes on the prepared mixed-mode monolithic stationary phases. In addition to hydrophobic interactions, polar interactions contribute also for the separation of neutral polar analytes. Both hydrophobic and ion-exchange interactions enable the separation of charged analytes.

6 References

[1] K. D. Bartle, P. Myers, *Capillary electrochromatography*, The Royal Society of Chemistry, Cambridge, **2001**.

[2] I. S. Krull, R. L. Stevenson, K. Mistry, M. E. Swartz, *Capillary electrochromatography and pressurized flow capillary electrochromatography*, HNB publishing, New York, **2000**.

[3] S. Eeltink, W. T. Kok, *Electrophoresis*, **2006**, *27*, 84-96.

[4] J.W. Jorgenson, K. D. Lukacs, *Anal. Chem*., **1981**, *53*, 1298-1302.

[5] M. Lämmerhofer, W. Lindner, *Capillary electrochromatography*, pp. 489-559, in: F. Svec, T. B. Tennikova, Z. Deyl (Eds.), monolithic materials: preparation, properties and applications, Elsevier, Amsterdam, **2003**.

[6] U. Pyell, *Fundamentals of capillary electrochromatography*, pp. 1-51, in: P. R. Brown, E. Grushka (Eds.), Advances in Chromatography. Vol. 41, Marcel Dekker, New York, **2001**.

[7] D. A. Skoog, J. J. Leary, *Principles of instrumental analysis*, Saunders College Publishing, New York, **1992**.

[8] A. J. P. Martin, R. L. M. Synge, *Biochem. J*., **1941**, *35*, 1358-1368.

[9] T. Jiang, J. Jiskra, H. A. Claessens, C. A. Cramers, *J. Chromatogr. A*, **2001**, *923*, 215-227.

[10] K. Mistry, I. Krull, N. Grinberg, *J. Sep. Sci*., **2002**, *25*, 935-958.

[11] E. Wen, R. Asiaie, C. Horvath, *J. Chromatogr. A*, **1999**, *855*, 349-366.

[12] E. R. Verheij, U. R. Tjaden, W. M. A. Niessen, J. van der Greef, *J. Chromatogr*., **1991**, *554*, 339-349.

[13] A. Apffel, H. Yin, W. S. Hancock, D. McManigill, J. Frenz, S. L. Wu, *J. Chromatogr. A*, **1999**, *832*, 149-163.

[14] K. Pusecker, J. Schewitz, P. Gförer, L. H. Tseng, K. Albert, E. Bayer, *Anal. Chem*., **1998**, *70*, 3280-3285.

[15] D.A. Stead, R.G. Reid, R.B. Taylor, *J. Chromatogr. A*, **1998**, *798*, 259–267.

[16] A. Banholczer, U. Pyell, *J. Chromatogr. A*, **2000**, *869*, 363-374.

[17] J. Jiskra, H. A. Claessens, C. A. Cramers, *J. Sep. Sci*, **2003**, *26*, 1305-1330.

[18] U. Pyell, *J. Chromatogr. A*, **2000**, *892*, 257-278.

[19] J. W. Jorgenson, K. D. Lukacs, *J. Chromatogr*., **1981**, *218*, 209-212.

[20] H. Yamamoto, J. Baumann, F. Erni, *J. Chromatogr. A*, **1992**, *593*, 313-319.

[21] S. Lüdtke, T. Adam, K. K. Unger, *J. Chromatogr. A*, **1997**, *786*, 229-235.

[22] C. G. Bailey, C. Yan, *Anal. Chem*., **1998**, *70*, 3275-3279.

[23] R. M. Seifar, J. C. Kraak, W. T. Kok, H. Poppe, *J. Chromatogr. A*, **1998**, *808*, 71-77.

[24] R. Dadoo, R. N. Zare, C. Yan, D. S. Anex, *Anal. Chem*., **1998**, *70*, 4787-4792.

[25] L. A. Colon, G. Burgos, T. D. Maloney, J. M. Cintron, R. L. Rodriguez, *Electrophoresis*, **2000**, *21*, 3965-3993.

[26] G. Vanhoenacker, T. Van den Bosch, G. Rozing, P. Sandra, *Electrophoresis*, **2001**, *22*, 4064-4103.

[27] H. Rebscher, U. Pyell, *Chromatographia,* **1994**, *38*, 737-743.

[28] T. Tsuda, K. Nomura, K. Nagagawa, *J. Chromatogr*., **1982**, *248*, 241-247.

[29] G. J. M. Bruin, P. P. H. Tock, J. C. Kraak, H. Poppe, *J. Chromatogr*., **1990**, *517*, 557-572.

[30] J. J. Pesek, M. T. Matyska, S. Cho, *J. Chrom.A*, **1999**, *845*, 237-246.

[31] Z. Liu, K. Otsuka, S. Terabe, *J. Chromatogr. A*, **2002**, *961*, 285-291.

[32] A. Malik, *Electrophoresis*, **2002**, *23*, 3973-3992.

[33] S. Constatin, R. Freitag, *J. Sep. Sci*, **2002**, *25*, 1245-1251.

[34] Y. Zhao, R. Zhao, D. Shangguan, G. Liu, *Electrophoresis*, **2002**, *23*, 2990-2995.

[35] C. P. Kapnissi, C. Akbay, J. B. Schlenoff, I. M. Warner, *Anal. Chem*., **2002**, *74*, 2328-2335.

[36] M. W. Kamande, C.P. Kapnissi, X. Zhu, C. Akbay, I. M. Warner, *Electrophoresis*, **2003**, *24*, 945-951.

[37] A. Maruska, *Monolithic Continuous Beds Prepared from Water-Soluble Acrylamide-Based Monomers*, pp. 141-170, in: F. Svec, T.B. Tennikova, Z. Deyl, (Eds), monolithic materials: preparation, properties and applications, Elsevier, Amsterdam, **2003**.

[38] S. Hjerten, J. L. Liao, R. Zhang, *J. Chromatogr. A*, **1989**, *473*,273-275.

[39] C. Ericson, J. L. Liao, K. Nakazato, S. Hjerten, *J. Chromatogr. A*, **1997**, *767*, 33-41.

[40] C. Ericson, S. Hjerten, *Anal. Chem*., **1999**, *71*, 1621-1627.

[41] J.L. Liao, N. Chen, C. Ericson, S. Hjerten, *Anal. Chem*., **1996**, *68*, 3468-3472.

[42] C. Fujimoto, J. Kino, H. Sawada, *J. Chromatogr. A*, **1995**, *716*, 107-113.

[43] S. Hjerten, D. Eaker, K. Elenbring, C. Ericson, K. Kubo, J.L.Liao, C.M. Zeng, P.A. Lindström, C. Lindh, A. Palm, T. Srichiayo,L. Valcheva, R. Zhang, *Jpn. J. Electrophor*., **1995**, *39*, 105-118

[44] E.C. Peters, M. Petro, F. Svec, J.M.J. Frechet, *Anal. Chem*., **1997**, *69*, 3646–3649.

[45] A. Palm, M.V. Novotny, *Anal. Chem*., **1997**, *69*, 4499–4507.

[46] L. Schweitz, L.I. Andersson, S. Nilsson, *Anal. Chem*., **1997**,*69*, 1179–1183.

[47] M.T. Dulay, R.P. Kulkarni, R.N. Zare, *Anal. Chem*., **1998**, *70*,5103–5107.

[48] I. Gusev, X. Huang, C. Horvath, *J. Chromatogr. A,* **1999**,*855*, 273–290.

[49] G. Chirica, V.T. Remcho, *Electrophoresis,* **1999**, *20*, 50–56.

[50] Q.L. Tang, B.M. Xin, M.L. Lee, *J. Chromatogr. A,* **1999**, *837*,35–50.

[51] N. Tanaka, H. Nagayama, H. Kobayashi, T. Ikegami, K. Hosoya,N. Ishizuka, H. Minakuchi, K. Nakanishi, K. Cabrera, D.Lubda, *J. High Resol. Chromatogr*., **2000**, *23*, 111–116.

[52] B. Eeltink, F. Svec, *Electrophoresis*, **2007**, *28*, 137-147.

[53] F. Svec, C.G. Huber, *Anal. Chem.,* **2006**, *78*, 2100-2107.

[54] F. Svec, *J. Sep. Sci*, **2005**, *28*, 729-745.

[55] E. F. Hilder, F. Svec, J. M. J. Frechet, *J. Chrom. A*, **2004**, *1044*, 3-22.

[56] E. F. Hilder, F. Svec, J. M. J. Frechet, *Electrophoresis*, **2002**, *23*, 3934-3953

[57] Y. Baba, M. Tsuhako, *Trends Anal. Chem*., **1992**, *11*, 280-287.

[58] C. Fujimoto, *Anal. Chem*., **1995**,*67*, 2050-2053.

[59] C. Fujimoto, *Analusis*, **1998**, *26*, M49-M52.

[60] A. Palm, M.V. Novotny, *Anal. Chem*., **1997**, *69*, 4499-4507.

[61] J.A. Starkey, Y. Mechref, C.K. Byun, R. Steinmetz, J.S. Fuqua, O.H. Pescovitz, M.V. Novotny, *Anal. Chem*., **2002**, *74*, 5998-6005.

[62] M.Q. Zhang, Z. El Rassi, *Electrophoresis*, **2001**, *22*, 2593-2599.

[63] D. Hoegger, R. Freitag, *J. Chrom. A*, **2001**, *914*, 211-222.

[64] D. Hoegger, R. Freitag, *J. Chrom. A*, **2003**, *1004*, 195-208.

[65] D. Hoegger, R. Freitag, *Electrophoresis*, **2003**, *24*, 2958-2972.

[66] R. Freitag, *J. Chromatogr. A*., **2004**, *1033*, 267-273.

[67] I. Gusev, X. Huang, Cs. Horváth, *J. Chromatogr. A*, **1999**, *855*, 273-290.

[68] S.H. Zhang, J. Zhang, Cs. Horváth, *J. Chromatogr. A*, **2001**, *914*, 189-200.

[69] W. Jin, H. Fu, X. Huang, H. Xiao, H. Zou, *Electrophoresis*, **2003**, *24*,3172-3180.

[70] E.C. Peters, M. Petro, F. Svec, J.M.J. Fréchet, *Anal. Chem*., **1997**, *69*, 3646-3649.

[71] E.F. Hilder, F. Svec, J.M.J. Frechet, *Electrophoresis*, **2002**, *23*, 3934-3953.

[72] E.F. Hilder, F. Svec, J.M.J. Frechet, *J. Chromatogr. A*, **2004**, *1044*, 3-22.

[73] F. Svec, *J. Sep. Sci*, **2005**, *28*, 729-745.

[74] L.I. Zhang, G. Ping, L. Zhang, W. Zhang, Y. Zhang, *J. Sep. Sci*., **2003**, *26*, 331-336.

[75] G.C. Ping, Y.K. Zhang, W.B. Zhang, L. Zhang, L.H. Zhang, P. Schmitt-Kopplin, A. Kettrup, *Electrophoresis*, **2004**, *25*, 421-427.

[76] V. Augustin, A. Jardy, P. Gareil, M. C. Hennion, *J. Chromatogr. A*, **2006**, *1119*, 80-87.

[77] J.P. Kutter, S.C. Jacobson, N. Matsubara, J.M. Ramsey, *Anal. Chem*., **1998**, *70*, 3291–3297.

[78] B.E. Slentz, N.A. Penner, F.E. Regnier, *J. Chromatogr. A,* **2002**, *948*, 225–233.

[79] C. Ericson, J. Holm, T. Ericson, S. Hjerten, *Anal. Chem*., **2000**, *72*, 81–87.

[80] H. Ritter, M. Tabatabai, *Trends Polym. Sci*, **2002**, *27*, 1713-1720.

[81] J. Szejtli, *Chem. Rev*., **1998**, *98*, 1743-1753.

[82] A. Schornick, A. Kistenmacher, H. Ritter, J. Jeromin, O. Noll, M. Born, German Pat., DE 19533269, **1997**.

[83] J. Jeromin, H. Ritter, *Macromol. Rapid Commun*., **1998**, *19*, 377-379.

[84] J. Jeromin, O. Noll, H. Ritter, *Macromol. Chem. Phys*., **1998**, *199*, 2641-2645.

[85] P. Glöckner, H. Ritter, *Macromol. Rapid Commun*., **1999**, *20*, 602-605.

[86] P. Casper, P. Glöckner, H. Ritter, *Macromolecules*, **2000**, *33*, 4361-4364.

[87] S. Bernhardt, P. Glöckner, A. Theis, H. Ritter, *Macromolecules*, **2001**, *34*, 1647-1649.

[88] S. Bernhardt, P. Glöckner, H. Ritter, *Polymer Bulletin*, **2001**, *46*, 153-157.

[89] S. Schwarz-Barac, H. Ritter, *J. Macromol. Sci*., **2003**, *40*, 437-448.

[90] O. Kretschmann, C. Steffens, H. Ritter, *Angew. Chem. Int. Ed*., **2007**, *46*, 2708-2711.

[91] A. Wahl, I. Schnell, U. Pyell, *J. Chromatogr. A*, **2004**, *1044*, 211-222.

[92] S. Hjerten,, *J.Chromatogr*., **1985**, *347*, 191-198

[93] Y. Liu, Y. Zhao, H. Zhang, Z. Fan, G. Wen, F. Ding, *J. Phys. Chem.B*, **2004**, *108*, 8836-8843.

[94] L. Fielding, *Tetrahedron*, **2000**, *56*, 6151-6170.

[95] S. Terabe, Y. Miyashita, O. Shibata, E.R. Barnhart, L.R. Alexander, D.G. Patterson, B.L. Karger, K. Hosoyo, N. Tanaka, *J. Chromatogr*., **1990**, *516*, 23-31.

[96] S. Terabe, K. Otsuka, K. Ichikawa, A. Tsuchiya, T. Ando, *Anal. Chem.,* **1984**, *56*, 111-113.

[97] K. Fujimura, T. Ueda, M. Kitagawa, H. Takayanagi, T. Ando, *Anal. Chem*., **1986**, *58*, 2668-2674.

[98] J. Lipkowski, O.I. Kalchenko, J. Slowikowska, V.I. Kalchenko, O.V. Lukin, L.N. Markovsky, R. Nowakowski, *J. Phys. Org. Chem.,* **1998**, *11*, 426-435.

[99] U.B. Nair, K.L. Rundlett, D.W. Armstrong, D. W., *J. Liq. Chrom.* **1997**, *20*, 203-216.

[100] J. Lipkowski, O.I. Kalchenko, J. Slowikowska, V.I. Kalchenko, O.V. Lukin, L.N. Markovsky, R. Nowakowski, *J. Phys. Org. Chem.,* **1998**, *11*, 426-435.

[101] D.W. Armstrong, F. Nome, L. Spino, T. Golden, *J. Am. Chem. Soc.,* **1986**, *1084*, 1418-1421.

[102] D. W. Armstrong, F. Nome, L. Spino, T. Golden, *J. Am. Chem. Soc*., **1986**, *1084*, 1418-1421.

[103] Y. Liu, Y. Zhao, H. Zhang, Z. Fan, G. Wen, F. Ding, *J. Phys. Chem. B*., **2004**, *108*, 8836-8843.

[104] M.T. Bowser, A.R. Kranack, D.D.Y. Chen, *Trends in Analytical Chemistry,* **1998**, *17*, 424-434.

[105] Y. Yamamoto, M. Onda, M. Kitagawa, Y. Inoue, R. Chujo, *Carbohydr. Res*., **1987**, *167*, C11-C16.

[106]. A.M. Krstulovic, H. Colin, A. Tchapla, G. Guiochon, *Chromatographia*, **1983**, *17*, 228-230.

[107] C. Schwer, E. Kenndler, *Anal. Chem*., **1991**, *63*, 1801-1807.

[108] R. Appel, K. Cruse, P. Drossbach, H. Falkenhagen, G. G. Grau, G. Kelbg, E. Schmutzer, H. Strehlow, Landolt-Boernstein, Zahlenwerte und Funktionen aus Physik, Chemie, Astronomie, Geophysik, Technik, 6. Auflage, II. Band, 7. Teil, Elektrische Eigenschaften II (elektrochemische Systeme), Springer-Verlag, 1960.

[109] M. Al-Bokari, D. Cherrak, G. Guiochon, *J. Chromatogr. A*, **2002**, *975*, 275-284.

[110] D. Lubda, W. Lindner, M. Quaglia, C. Fresne von Hohenesche, K. K. Unger, *J. Chromatogr. A*, **2005**, *1083*, 14-22.

[111] H. Guan, G. Guiochon, *J. Chromatogr. A*, **1996**, *731*, 27-40.

[112] V. Szucs, R. Freitag, *J. Chromatogr. A*, **2004**, *1044*, 201-210.

[113] K. Sarmini, E. Kenndler, *J. Biochem. Biophys. Methods*, **1999**, *38*, 123-137.

[114] A.S. Rathore, C. Horvath, *Electrophoresis*, **2002**, *23*, 1211-1216.

[115] X. Yang, J. Dai, P. W. Carr, *J. Chromatogr. A*., **2003**, *996*, 13-31.

[116] U. D. Neue, C. H. Phoebe, K. Tran, Y. F. Cheng, Z. Lu, *J. Chromatogr. A*., **2001**, *925*, 49-67.

[117] G. Vigh, Z. Varga-Puchony, *J. Chromatogr*., **1980**, *196*, 1-9.

[118] A. Sokolowski, K. G. Wahlund, *J. Chromatogr*., **1980**, *189*, 299-316.

[119] A. Nahum, C. Horvath, *J. Chromatogr*., **1981**, *203*, 53-63.

[120] A. Rahman, N. E. Hoffman, *J. Chromatogr. Sci*., **1990**, *28*, 157-161.

[121] J. C. Miller, J. N. Miller, *Statistics for Analytical Chemistry*, Ellis Horwood Limited, London, **1993**.

[122] D. Briers, I. Picard, T. Verbiest, A. Persoons, C. Samyn, *Polymer*, **2004**, *45*, 19-24.

7 Summary

Highly crosslinked, macroporous mixed-mode monolithic stationary phases were synthesized for capillary electrochromatography (CEC). Free radical copolymerization was performed in aqueous solution with a cyclodextrin-solubilized hydrophobic monomer, a water-soluble crosslinker (piperazinediacrylamide), and a negatively charged monomer (vinylsulfonic acid) in bind silane-pretreated fused-silica capillaries. Different hydrophobic methacrylate monomers (isobornyl, adamantyl, cyclohexyl, and phenyl methacrylate) were investigated. The best cyclodextrin as solubilizing agent for the hydrophobic monomers was selected by using cyclodextrin-modified micellar electrokinetic chromatography in which the presence of cyclodextrin in the aqueous buffer solution will influence the partitioning of solutes between the pseudostationary phase and the surrounding aqueous phase. A quantitative measurement of this influence was used as a tool in the investigation of complex formation between cyclodextrin (host) and methacrylate monomers (guests). This method showed that methylated-ß-cyclodextrin is the best solubilizing agent. Complex forming constants of methacrylate monomers with methylated-ß-cyclodextrin were determined by cyclodextrin-modified CEC and ^{1}H NMR spectroscopy. In cyclodextrin-modified CEC, the presence of cyclodextrin in the mobile phase will influence the partitioning of solutes between the stationary phase and the mobile phase. Using this method, the effect of various concentrations of cyclodextrin in the mobile phase on observed retention factors was used to calculate complex formation constants for complexes with low complex forming constants. Using ^{1}H NMR method, the proton chemical shift changes for methacrylates were monitored as a function of the molar concentration of cyclodextrin. This quantity is used for the determination of complex forming constants of strong complexes.

Employing solubilization by complexation with cyclodextrins, hydrophobic methacrylate-based monoliths were synthesized in aqueous solution. The hydrophobic structure units enable reversed-phase chromatographic separations. The incorporation of sulfonic acid groups is needed to produce the required electroosmotic flow (EOF) for the propulsion of the mobile phase through the chromatographic bed. Ammonium sulfate salt is added to the polymerization mixture to promote pore formation (and permeability) of the monolith by hydrophobic interaction (salting out of the polymer chains). Ammonium persulfate (APS) and tramethylethylenediamine (TEMED) were used as a free radical starter and accelerator for the free radical polymerization reaction, respectively.

The prepared monolithic stationary phases were used for the separation of neutral hydrophobic (alkylphenones) and neutral polar (phenolic and nitrotoluene solutes) analytes by CEC. Chromatographic properties of the synthesized monoliths were studied with aqueous and non-aqueous mobile phases with hydrophobic and with polar analytes. Due to the amphiphilic nature of the polymers synthesized, the elution orders obtained correspond to the reversed-phase mode and to the normal-phase mode depending on the polarity of the mobile phase. However, observations made with polar solutes and polar mobile phase can only be explained by a mixed-mode retention mechanism. Comparison of retention data with those of a commercial octadecyl silica gel HPLC column reveals that the hydrophobicity of alkylphenones (expressed as methylene selectivity) of the monolithic capillaries prepared in this study is very similar to that of routinely used octadecyl silica gels.

The potential of methacrylate-based mixed-mode monolithic stationary phases bearing sulfonic acid groups for the separation of positively charged analytes (alkylanilines, amino acids, and peptides) by CEC is investigated. The retention mechanism of these charged solutes on these negatively charged mixed-mode stationary phases is investigated by studying the influence of mobile phase and stationary phase parameters on the corrected retention factor, which was calculated by taking the electrophoretic mobility of the solutes into consideration. These parameters include volume fraction of methanol, pH*, concentration of counter ion in the mobile phase, concentration of vinylsulfonic acid and concentration of hydrophobic monomer present in the polymerization mixture. Results show that both hydrophobic and ion-exchange interactions contribute to the retention of these analytes. The quantitative relationship between hydrophobic and ion-exchange interactions is investigated by comparing two different retention models for charged analytes on a mixed-mode stationary phase: the one site and the two-site model. The dependence of the corrected retention factor on (1) the concentration of the counter ion ammonium and (2) the number of methylene groups in the alkyl chain of the model analytes investigated shows clearly that a one-site model (hydrophobic and ion-exchange interactions take place simultaneously at a single type of site) has to be taken to describe the retention behaviour observed. Comparison of the CEC-separation of these charged analytes with electrophoretic mobilities determined by open-tubular capillary electrophoresis shows that mainly chromatographic interactions (hydrophobic and ion-exchange interactions) are responsible for the selectivity observed in CEC, while the electrophoretic migration of these analytes plays only a minor role. The separation selectivity of the charged analytes in CEC was compared with the separation selectivity obtained via open-tubular CE. Alkylanilines are separated by CE at optimized

conditions with very low resolution and with comigration of 4-pentylaniline and 4-hexylaniline. Amino acids are separated by CE at optimized conditions with comigration of phenylalanine and tryptophan. Peptides were separated by CE at optimum pH* (7.05) with comigration of the EOF marker (DMF) and Phe-Phe-Phe, and at pH* 4.0 with comigration of Phe-Phe, Phe-Tyr, and Phe-Phe-Phe. In contrast to these results, in CEC good peak resolutions were obtained for all solutes selected. Run-to-run, day-to-day, and capillary-to-capillary reproducibility of the elution time of an unretained marker and the retention factors for selected neutral solutes demonstrated that the synthesis procedure, as well as the homebuilt-CEC instrument can be used to achieve reproducible and reliable separations.

8 Summary in German (Zusammenfassung)

Hochquervernetzte makroporöse monolithische stationäre Phasen wurden für die Kapillarelektrochromatographie (CEC) synthetisiert. Radikalische Copolymerisationen wurden in wässriger Lösung mit einem durch Cyclodextrin in Lösung gebrachten hydrophoben Monomer, einem wasserlöslichen Vernetzer (Piperazindiacrylamid) und einem negativ geladenen Monomer (Vinylsulfonsäure) in einer mit Bindsilan-modifizierten Kapillare durchgeführt. Verschiedene hydrophobe Methacrylate (Isobornyl-, Adamantyl-, Cyclohexyl- und Phenylmethacrylat) wurden in die Untersuchungen einbezogen. Das Cyclodextrin, welches als Solubilisierungsmittel für diese hydrophoben Monomere am besten geeignet ist, wurde über Messungen mittels MEKC ausgewählt, in denen das Vorhandensein des Cyclodextrins in der wäßrigen Pufferlösung die Verteilung der Analyte zwischen der pseudo-stationären mizellaren Phase und der umgebenden wässrigen Phase beeinflusst. Diese Methode gestattet eine qualitative Untersuchung der Komplexbildung zwischen Cyclodextrin (Wirt) und Methacrylat (Gast) und weist nach, dass methyliertes ß-Cyclodextrin das beste Solubilisierungmittel ist. Die Komplexbildungskonstante der hydrophoben Monomere mit methyliertem ß-Cyclodextrin wurde durch Cyclodextrin-modifizierte CEC und ^{1}H NMR-Spektroskopie bestimmt. In Cyclodextrin-modifizierter CEC beeinflusst das Vorhandensein des Cyclodextrins in der mobilen Phase die Verteilung der Analyte zwischen der stationären Phase und der mobilen Phase. Der Einfluss der verschiedenen Konzentrationen des Cyclodextrins in der mobilen Phase auf den beobachteten Retentionsfaktor wurde verwendet, um Komplexbildungskonstanten für Komplexe mit niedriger Komplexbildungskonstante zu errechnen. Mittels ^{1}H-NMR wurde die chemische Verschiebung eines ausgewählten Protons des Methacrylats als Funktion der Stoffmengenkonzentration des Cyclodextrins erfasst. Aus diesen Daten wurden die Komplexbildungskonstanten für besonders stabile Komplexe berechnet.

Die Solubilisierung hydrophober Monomere durch Komplexbildung mit Cyclodextrinen ermöglichte die Synthese von hydrophoben Methacrylat-Monolithen in wässriger Lösung. Methacrylatmonomere wurden eingesetzt, um Umkehrphasen-chromatographische Trennungen zu ermöglichen. Vinylsulfonsäure als geladenes Monomer wurde zugesetzt, um den erforderlichen elektroosmotischen Fluss (EOF) für den Transport der mobilen Phase durch das chromatographische Bett zu generieren. Ammoniumsulfat wird der Polymerisationslösung zugefügt, um Porenbildung (und Permeabilität) des Monolithen durch hydrophobe Wechselwirkungen der Polymerketten (Aussalzen) zu steuern.

Diammoniumperoxodisulfat (APS) wurde als Radikalstarter und Tetramethylethylendiamin (TEMED) als Redox-Beschleuniger der radikalischen Copolymerisation in freier Lösung verwendet.

Die hergestellten monolithischen stationären Phasen wurden für die Trennung hydrophober Alkylphenone und weiter polarer Analyte (Phenole und Nitrotoluole) mittels CEC eingesetzt. Die chromatographischen Eigenschaften des synthetisierten Monolithen wurden mit wässrigen und nichtwässrigen mobilen Phasen über die Trennung der hydrophoben und der polaren Analyte ermittelt. Wegen der Amphiphilie des synthetisierten Monolithen entsprechen die erhaltenen Elutionsreihenfolgen sowohl dem Umkehrphasenmodus als auch dem Normalphasenmodus je nach Polarität der mobilen Phase. Jedoch können die Ergebnisse, die mit polaren Analyten und mit polarer mobiler Phase erhalten wurden, nur durch einen gemischtmodigen Retentionsmechanismus erklärt werden. Ein Vergleich von Retentionsdaten mit denen einer kommerziellen Octadecyl-Silicagel-HPLC-Säule zeigt, dass die Hydrophobizität (ausgedrückt als Methylenselektivität) der monolithischen Kapillaren in der gleichen Größenordnung liegt.

Von Interesse ist das Potential dieser monolithischen stationären Phasen mit kovalent immobilisierten Sulfonsäuregruppen für die Trennung von positiv-geladenen Analyte (Alkylaniline, Aminosäuren und Peptide) mittels CEC. Der Mechanismus der Retention dieser positiv-geladenen Analyte auf der negativ-geladenen stationären Phase wurde durch Erfassung des Einflusses der Zusammensetzung der mobilen Phase und der stationären Phase auf den korrigierten Retentionsfaktor untersucht. Der korrigierte Retentionsfaktor berücksichtigt die effektive elektrophoretische Mobilität der Analyte. Die in diesen Untersuchungen variierten Parameter umfassen den Volumenanteil Methanol, den pH*, die Konzentration des Gegenions in der mobilen Phase und die Konzentration der Vinylsulfonsäure und die Konzentration des hydrophoben Monomers in der Polymerisationsmischung. Die Resultate zeigen, dass sowohl hydrophobe Wechselwirkungen als auch Ionenaustausch zur Retention dieser Analyte beitragen. Das quantitative Verhältnis zwischen den hydrophoben und den Coulomb-Wechselwirkungen wurde untersucht, indem zwei unterschiedliche Modelle für die Wechselwirkung geladener Analyte mit der stationären Phase miteinander verglichen werden: das one-site-Modell und das two-site-Modell. Die Abhängigkeit des korrigierten Retentionsfaktors von (1) der Konzentration des Gegenions und (2) der Zahl der Methylengruppen in der Alkylkette der Analyten zeigt, dass das one-site-Modell (hydrophobe Wechselwirkung und Ionenaustausch finden gleichzeitig statt)

herangezogen werden muss, um die beobachtete Retention zu beschreiben. Der Vergleich der CEC-Trennung dieser geladenen Analyte mit elektrophoretischen Mobilitäten, die über Kapillarelektrophorese (CE) bestimmt wurden, zeigt, dass hauptsächlich chromatographische Wechselwirkungen für die in der CEC beobachtete Selektivität verantwortlich sind, während die elektrophoretische Migration dieser Analyte nur eine untergeordnete Rolle spielt.

Die Selektivität der Trennung der geladenen Analyte in der CEC wurde mit der Selektivität der Trennung durch CE verglichen. Alkylaniline werden in der CE unter optimierten Bedingungen mit sehr niedriger Auflösung bei Comigration von 4-Pentylanilin mit 4-Hexylanilin getrennt. Aminosäuren werden in der CE bei optimierten Bedingungen unter Comigration des Phenylalanins und des Tryptophans getrennt. Peptide werden in der CE am optimalen pH* (7.05) unter Comigration des EOF Markers (DMF) und Phe-Phe-Phe und bei pH* 4.0 unter Comigration von Phe-Phe, Phe-Tyr und Phe-Phe-Phe getrennt. Im Gegensatz hierzu wurden alle Analyte mittels CEC mit guter Auflösung getrennt. Die Wiederholbarkeit der elektroosmotischen Mobilität μ_{eo}, und des Retentionsfaktors k eines unpolaren neutralen Analyten (als relative Standardabweichung) von Lauf zu Lauf, von Tag zu Tag und von Kapillare zu Kapillare zeigte, dass das entwickelte Syntheseverfahren und das selbstgebaute CEC-Instrument routinemäßig verwendet werden können, um reproduzierbare und zuverlässige Trennungen zu erzielen.

9 Appendices

9.1 Materials

All chemicals were used without further purification. 3-(trimethoxysilyl) propyl methacrylate (bind silane), piperazinediacrylamide, N,N-dimethylformamide (DMF), ammonium sulfate, and 2-hydroxypropyl-γ-cyclodextrin are from Fluka (Buchs, Switzerland). Hydroxypropyl-ß-cyclodextrin, α-cyclodextrin, vinylsulfonic acid (25% w/v), N,N,N',N'-tetramethylethylenediamine (TEMED), N-isopropylacrylamide, and alkylanilines are from Sigma-Aldrich (Milwaukee, USA). Methacrylamide, ammonium persulfate, acetic acid, alkylphenones (acetophenone, propiophenone, butyrophenone, and valerophenone), 3-ethoxy-4-hydroxybenzaldehyde, 3-methoxy-4-hydroxybenzaldehyde are from Merck (Darmstadt, Germany). Dodecyl methacrylate is from Merck-Schuchardt (Hohenbrunn, Germany). Octadecyl methacrylate is from ABCR GmbH & Co. KG (Karlsruhe, Germany). Phenyl methacrylate is from Lancaster (England). Cyclohexyl methacrylate is from Lancaster (Mühlheim, Germany). Isobornyl methacrylate is from Acros Organics (New Jersy, USA). Statistically 2,6-methylated-ß-cyclodextrin (degree of methylation 1.7-1.9 methyl groups per glucose unit, statistical distribution) is from Wacker-Chemie (Burghausen, Germany). Acetonitrile is from LGC Promochem GmbH, Germany. Methanol is from Fisher Scientific UK limited (UK). Deuterated Methanol-d_4 was from Deutero GmbH (Kastellaun, Germany). Deuterium oxide was from Cambridge Isotope Laboratories (USA). Phe-Phe, Phe-Tyr, Phe-Arg, and Phe-Glu are from Bachem (Switzerland). The amino acids and Phe-Phe-Phe are from MP Biomedicals (Illkirch, France).

Fused-silica capillaries (100 μm I.D × 360 μm O.D.) were from Polymicro Technologies (Phoenix, AZ, USA).

9.2 Synthesis and characterization of adamantyl methacrylate

Adamantyl methacrylate was synthesized according to [122]. 8.3 g (78.8 mmol) of methacryloyl chloride was added dropwise under cooling to a stirred solution of 10.0 g (65.7 mmol) of 1-adamantanol and 12.0 g (119.0mmol) of triethylamine in 100 mL of dichloromethane. After three days of stirring in the refrigerator, the organic layer was treated with a bicarbonate solution (50 mL) followed by water (50 mL). After drying over magnesium sulfate and removal of the solvent under reduced pressure, followed by column chromatography (silica gel with particle size 0.040-0.063 mm (230-400 mesh), Merck,

Germany, eluent: dichloromethane), pure adamantyl methacrylate was obtained as an oil. Characterization was done by ^{1}H- and ^{13}C-NMR spectroscopy:

^{1}H NMR (200 MHz, CD_3OD, ppm): δ = 5.87 (s, 1H, Ha), 5.41 (s, 1H, Hb), 2.05 (s, 9H, H_2+H_3), 1.75 (s, 3H, CH_3), 1.61 (s, 6H, H_4). s: singlet.

^{13}C NMR (200 MHz, CD_3OD, ppm) δ: 168.3 (), 139.7 (), 125.5 (), 82.0 (C_1), 42.8 (C_2), 37.7 (C_4), 32.7 (C_3), 18.9 (CH_3).

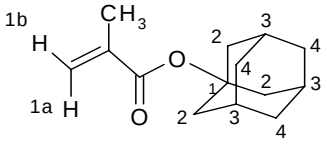

9.3 Preparation of the phosphate buffer

Phosphate buffer needed for the polymerisation mixture was prepared by dissolving 0.39 g (50 mmol L^{-1}) of sodium dihydrogenphosphate and 0.445 g (50 mmol L^{-1}) of disodium hydrogenphosphate in 100 mL of distilled water. The pH of the resulting buffer was measured with the pH meter.

9.4 SEM experiments

1. Capillaries were cut into three segments, one from the detection-window end, the other from the middle of the capillary, and the third segment from the end of the capillary.

2. These cross sections were coated with gold to make them electrically conductive.

3. Then SEM photographs were taken for these segments with different magnification using SEM instrumentation at Electron Microscopy & Microanalysis (EM&M) Laboratory, Institute of Geology, University of Marburg.